POLYPEPTIDE

BASED HYDROGELS

Saltuk B. Hanay (M.Sc.)

Supervisor: Prof. Dr. Andreas Heise

A thesis submitted to Dublin City University
in partial fulfilment of the requirements
for the degree of
Doctor of Philosophy

January 2018

Declaration

I hereby certify that this material, which I now submit for assessment on the programme of study leading to the award of a degree of Doctor of Philosophy is entirely my own work, that I have exercised reasonable care to ensure that the work is original, and does not to the best of my knowledge breach any law of copyright, and has not been taken from the work of others save and to the extent that such work has been cited and acknowledged within the text of my work.

Signed: _____(Saltuk B. Hanay) ID No. 13210077 Date: 01.01.2018

Dedicated to my father Abdullah Hanay, MD, PhD,

& to my niece Misaki and Miray.

Acknowledgements

Every Ph.D. has its own challenges… The mandatory mobility in the Neogel project was my challenge. I don't remember how many times I flied between Ireland and the Netherlands. I had to apply for visa each time, then find a new room in other country and put all my life into one luggage to fly over. I had to adapt to different cultures, colleagues and laboratories. This movement indeed costed me valuable research time but in return I gained ultimate experience for becoming a global scientist.

First of all, I would like to thank my supervisor Prof. Andreas Heise for this Ph.D. opportunity and supporting me until the end. He always helped me whenever I encountered a problem, not only in science but also in life. Thanks to his guidance I could manage to produce good work from this highly mobile project. I would also like to thank Dr. Aylvin Dias and Prof. Dermot Brougham for this opportunity. Their comments, supervising and help during the project were truly unforgettable. My Neogel mates Dr. Bing, Dr. Timo and Kevin (will be Dr. soon), you guys are really amazing friends and we had many good memories that I will remember. I would like to thank Dr. Peter Quaedflieg and Dr. Bas Ritzen for giving me a place in their lab and guidance. I would also like to thank my previous supervisors Prof. Amitav Sanyal and Assoc. Prof. Donus Tuncel for giving me position in their group and helping me to improve my polymer chemistry skills.

I would like to thank Prof. Filip Du Prez for accepting the external examiner position, spending his time to evaluate my work and comments. I would also like to thank Prof. Kiaran Nolan for being my former internal examiner until an unfortunate accident. Very special thanks to Prof. Mary Price for accepting the internal examiner position in such a short time and for her comments on the thesis.

I would like to thank all the members of DCU PRG group – Tushar, Rob, Zeliha, Elena, Fernando, Mark, Anton, Jaco, Fabrice, Jin, Ida, Marcelo. Very special thanks to the people who made an enormous effort for moving the lab from DCU to RCSI and ordering chemicals, glasswares and making the new lab ready in a short time; Hannah, Shoana, Scott, Seamus, Drazen, Trisha, Ruari, Emmet, Graeme.

I would like to thank very much to the technical staff at the School of Chemical Sciences at DCU; Ambrose, Veronica, John, Vinny, Catherine, Damien. Your help with chemical orders, fast replies with NMRs, fixing the lab issues quickly and allowing us to use instruments in DCU (also after moving to RCSI) helped me a lot during this Ph.D. I would also like to thank school secretary Julie for her help and quick replies.

Special thanks to Burcu, Zeliha, Fadwa, Teresa, Safa and Alper for their help and friendship. Thanks to Nilesh, Rory and the soccer guys for the matches and good time. I would also like to thank Chris for his help in DSM and Cristina for her help with SEC in Eindhoven. Very special thanks to Assoc. Prof. Ünsal Koldemir for his amazing TA during 2nd year organic chemistry labs and also for his invitation to a constructive talk prior to my Ph.D. viva.

Finally, I would like to thank my brothers Asst. Prof. Selim Hanay, Asst. Prof. Sinan Hanay and my mother Nimet Hanay for their support during this Ph.D. study.

Content

Abbreviations

AMM	Activated monomer mechanism
ATRP	Atom transfer radical polymerization
BLG	γ-benzyl-L-glutamate
Cbz	Carboxybenzyl
CDI	Carbonyldiimidazole
$CHCl_3$	Chloroform
DBDMH	1,3-Dibromo-5,5-dimethylhydantoin
DMEQ	4-[2-(3,4-Dihydro-6,7-dimethoxy-4-methyl-3-oxo-2-quinoxalinyl)ethyl]-3H
DMF	Dimethylformamide
DPPA	Diphenyl phosphoryl azide
DRI	Differential refractive index (detector)
ESEM	Environmental scanning electron microscope
IR	Infrared spectroscopy
HBr	Hydrobromic acid
HDMS	Bis(trimethylsilyl)amine
HRP	Horseradish peroxidase
LS	Light scattering (detector)
Lys	Lysine
MWCO	Molecular weight cut-off
NAM	Normal amine mechanism
NCA	N-Carboxyanhydride
NMR	Nuclear magnetic resonance
OBT	O-benzyltyrosine
PBLG	Poly(γ-benzyl-L-glutamate)
PDMS	Polydimethylsiloxane

PEG	Poly(ethyleneglycol)
PTAD	4-phenyl-1,2,4-triazole-3,5-dione
PBS	Phosphate buffer saline
ROP	Ring opening polymerization
SEC	Size exclusion chromatography
SEM	Scanning electron microscope
SPPS	Solid phase peptide synthesis
TAD	1,2,4-triazole-3,5-dione
TFA	Trifluoroacetic acid
THF	Tetrahydrofuran
TLC	Thin layer chromatography
TMS	Trimethylsilyl
TRIS	[Tris(hydroxymethyl)aminomethane]
TRP	Tryptophan
TYR	Tyrosine
ZLL	ε-carbobenzyloxy-L-lysine

Abstract

Saltuk B. Hanay

Polypeptide Based Hydrogels

There is a need for biocompatible, biodegradable, 3-D printable and stable hydrogels especially in the areas of tissue engineering, drug delivery, bio-sensing technologies and antimicrobial coatings. The main aim of this Ph.D. work was to fabricate polypeptide based hydrogel which may find a potential application in those fields. Focusing on tyrosine or tryptophan-containing copolypeptides prepared by N-Carboxyanhydride (NCA) polymerizations, three different crosslinking strategies have been tested to obtain polypeptide hydrogels.

1- Enzymatic crosslinking of tyrosine (Chapter 2): Horseradish peroxidase (HRP) enzyme crosslinks tyrosine via a radical formation mechanism. There are several reports of HRP crosslinked tyramine modified natural polymers such as chitosan, hyaluronic acid. However, when a library of tyrosine containing synthetic polypeptides was tested for HRP crosslinking, none of resulted in gel formation.

2- TAD click crosslinking of tyrosine (Chapter 3): 4-Phenyl-1,2,4-triazole-3,5-dione reacts (PTAD) with tyrosine in a click-like manner.[1] Tyrosine copolypeptides were successfully reacted with commercially available PTAD. Then, a series of monofunctional and bifunctional TAD compounds were synthesized and tested. Hydrogels were obtained by crosslinking copolypeptides with hexamethylene-bisTAD. Although TAD-tyrosine reaction is fast and selective, TADs' instability in aqueous conditions is a limitation for this system.

3- TAD click crosslinking of tryptophan (Chapter 4): Methyl-TAD reacts with indole groups very fast, efficiently and reversibly in organic solvents.[2] Tryptophan (indole-containing amino acid) NCA monomer was synthesized, characterized and copolymerized with PEG-amine, Z-Lys, and BLG NCAs. Novel mono and bifunctional PEG-TADs were also synthesized. The polypeptides were PEGylated and crosslinked to produce hydrogels.

4- Novel organohydrogels (Chapter 5): The successfull strategy from Chapter 4 was further applied to produce novel organohydrogels gels with defined segments. Control over gelation kinetics was demonstrated by the hexamethylene-bisTAD reaction with tryptophan containing copolypeptides. Applying controlled lysine and glutamic acid deprotection, non-toxic organohydrogel consisting of a hydrophobic core and a hydrophilic shell were obtained.

Chapter 1
Polypeptide-Based Hydrogels

1.1. Introduction

Polypeptides (or proteins) are common building blocks of living matter as they play a crucial role in metabolic activities and the interaction between organisms and the environment. Polypeptide-based hydrogels hold great potential to be used as biomedical responsive materials for tissue engineering, drug delivery and therapeutics.[1–3] The last decade has shown that there is still a need for new smart materials which can mimic natural tissues and interact with cells without causing a foreign body reaction.[4–7] For example, the fabrication of an artificial extracellular matrix (where cells can grow, migrate and form tissues inside) is still a challenge because a polymeric scaffold must meet many criteria such as being biocompatible, scalable and meeting the desired mechanical properties.[6,8–10]

1.1.1 Tissue Engineering Applications

Tissue engineering is a recently established interdisciplinary field covering medicine, molecular biology, chemistry and engineering.[11–13] The first tissue engineered examples were reported in 1981 when scientists developed an artificial skin used to treat burn victims.[14,15] The main steps of tissue engineering are shown in Figure 1. It starts with proliferation of stem cells which are taken from the patients' body. One strategy involves printing cells and polymer together (bioprinting) during scaffold fabrication utilizing UV-curing approaches. However, crosslinkers or UV irradiations are not generally compatible with cells. The other strategy is to load proliferated stem cells into a pre-made synthetic scaffold or into a decellularized donor organ.[16–18] Premade scaffolds can be washed to remove non-compatible reagents and be sterilized

to make hydrogels biocompatible. Recently, 3D-printing and 3D-bioprinting technologies were utilized to create hydrogels with complex shapes and geometries.[19–25]

Hydrogels for tissue engineering can be prepared from natural polymers such as collagen, chitosan, silk or from synthetic polymers such as polyethylene glycol, polyphosphazene or polypeptides.[26,27] Natural polymers have the advantage of biocompatibility which is a prime requirement for tissue engineering.[28] However, drawbacks of natural polymers are related to their scalability and compositional inconsistency depending on the source which they are isolated from.[29] On the contrary, synthetic polymers can be produced industrially in large scales and their chemical composition can be controlled to a large extent. The main challenges for synthetic polymers are generally related to their biocompatibility. In this context, synthetic polypeptides hold great potential for future biomaterials as they combine natural building blocks (biocompatibility, biodegradability) with the advantages of synthetic flexibility.

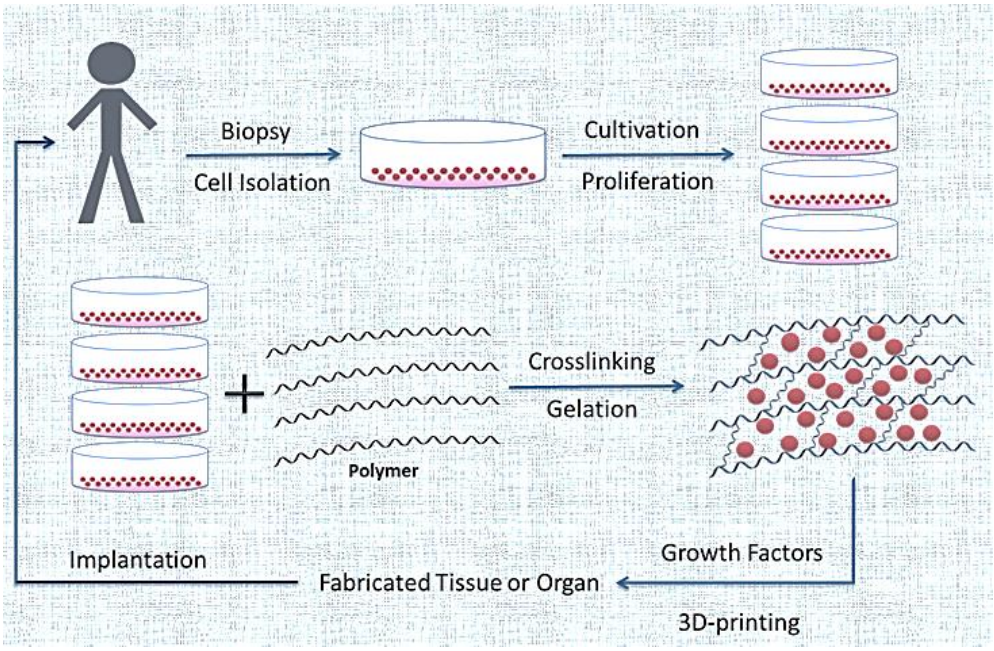

Figure 1.1. The general approach for fabricating tissues using the patient's own cells.

1.1.2 Drug Delivery Applications

Stimuli-responsive hydrogels can be used to create advanced drug delivery systems.[30] For example, Kopecek's and co-workers demonstrated that a pH responsive and biodegradable hydrogel releases drugs mostly in the colon after enzymatic degradation of the hydrogel network.[31] As seen in Figure 1.2, carboxylates (COO^-) become non-ionized due to low pH of the stomach. The neutralization of carboxylic acid causes shrinkage of the hydrogel network. Therefore, the diffusion of the drug becomes minimized in the stomach. When the hydrogel passes into the small intestine, higher pH causes reionization of COOH groups. Thus, the hydrogel swells again and the gel network expands. At this stage, the release of the drug becomes much higher as pores increase. Finally, the azoaromatic crosslinks are broken by colon enzymes and all the drug molecules released at much higher rate. Similarly, a hydrogel having cationic side groups (such as lysine) swells under acidic conditions and shrinks under basic conditions. In addition to pH, electric[32,33],light[34–36], pressure[37], glucose[38–40], and antigen[41] sensitive hydrogels are reported.

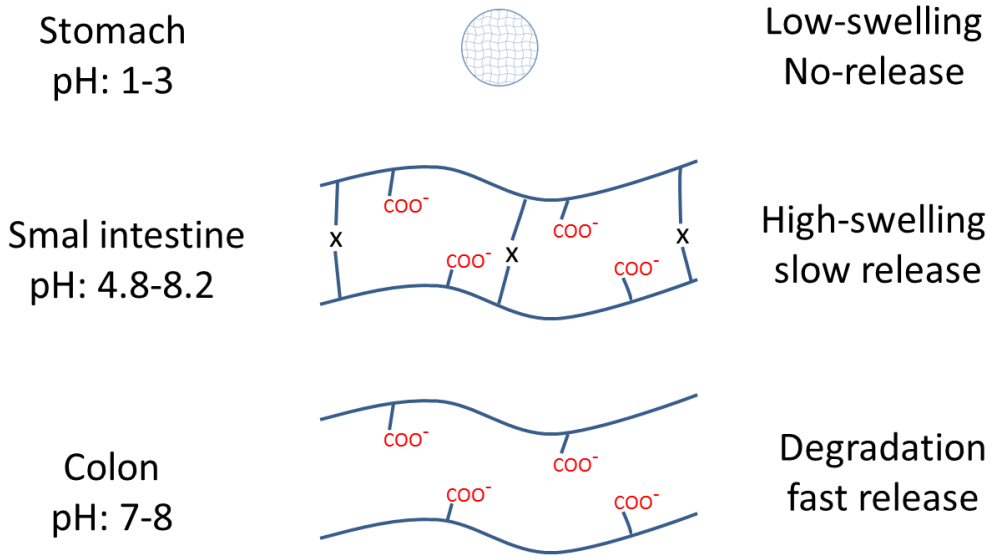

Figure 1.2. Stimuli-responsive biodegradable hydrogel with controlled drug release.[31]

1.1.3 Synthesis of Polypeptides

Biodegradability is a common challenge in the design of advanced drug delivery systems. Synthetic polypeptides might overcome this since the peptide bonds are enzymatically and chemically degradable. Synthetic polypeptides can be prepared by four different methods as briefly highlighted below. Each of these strategies has its specific advantages and disadvantages.

NCA Polymerization: Ring-opening polymerization of N-carboxyanhydrides (NCA) is a very convenient way to synthesize polypeptides in bulk amounts. High yield, ease of synthesis and control over molecular weight makes NCA polymerization one of the most common methods to prepare polypeptides. While an exact amino acid sequence cannot be achieved, homo polypeptides, block polypeptides, complex polypeptide architectures or glycopeptides can be prepared by this technique .[42–49]

Solid Phase Peptide Synthesis: In SPPS, amino acids are added to each other one by one. Monodisperse polypeptides with precisely controlled sequences can be obtained by this method. However, SPPS is not convenient to prepare large scale or long chain polypeptides (> 50 units) because of the lower yield and challenging purification after each addition of amino acid.[50–55]

Protein Engineering: Protein engineering is a method to prepare polypeptides by expression of artificial genes in a living organism such as bacteria. It has been shown that protein engineering can be used to synthesize natural proteins such as silk, collagen, and elastin.[56,57]

Self-Replication: In this technique, a template is used to synthesize sequentially controlled polypeptides. Reactants are pre-organized and catalyzed by a template to

replicate the template. Self-replication is complex but exciting field since it may find solution to how life started and evolved.[58]

1.1.4 Polypeptide-Based Hydrogels

Natural polypeptides are proteins which are isolated from animals or plants. The most common proteins used in biomaterial applications are collagen, gelatin, fibrinogen, and silk. Although the quality and type varies depending on the source, they have significant advantages such as degradability as well as having cell or growth factor binding sequences.[59] Additionally, their gelations are mostly due to self-assembly into specific chain formations such as α-helix, β-sheets, and fibrils.[60–62] The self-assembly character of these polypeptides can be exploited to prepare stimuli-responsive injectable hydrogels. For example, a collagen solution at room temperature forms a physically crosslinked hydrogel when the temperature is raised to 37^{o}C. The microstructure of these types of hydrogels can be easily tuned by pH, ionic strength or speed of heating to the desired temperature. The drawback of physically-crosslinked hydrogels is their low mechanical strength. In general, they are not mechanically robust materials. One way to increase the strength of these hydrogels is chemical crosslinking or modification of natural polypeptides. Bisaldehydes, amidation coupling agents, disocyanates or other functional groups can be used to covalently crosslink proteins or polypeptides. Alternatively, an acrylate modified gelatin can be hardened by UV or thermal irradiation.[63,64]

1.1.5 Hydrogels from synthetic polypeptides

Physical crosslinking of synthetic polypeptides can be achieved by non-covalent interactions such as H-bonding, hydrophobic interactions, van der Waals, coulombic interactions, and self-assembly.[1,9,65] Their crosslinking or properties can also be altered by an external stimulus such as pH, temperature or ionic strength.[66–68] Amphiphilic

diblock or triblock polypeptides prepared by NCA polymerization can form physically crosslinked hydrogels.[62,69–72]. These types of gels are mechanically weak but they are stimuli-responsive. On the other hand, covalent crosslinking provides stronger materials.

Ahrens *et al.* prepared polypeptides having alkyne side groups and functionalized them with N_3-PEG-maleimide and N_3-PEG-Norbornene.[73] Additionally, hydrogels were obtained by crosslinking maleimide groups with 4-arm PEG-thiol. The authors showed that the attachment of human mesenchymal stem cell (hMSC) in peptide-PEG hybrid is more effective than in PEG-only gels. It is important to notice that this hydrogel is uncharged. It was shown that charged polypeptide materials cause cytotoxicity or non-binding of cells when the chain length is small. However, longer chain copolypeptides of charged amino acids such as poly(L-lysine)-block-poly(L-leucine) displayed good biocompatibility.[74] Wang *et al.* used the non-toxic crosslinking agent genipin to obtain hydrogels from lysine containing copolypeptides.[75] They demonstrated that block copolypeptides of lysine-alanine and lysine-glycine have good biocompatibility. Additionally, control over mechanical properties, enzymatic degradability, and successful cell attachments were achieved. Hartgerink's group also reported a lysine-containing polypeptide hydrogel which was crosslinked in mammalian cell culture conditions. The crosslinking was due to oxidation of lysine and Schiff base formation by lysyl oxidize enzyme which naturally occurs in the serum (Figure 1.3).[76]

Not relying on NCA polymerization or SPPS, Lim *et al.* obtained hydrogels from a synthetic polypeptide synthesized by E. coli.[77] They genetically modified E.coli to produce elastin-like polypeptides (ELP). ELP consist of repeating Valine-Proline-Glycine-X-Glycine where X is a natural amino acid but different from proline. They

have periodically introduced lysine groups to the X position. Then hydrogels were obtained by crosslinking lysine residues with [tris(hydroxymethyl)phosphino] propionic acid.

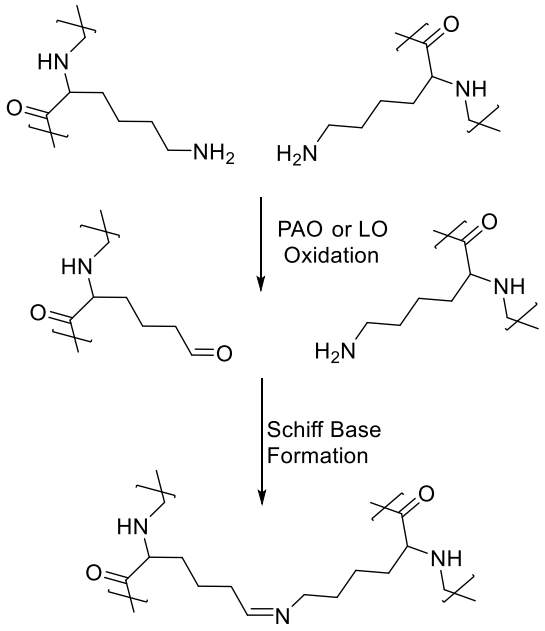

Figure 1.3. Schiff base crosslinking of lysine by polyamine oxidase or lysyl oxidase.[76]

Synthetic polypeptides are not limited to natural amino acids. To date, many non-natural amino acids containing unique functional groups are reported. For example, alkene[78] or alkyne-azido[79–83] groups can be incorporated to polypeptides by NCA. Hydrogels can be obtained by crosslinking these groups with azide-alkyne cycloadditions thiol-ene reaction.

1.2. Details of NCA Polymerization

The first synthetic polypeptides were prepared by Curtius and Wessely in the 1920s. They showed that high molecular weight polypeptides can be prepared by ring-opening polymerization of NCAs, which is initiated by a nucleophile such as alcohol or a primary amine.[84] Despite being well known, NCA polymerization has only gained its popularity in last two decades. The recent developments in NCA polymerization have

enabled the preparation of polypeptides with control over the molecular weight and the chain architecture. Additionally, self-assembling properties of polypeptides and their high biocompatibility have made them strong candidates for the next generation smart biomaterials.

1.2.1. NCA Monomers: Synthesis and Purification

The synthesis of NCAs via halogenating agents was firstly reported by Leuchs in 1906.[85] There have been many alternative ways proposed for the synthesis of α-amino acid NCAs since then. One very efficient way is the Fuchs-Farthing method which utilizes phosgenation chemistry (Figure 1.4).[86] Due to the high health risk of phosgene gas, its commercially available derivatives offer a safer and more practical usage. Liquid Diphosgene and solid triphosgene are easier to handle and store compared to phosgene gas.

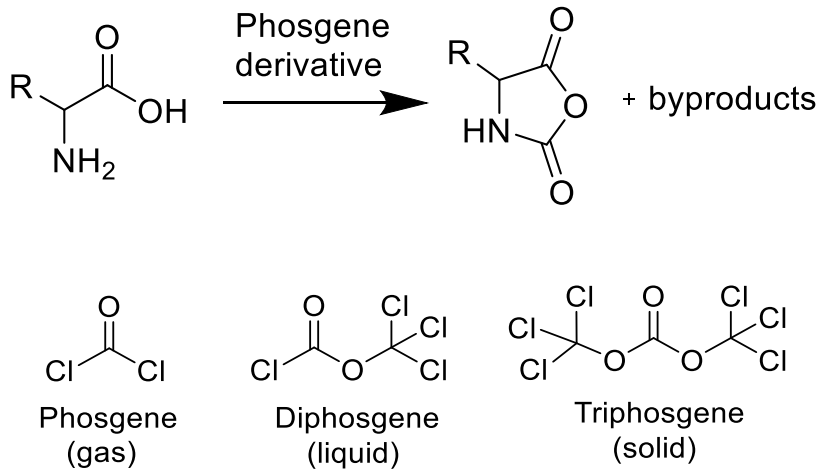

Figure 1.4. NCA synthesis by the Fuchs-Farthing method and phosgene derivatives.

Phosgene free syntheses of NCAs have also been reported for specific amino acids. Recently, Endo and his group have shown that bisarylcarbonates can be used to convert amino acid into NCAs.[87] The same group has also demonstrated that imidazolium salts of amino acids can be converted into NCA by using

phenylcarbonate.[88] However, these methods do not apply to all amino acids easily and yields are lower compared to phosgenation.

The syntheses of NCA monomers are always accompanied by side-products. Depending on the synthetic route these side products can be a mixture of HCl, aminoacid HCl salts, alkyl halides etc.[89] Some of these side products may inhibit polymerization causing a lower degree of polymerization. Others may initiate polymerization causing low stability of the monomers or control over polymerization. Therefore, it is very important to remove by-products and prepare pure monomers for a controlled polymerization.

Some side products can be removed by extraction and washing.[90] Addition of α-pinene to the reaction mixture scavenges HCl and related side product.[91] However, further purification is always needed. Crystallization is the most common method for purification of NCA monomers. Multiple recrystallizations are crucial to achieving the desired purity. Depending on the amino acid and its protecting group, the number of recrystallization varies from two to six or more. In some cases, NCA monomer cannot be isolated as crystals. Especially, NCAs having lower melting points or long n-alkyl chains do not give crystalline products. In these cases, using silica gel column chromatography under dry and inert conditions may help for purification.[89]

1.2.2 Mechanism of NCA polymerization

NCA polymerization can be initiated by different methods. The most common methods to initiate NCA polymerization are the normal amine mechanism (NAM) and activated monomer mechanism (AMM). In NAM, a non-bulky nucleophile attacks the carbonyl of NCA to form a carbamic acid intermediate. Decarboxylation of this intermediate produces a primary amine which can propagate the polymerization (Figure 1.5). AMM starts by abstraction of H from N of the NCA ring by a non-

nucleophilic base. Then, activated NCA initiates the polymerization in a similar manner to NAM. Amino acids with reactive side groups such lysine and tyrosine may initiate the polymerization. Therefore, protection of reactive groups must be done before NCA monomer synthesis.

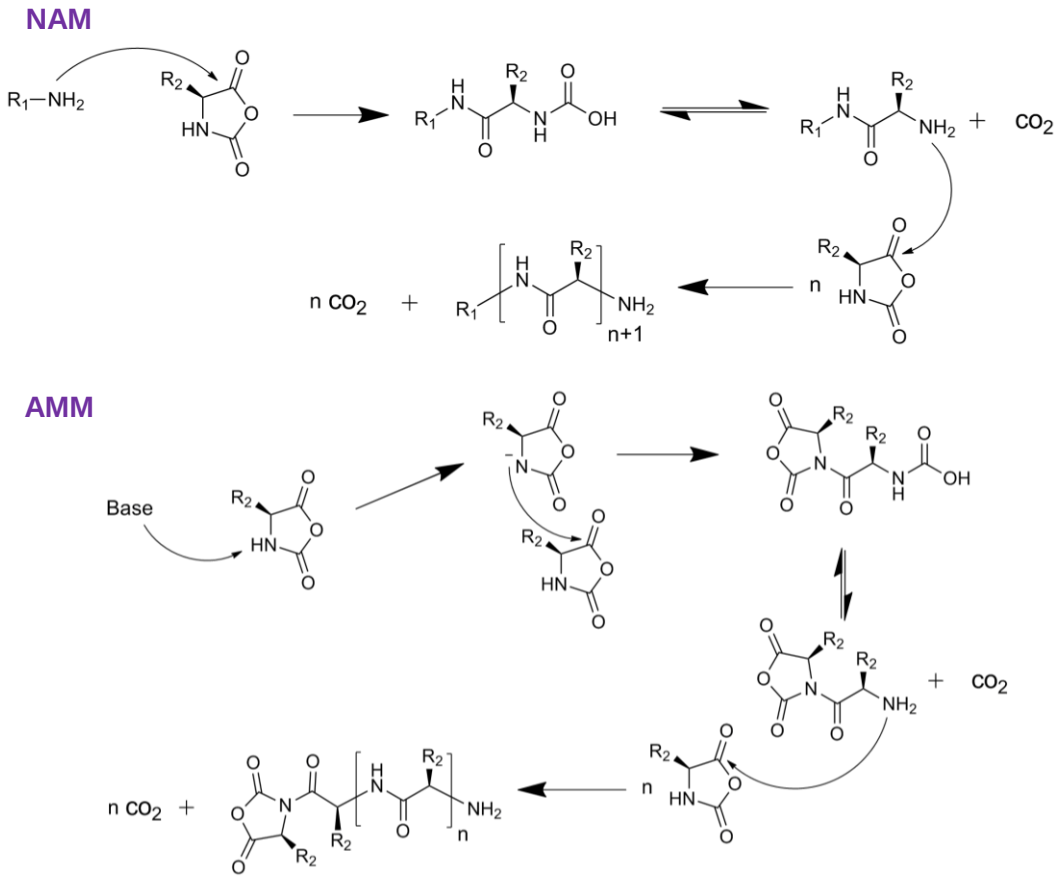

Figure 1.5. The detailed mechanism of the N-Carboxyanhydride polymerization.

An example of NCA in figure 1.6 shows the type of monomers, initiator, and removal of the protection groups.

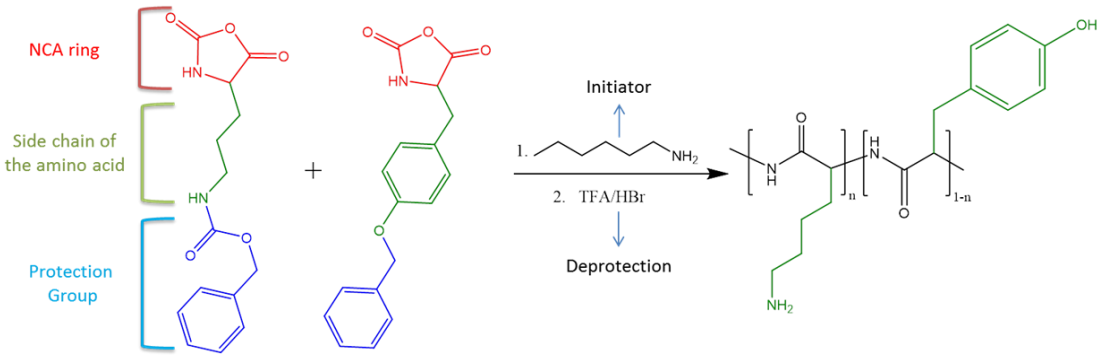

Figure 1.6. NCA ROP of Z-Lysine and O-benzyl Tyr and removal of protection groups.

1.2.3 Recent Methods and Developments in NCA-ROP

When NCA polymerization is carried out under normal conditions (room temperature and atmospheric pressure), the control over the polymerization and the end group functionality is limited due to chain end termination by side reactions.[45,92,93]

Deming developed transition metal initiators to prevent side reactions. Successful preparation of triblock copolypeptides having very high molecular weight (over 200KDa) and low polydispersity (1.15) was achieved via initiation by cobalt, nickel and iron complexes such as bpyNi(COD), (PMe_3)Fe, (PMe_3)Co. Although the metal initiators needed to be removed after polymerization, this method provides excellent control over molecular weight, low dispersity, and high end-group functionality. [44,94–96]

In addition to transition metal complexes, optimization of reaction parameters in amine initiated polymerization also provides control over dispersity and end group functionality. Hadjichristidis and Messmann groups demonstrated that well-defined polypeptides with low dispersity can be obtained by highly pure monomers and high vacuum conditions.[47,97] Vayaboury *et al.* showed that temperature dramatically affects the end group functionality. Interestingly, living end groups increased from 22% to 99% by just decreasing the reaction temperature from 20°C to 0°C.[93] The end group

termination was determined by non-aqueous capillary electrophoresis (NACE). It is found that dead chain ends have carboxylate and formyl groups (Figure 1.7). Formation of carboxylates was due to termination by an NCA anion (isocyanate resonance terminates amine ends). On the other hand, the formation of formyl end was due to the reaction with DMF.

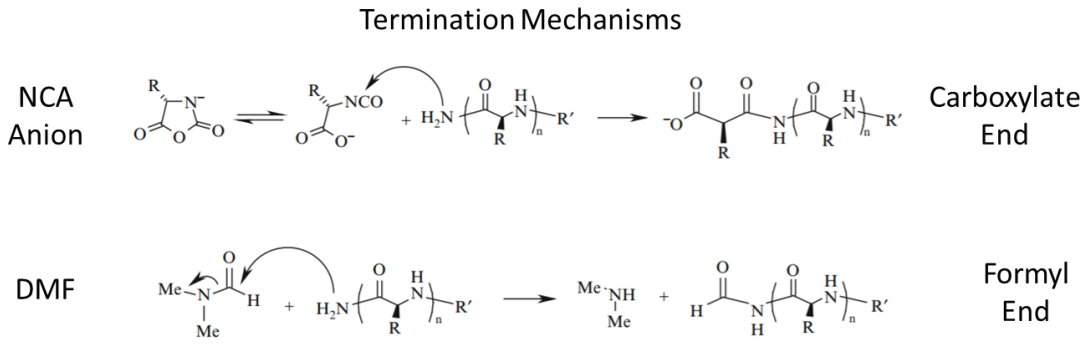

Figure 1.7. Living end group termination mechanisms.[93,98]

For the synthesis of block polypeptides it is important to carry out polymerization at low temperatures because living end groups are critical to obtain satisfactory results. However, lowering the temperature increases the polymerization time from hours to several days. Heise and Habraken demonstrated that high vacuum and low temperature conditions are ideal for NCA polymerization. Removal of CO_2 by vacuum shifts the CO_2 - carbamic acid equilibrium to the right and this accelerates the polymerization.[45] This condition provides control of NCA polymerization without metal complexes.

Another way of initiating NCA polymerization utilizes hexamethyldisilazane (HMDS). Although HMDS is a secondary amine, the initiation and propagation steps are different than in the normal amine mechanism or activated monomer mechanism. Firstly, the trimethylsilane group is transferred to C2 of the NCA after the cleavage of the Si-N bond during initiation. Then, TMS amine reacts with NCA-TMS to form

TMS-carbamate. Finally, polymerization is propagated by transfer of TMS groups from previous TMS-carbamate monomer (Figure 1.8).[98]

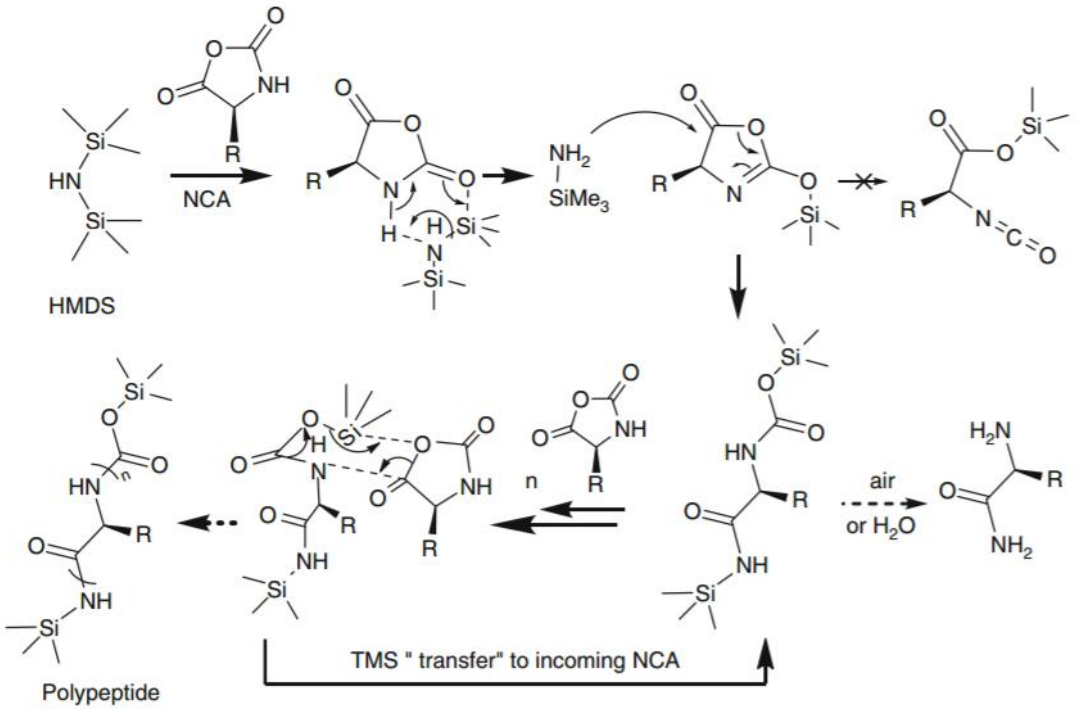

Figure 1.8. Mechanism of HMDS initiated NCA-ROP.[98]

1.3. Triazolinedione (TAD) Chemistry

1.3.1 Synthesis of TADs

Triaziolinediones are one of the most reactive dienophiles and enophiles ever known[99]. The first reports on syntheses of TADs via the oxidation of 4-phenylurazole were given by Thiele in 1894 and by Stolle in 1912[100]. However, both reported only low yields. Cookson's work in 1962[100] and 1967[101] is considered to be a milestone in TAD syntheses where he achieved high yields and demonstrated Diels-Alder reaction with 4-Phenyl-3H-1,2,4-triazole-3,5(4H)-dione (PTAD).[102] In the 1980s and 1990s, simple TADs such as PTAD, Methyl-TAD were used to modify and crosslink polymers to alter mechanical or optical properties of materials. Additionally, bisTADs were reported to be used in step-growth polymerization.[99,103–105] TAD chemistry has

regained attention in this millennium due to the improvements in its synthesis[106,107] and the success in applications such as total synthesis[108], bioconjugation[109,110], polymer chemistry and material chemistry[111–116]. Du Prez and co-workers has reported an extensive review on TADs which includes its history, synthesis (precursor and oxidation), reactivity and applications in polymer and material science.[102]

In general, TADs are synthesized from their corresponding urazoles via oxidation. Urazoles can be synthesized from amines, anilines, isocyanates and carboxylic acids in two or three steps (Figure 1.9). Little *et al.* reported 100 g scale urazole synthesis from these precursors.[106] The first step of urazole synthesis is the formation of semicarbazide (**1**) or sometimes referred as hydrazinecarboxylate. Then, urazole (**2**) forms upon cyclization of **1** in strong basing conditions such as refluxing in 4N KOH or K_2CO_3/EtOH.

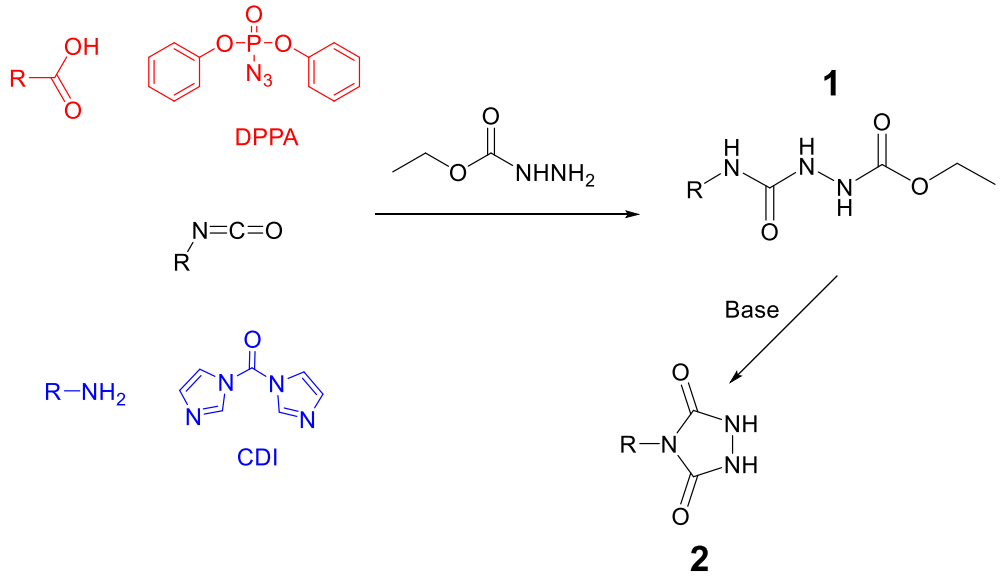

Figure 1.9. Urazole synthesis

The final step in TAD synthesis, the oxidation of urazole, is the most challenging step. There are numerous methods proposed, especially by Mallakpour, to oxidize urazoles to the corresponding TADs.[107,117–122] Du Prez classified the oxidizing agents for TAD

synthesis as nitrogen(IV) & nitrogen(V) oxide-based, halogen-mediated, activated DMSO & selenic acid-mediated, metal ion/metal oxide-mediated, electrochemical oxidation and others.[102] The choice of oxidizing agent should be guided by the urazole structures. A mild oxidizing agent is more suitable for urazoles having oxidizable functional groups. Additionally, it is important to test different classes of oxidizing agents to obtain TADs in satisfactory yield and purity.

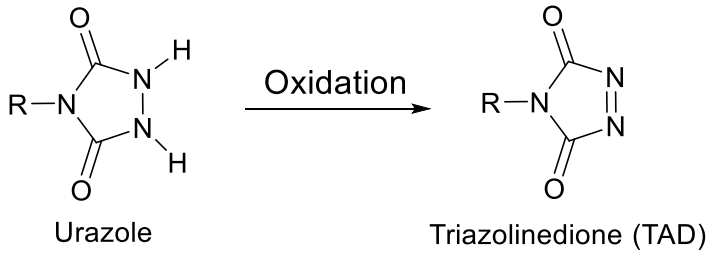

Figure 1.10. Final step in TAD synthesis.

Commercially available oxidizing agents such as 1,3-dibromo-5,5-dimethylhydantoin or 1,3-dichloro-5,5-dimethylhydantoin can be used as a convenient option.[119] However, removal of hydantion related side products presents a challenge. Additionally, this method produces hydrogen halides (4 equivalent of HX per urazole). For some applications such as gel formation, these side products can be washed off after crosslinking. Therefore, side products might not be a problem. On the other hand, if a pure TAD is needed, alternative methods should be chosen because the purification might be very challenging due to the high reactivity of TADs. Heterogeneous oxidizing agents are promising to obtain pure TADs. Silica-bound nitric acid was shown to be effective and it can be removed by filtration. However, water coming of nitric acid may decompose TAD if the oxidation is done in a hygroscopic solvent. For other solvent, drying solution with anhydrous $MgSO_4$ just after oxidation gives good results. Otherwise, water decomposes TAD especially when water gets concentrated during evaporation of the organic solvent.

1.3.2 Novel TAD Compounds

Previously, simple TADs such as PTAD or Mehtyl-TAD (and their bifunctional counterparts) were used in polymer modifications. Recent developments in TAD synthesis and demonstration of click-like behaviour has attracted scientist to synthesize new TAD compounds with more exotic functionalities. The reactivity and stability of the new compounds may differ depending on adjacent groups of TAD moiety. Some TADs can be isolated and stored for months but others may require in-situ preparation and immediate use. Additionally, incompatibility of the oxidation method may lower their stability.

Some of the recently reported TADs are shown in Figure 1.11. Azide (**1**) and alkyne (**2**,**3**) TADs were used in the bioconjugation of tyrosine.[110,123,124] Urazole precursors of **2** and **3** were reacted with PEG-azide and then oxidized to form pseudo PEG-TAD. The PEGylation of chymotrypsinogen (a digestive enzyme) and aplaviroc (anti-HIV drug) was done by using pseudo PEG-TAD. The PEGylation is an important reaction in pharmaceutical applications and this method is more convenient (due to its click-like character) than previously reported PEGylation of tyrosine.[125] However, the reported pseudo PEG-TAD requires tedious synthesis of **2** and **3** and was not isolated and characterized after reaction of 2,3 with PEG-azide.

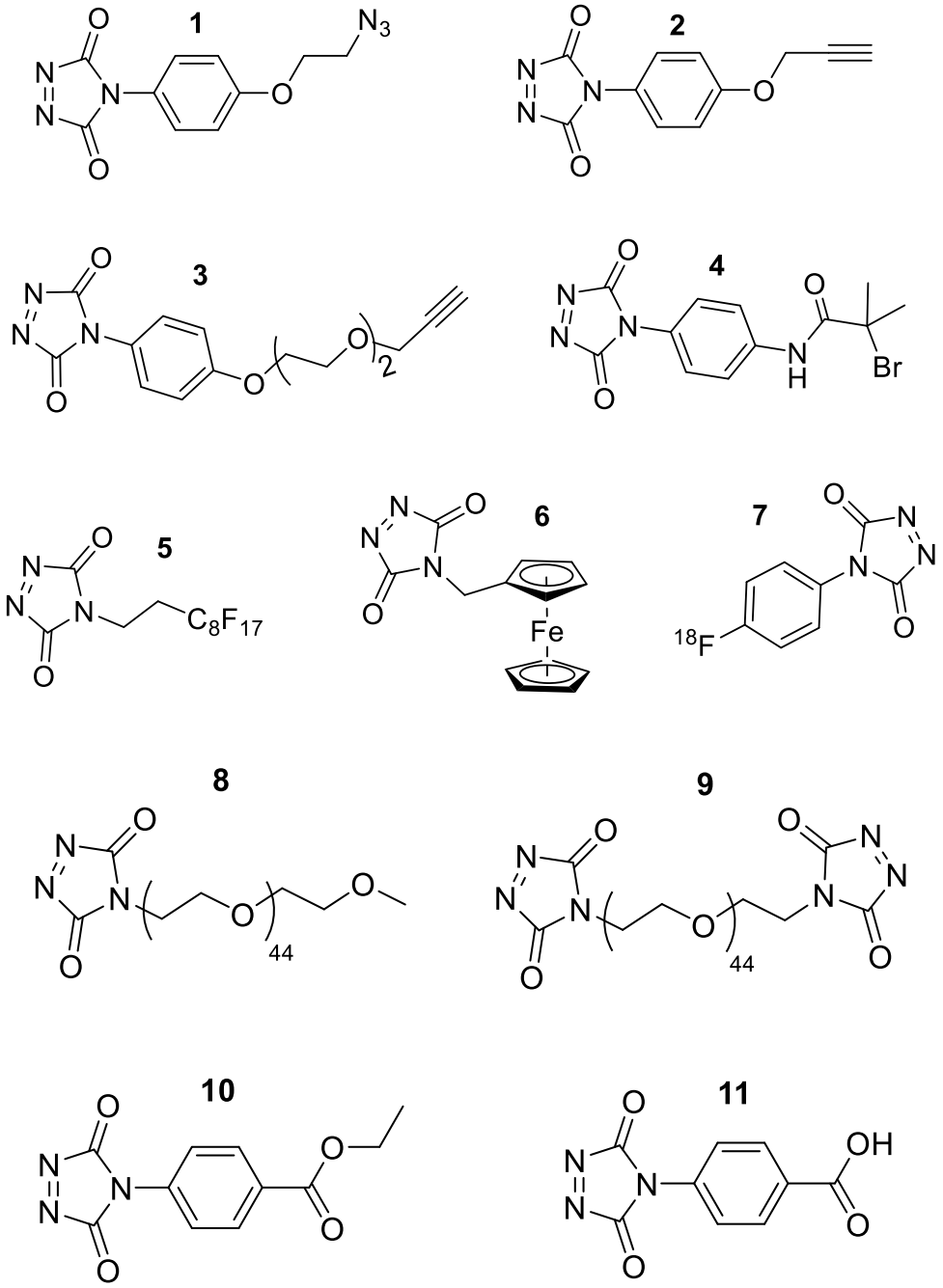

Figure 1.11 Some of the recently reported TAD compounds.

ATRP-TAD (**4**) compound was reported by Du Prez and co-workers.[111] Later this initiator was used to create rewritable polymer brushes (Figure 1.12)[112]. Indole-functionalized glass or silicon surfaces were prepared by the thiol-ene reaction. Then PDMS stamp having the initiator was printed on this surface by reversible TAD-indole click reaction. Patterned polymer brushes were grown by surface-induced ATRP and these brushes were erased at high temperature due to reversible nature of the

reaction[108]. The re-writing was done with the same cycle and this process was repeated 4 times to demonstrate the robustness of the method.

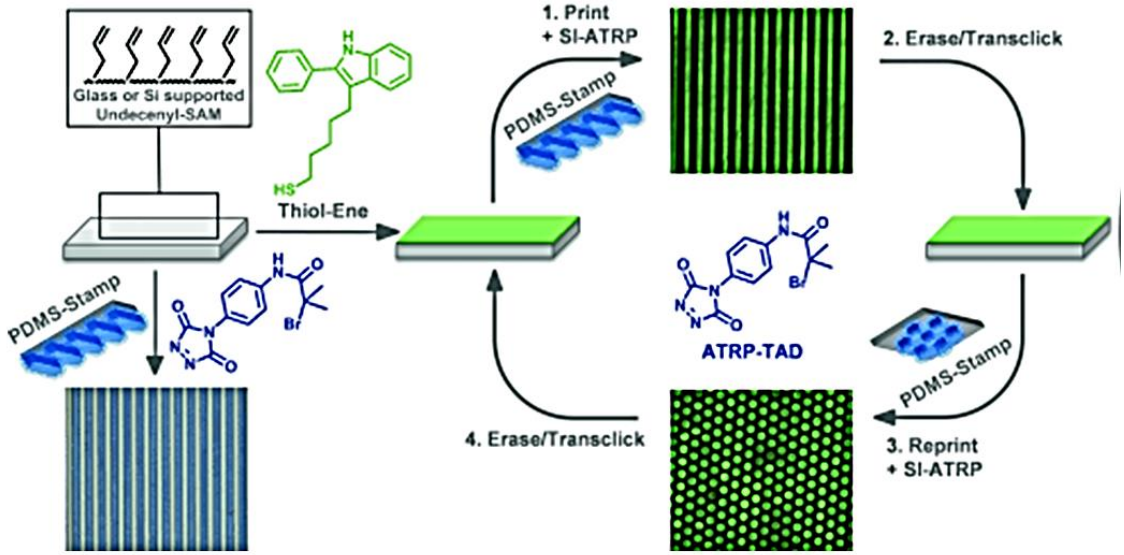

Figure 1.12. Rewritable surfaces by using reversible TAD-indole reaction.[112]

and Curran.[126] Fluorous TAD (**5**) was used to scavenge excess dienes after Diels-Alder reaction (Figure 1.13). Due to its high reactivity and distinct color, scavenging reactions can be done in seconds and monitored by the naked eye. Scavenged dienes can be removed by solid-phase extraction on fluorous silica gel (FSPE).

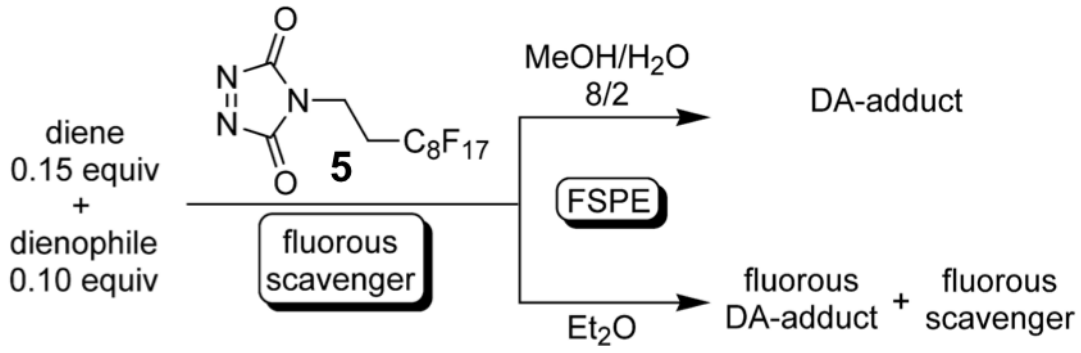

Figure.1.13. Scavenging dienes by fluorus TAD and purification by FSPE.

Commercially available DMEQ-TAD (described in Chapter 4) and TAD-Ferrocene (**6**) was used to tag vitamin D. Then, quantification of vitamin D metabolites was done by

fluorescence spectroscopic methods (for DMEQ)[127] and by mass spectrometry (for ferrocene).[128] Jessica *et al.* demonstrated that novel [18F]-4-(4-fluorophenyl)-1,2,4-triazole-3,5-dione **(7)** can be used to radiolabel tyrosine on short peptides and proteins. This agent has potential to be used in positron emission tomography (PET) imaging

In chapter 4, we report the synthesis and use of mono and bifunctional PEG-TAD (**8**, **9**) which are directly synthesized from PEG-amine, isolated as powder and characterized by NMR and IR. Additionally, synthesis and characterization of ester-TAD (**10**) and carboxylic acid TAD (**11**) are reported in Chapter 3.

1.4. Aim of the work

The main aim of the project is the synthesis of polypeptide-based hydrogels which may find application in tissue engineering, drug delivery and related fields. The approach follows three steps. The first step involves the synthesis of polypeptides by NCA polymerization. Secondly, TAD crosslinkers are synthesized. Finally, the polypeptides are crosslinked to obtain hydrogels. The project is designed to crosslink natural amino acids by a fast, efficient and selective reaction. For this reason, TAD-tyrosine and TAD-tryptophan reactions were examined and utilized. Details are described in the following chapters 3-5, which have been drafted for publications.

1.5. References

(1) Huang, J.; Heise, A. *Chem. Soc. Rev.* **2013**, *42* (17), 7373–7390.

(2) Zhang, S.; Li, Z. *J. Polym. Sci. Part B Polym. Phys.* **2013**, *51* (7), 546–555.

(3) He, X.; Fan, J.; Wooley, K. L. *Chemistry - An Asian Journal*. 2016, pp 437–447.

(4) Bianco, P.; Robey, P. G. *Nature* **2001**, *414* (6859), 118–121.

(5) Caplan, A. I. *J. Cell. Physiol.* **2007**, *213* (2), 341–347.

(6) Langer, R. *Nat Biotechnol* **1994**.

(7) Hu, W.-J.; Eaton, J. W.; Ugarova, T. P.; Tang, L. *Blood* **2001**, *98* (4), 1231–1238.

(8) Gunatillake, P. A.; Adhikari, R. *Eur Cell Mater* **2003**, *5* (1), 1–16.

(9) Matson, J. B.; Stupp, S. I. *Chem. Commun.* **2012**, *48* (1), 26–33.

(10) Lee, K. Y.; Mooney, D. J. *Chem. Rev.* **2001**, *101* (7), 1869–1880.

(11) Langer, R.; Vacanti, J. P. *Science* **1993**, *260* (5110), 920–926.

(12) Ikada, Y. *J. R. Soc. Interface* **2006**, *3* (10), 589–601.

(13) Van Vlierberghe, S.; Dubruel, P.; Schacht, E. *Biomacromolecules*. 2011, pp 1387–1408.

(14) Bell, E.; Ehrlich, H. P.; Buttle, D. J.; Nakatsuji, T. *Science (80-.).* **1981**, *211* (4486), 1052–1054.

(15) Burke, J. F.; Yannas, I. V; Quinby Jr, W. C.; Bondoc, C. C.; Jung, W. K. *Ann. Surg.* **1981**, *194* (4), 413.

(16) Badylak, S. F.; Taylor, D.; Uygun, K. *Annu. Rev. Biomed. Eng.* **2011**, *13*, 27–53.

(17) Uygun, B. E.; Soto-Gutierrez, A.; Yagi, H.; Izamis, M.-L.; Guzzardi, M. A.; Shulman, C.; Milwid, J.; Kobayashi, N.; Tilles, A.; Berthiaume, F. *Nat. Med.* **2010**, *16* (7), 814–820.

(18) Gilbert, T. W.; Sellaro, T. L.; Badylak, S. F. *Biomaterials* **2006**, *27* (19), 3675–3683.

(19) Trachtenberg, J. E.; Placone, J. K.; Smith, B. T.; Piard, C. M.; Santoro, M.; Scott, D. W.; Fisher, J. P.; Mikos, A. G. *ACS Biomater. Sci. Eng.* **2016**, *2* (10), 1771–1780.

(20) Kuo, C. Y.; Eranki, A.; Placone, J. K.; Rhodes, K. R.; Aranda-Espinoza, H.; Fernandes, R.; Fisher, J. P.; Kim, P. C. W. *ACS Biomater. Sci. Eng.* **2016**, *2* (10), 1817–1826.

(21) Murphy, S. V; Atala, A. *Nat. Biotechnol.* **2014**, *32* (8), 773–785.

(22) Kolesky, D. B.; Truby, R. L.; Gladman, A. S.; Busbee, T. A.; Homan, K. A.; Lewis, J. A. *Adv. Mater.* **2014**, *26* (19), 3124–3130.

(23) Pereira, R. F.; Bártolo, P. J. *Journal of Applied Polymer Science*. 2015.

(24) Jose, R. R.; Rodriguez, M. J.; Dixon, T. A.; Omenetto, F.; Kaplan, D. L. *ACS Biomaterials Science and Engineering*. 2016, pp 1662–1678.

(25) Wang, Z.; Abdulla, R.; Parker, B.; Samanipour, R. *Biofabrication* **2015**, *7* (4), 1–29.

(26) Suh, J.-K. F.; Matthew, H. W. T. *Biomaterials* **2000**, *21* (24), 2589–2598.

(27) Drury, J. L.; Mooney, D. J. *Biomaterials* **2003**, *24* (24), 4337–4351.

(28) POLAK, J. M.; BISHOP, A. E. *Ann. N. Y. Acad. Sci.* **2006**, *1068* (1), 352–366.

(29) Hoffman, A. S. *Adv. Drug Deliv. Rev.* **2012**, *64*, 18–23.

(30) Qiu, Y.; Park, K. *Adv. Drug Deliv. Rev.* **2001**, *53* (3), 321–339.

(31) Ghandehari, H.; Kopečková, P.; Kopecek, J. *Biomaterials* **1997**, *18* (12), 861–872.

(32) Tanaka, T.; Nishio, I.; Sun, S.-T.; Ueno-Nishio, S. *Science (80-.).* **1982**, *218* (4571), 467–469.

(33) Sawahata, K.; Hara, M.; Yasunaga, H.; Osada, Y. *J. Control. Release* **1990**, *14* (3), 253–262.

(34) Suzuki, A.; Tanaka, T. *Nature* **1990**, *346* (6282), 345–347.

(35) Suzuki, A.; Ishii, T.; Maruyama, Y. *J. Appl. Phys.* **1996**, *80* (1), 131–136.

(36) Zhang, X.; Li, Y.; Hu, Z.; Littler, C. L. *J. Chem. Phys.* **1995**, *102* (1), 551–555.

(37) Zhong, X.; Wang, Y.-X.; Wang, S.-C. *Chem. Eng. Sci.* **1996**, *51* (12), 3235–3239.

(38) Lee, S. J.; Park, K. *J. Mol. Recognit.* **1996**, *9* (5-6), 549–557.

(39) Obaidat, A. A.; Park, K. *Pharm. Res.* **1996**, *13* (7), 989–995.

(40) Obaidat, A. A.; Park, K. *Biomaterials* **1997**, *18* (11), 801–806.

(41) Miyata, T.; Asami, N.; Uragami, T. *Nature* **1999**, *399* (6738), 766–769.

(42) Deming, T. J. *Prog. Polym. Sci.* **2007**, *32* (8), 858–875.

(43) Deming, T. J. *Adv. Mater.* **1997**, *9* (4), 299–311.

(44) Deming, T. J. *Nature* **1997**, *390* (6658), 386–389.

(45) Habraken, G. J. M.; Wilsens, K. H. R. M.; Koning, C. E.; Heise, A. *Polym. Chem.* **2011**, *2* (6), 1322–1330.

(46) Habraken, G. J. M.; Peeters, M.; Dietz, C. H. J. T.; Koning, C. E.; Heise, A. *Polym. Chem.* **2010**, *1* (4), 514–524.

(47) Aliferis, T.; Iatrou, H.; Hadjichristidis, N. *Biomacromolecules* **2004**, *5* (5), 1653–1656.

(48) Byrne, M.; Murphy, R.; Kapetanakis, A.; Ramsey, J.; Cryan, S.; Heise, A. *Macromol. Rapid Commun.* **2015**, *36* (21), 1862–1876.

(49) Huang, J.; Habraken, G.; Audouin, F.; Heise, A. *Macromolecules* **2010**, *43* (14), 6050–6057.

(50) Merrifield, R. B. *J. Am. Chem. Soc.* **1963**, *85* (14), 2149–2154.

(51) Amblard, M.; Fehrentz, J.-A.; Martinez, J.; Subra, G. *Mol. Biotechnol.* **2006**, *33*, 239–254.

(52) Fields, G. B.; Noble, R. L. *Int. J. Pept. Protein Res.* **1990**, *35* (3), 161–214.

(53) Merrifield, B. *Solid-Phase Peptide Synthesis*; 1997; Vol. 289.

(54) Palomo, J. M. *RSC Adv.* **2014**, *4* (62), 32658–32672.

(55) Albericio, F.; Carpino, L. A. *Methods Enzymol.* **1997**, *289* (1985), 104–126.

(56) Foo, C. W. P.; Kaplan, D. L. *Adv. Drug Deliv. Rev.* **2002**, *54* (8), 1131–1143.

(57) Brannigan, J. a; Wilkinson, A. J. *Nat. Rev. Mol. Cell Biol.* **2002**, *3* (12), 964–

970.

(58) Lee, D. H.; Granja, J. R.; Martinez, J. A.; Severin, K.; Ghadiri, M. R. *Nature* **1996**, *382* (6591), 525–528.

(59) Rutz, A. L.; Shah, R. N. In *Polymeric Hydrogels as Smart Biomaterials*; Springer, 2016; pp 73–104.

(60) Deming, T. J. *Soft Matter* **2005**, *1* (1), 28–35.

(61) Hamley, I. W. *Angew. Chemie Int. Ed.* **2007**, *46* (43), 8128–8147.

(62) Huang, J.; Hastings, C. L.; Duffy, G. P.; Kelly, H. M.; Raeburn, J.; Adams, D. J.; Heise, A. *Biomacromolecules* **2012**, *14* (1), 200–206.

(63) Chen, Y.; Lin, R.; Qi, H.; Yang, Y.; Bae, H.; Melero-Martin, J. M.; Khademhosseini, A. *Adv. Funct. Mater.* **2012**, *22* (10), 2027–2039.

(64) Nichol, J. W.; Koshy, S. T.; Bae, H.; Hwang, C. M.; Yamanlar, S.; Khademhosseini, A. *Biomaterials* **2010**, *31* (21), 5536–5544.

(65) Schneider, J. P.; Pochan, D. J.; Ozbas, B.; Rajagopal, K.; Pakstis, L.; Kretsinger, J. *J. Am. Chem. Soc.* **2002**, *124* (50), 15030–15037.

(66) Markland, P.; Zhang, Y.; Amidon, G. L.; Yang, V. C. *J. Biomed. Mater. Res.* **1999**, *47* (4), 595–602.

(67) Zhang, Z.; Chen, L.; Deng, M.; Bai, Y.; Chen, X.; Jing, X. *J. Polym. Sci. Part A Polym. Chem.* **2011**, *49* (13), 2941–2951.

(68) Chen, Y.; Pang, X.; Dong, C. *Adv. Funct. Mater.* **2010**, *20* (4), 579–586.

(69) Estroff, L. A.; Hamilton, A. D. *Chem. Rev.* **2004**, *104* (3), 1201–1218.

(70) Nowak, A. P.; Breedveld, V.; Pine, D. J.; Deming, T. J. *J. Am. Chem. Soc.* **2003**, *125* (50), 15666–15670.

(71) Breedveld, V.; Nowak, A. P.; Sato, J.; Deming, T. J.; Pine, D. J. *Macromolecules* **2004**, *37* (10), 3943–3953.

(72) Pochan, D. J.; Pakstis, L.; Ozbas, B.; Nowak, A. P.; Deming, T. J. *Macromolecules* **2002**, *35* (14), 5358–5360.

(73) Ahrens, C. C.; Welch, M. E.; Griffith, L. G.; Hammond, P. T. *Biomacromolecules* **2015**, *16* (12), 3774–3783.

(74) Pakstis, L. M.; Ozbas, B.; Hales, K. D.; Nowak, A. P.; Deming, T. J.; Pochan, D. *Biomacromolecules* **2004**, *5* (2), 312–318.

(75) Wang, S. S. S.; Hsieh, P.-L.; Chen, P.-S.; Chen, Y.-T.; Jan, J.-S. *Colloids Surfaces B Biointerfaces* **2013**, *111*, 423–431.

(76) Bakota, E. L.; Aulisa, L.; Galler, K. M.; Hartgerink, J. D. *Biomacromolecules* **2010**, *12* (1), 82–87.

(77) Lim, D. W.; Nettles, D. L.; Setton, L. A.; Chilkoti, A. *Biomacromolecules* **2007**, *9* (1), 222–230.

(78) Zhou, J.; Chen, P.; Deng, C.; Meng, F.; Cheng, R.; Zhong, Z. *Macromolecules* **2013**, *46* (17), 6723–6730.

(79) Rhodes, A. J.; Deming, T. J. *ACS Macro Lett.* **2013**, *2* (5), 351–354.

(80) Engler, A. C.; Lee, H.; Hammond, P. T. *Angew. Chemie Int. Ed.* **2009**, *48* (49), 9334–9338.

(81) Zhang, R.; Zheng, N.; Song, Z.; Yin, L.; Cheng, J. *Biomaterials* **2014**, *35* (10),

3443–3454.

(82) Shaikh, A. Y.; Das, S.; Pati, D.; Dhaware, V.; Sen Gupta, S.; Hotha, S. *Biomacromolecules* **2014**, *15* (10), 3679–3686.

(83) Xiao, C.; Zhao, C.; He, P.; Tang, Z.; Chen, X.; Jing, X. *Macromol. Rapid Commun.* **2010**, *31* (11), 991–997.

(84) Huang, J.; Heise, A. *Chem. Soc. Rev.* **2013**, *42* (17), 7373–7390.

(85) Kricheldorf, H. R. *Angew. Chemie Int. Ed.* **2006**, *45* (35), 5752–5784.

(86) Daly, W. H.; Poché, D. *Tetrahedron Lett.* **1988**, *29* (46), 5859–5862.

(87) Fujita, Y.; Koga, K.; Kim, H.; Wang, X.; Sudo, A.; Nishida, H.; Endo, T. *J. Polym. Sci. Part A Polym. Chem.* **2007**, *45* (22), 5365–5370.

(88) Koga, K.; Sudo, A.; Endo, T. *J. Polym. Sci. Part A Polym. Chem.* **2010**, *48* (19), 4351–4355.

(89) Kramer, J. R.; Deming, T. J. *Biomacromolecules* **2010**, *11* (12), 3668–3672.

(90) Poche, D. S.; Moore, M. J.; Bowles, J. L. *Synth. Commun.* **1999**, *29* (5), 843–854.

(91) Smeets, N. M. B.; Van Der Weide, P. L. J.; Meuldijk, J.; Vekemans, J.; Hulshof, L. A. *Org. Process Res. Dev.* **2005**, *9* (6), 757–763.

(92) Kricheldorf, H. R.; von Lossow, C.; Schwarz, G. *Macromolecules* **2005**, *38* (13), 5513–5518.

(93) Vayaboury, W.; Giani, O.; Cottet, H.; Deratani, A.; Schué, F. *Macromol. Rapid Commun.* **2004**, *25* (13), 1221–1224.

(94) Deming, T. J. *Macromolecules* **1999**, *32* (13), 4500–4502.

(95) Deming, T. J. *J. Am. Chem. Soc.* **1998**, *120* (17), 4240–4241.

(96) Deming, T. J.; Curtin, S. A. *J. Am. Chem. Soc.* **2000**, *122* (24), 5710–5717.

(97) Pickel, D. L.; Politakos, N.; Avgeropoulos, A.; Messman, J. M. *Macromolecules* **2009**, *42* (20), 7781–7788.

(98) Cheng, J.; Deming, T. J. *Top. Curr. Chem.* **2012**, *310*, 1–26.

(99) Butler, G. B. *Ind. Eng. Chem. Prod. Res. Dev.* **1980**, *19* (4), 512–528.

(100) Cookson, R. C.; Gilani, S. S. H.; Stevens, I. D. R. *Tetrahedron Lett.* **1962**, *3* (14), 615–618.

(101) Cookson, R. C.; Gilani, S. S. H.; Stevens, I. D. R. *J. Chem. Soc. C Org.* **1967**, 1905.

(102) De Bruycker, K.; Billiet, S.; Houck, H. A.; Chattopadhyay, S.; Winne, J. M.; Du Prez, F. E. *Chem. Rev.* **2016**, *116* (6), 3919–3974.

(103) Mallakpour, S. E.; Butler, G. B. *J. Polym. Sci. Part A Polym. Chem.* **1987**, *25* (10), 2781–2790.

(104) Mallakpour, S. E.; Asghari, J.; Schollmeyer, D. *Polym. Int.* **1996**, *41* (1), 43–52.

(105) Mallakpour, S. E.; Hajipour, A.-R.; Mahdavian, A.-R.; Khoee, S. *J. Polym. Sci. Part A Polym. Chem.* **1999**, *37* (8), 1211–1219.

(106) Little, T.; Meara, J.; Ruan, F.; Nguyen, M.; Qabar, M. *Synth. Commun.* **2002**, *32* (11), 1741–1749.

(107) Ghorbani-Choghamarani, A.; Chenani, Z.; Mallakpour, S. *Synth. Commun.*

2009, *39* (23), 4264–4270.

(108) Baran, P. S.; Guerrero, C. A.; Corey, E. J. *Org. Lett.* **2003**, *5* (11), 1999–2001.

(109) Ban, H.; Gavrilyuk, J.; Barbas III, C. F. *J. Am. Chem. Soc.* **2010**, *132* (5), 1523–1525.

(110) Adamo, R.; Allen, M.; Berti, F.; Danieli, E.; Hu, Q.-Y. Google Patents 2012.

(111) Billiet, S.; De Bruycker, K.; Driessen, F.; Goossens, H.; Van Speybroeck, V.; Winne, J. M.; Du Prez, F. E. *Nat. Chem.* **2014**, *6* (9), 815–821.

(112) Roling, O.; De Bruycker, K.; Vonhören, B.; Stricker, L.; Körsgen, M.; Arlinghaus, H. F.; Ravoo, B. J.; Du Prez, F. E. *Angew. Chemie Int. Ed.* **2015,** 54**,** 13126-13129 .

(113) Vonhören, B.; Roling, O.; De Bruycker, K.; Calvo, R.; Du Prez, F. E.; Ravoo, B. J. *ACS Macro Lett.* **2015**, *4* (3), 331–334.

(114) Vandewalle, S.; Billiet, S.; Driessen, F.; Du Prez, F. E. *ACS Macro Lett.* **2016**, *5*, 766–771.

(115) Wang, Z.; Yuan, L.; Trenor, N. M.; Vlaminck, L.; Billiet, S.; Sarkar, A.; Du Prez, F. E.; Stefik, M.; Tang, C. *Green Chem.* **2015**, *17* (7), 3806–3818.

(116) Wang, Z.; Zhang, Y.; Yuan, L.; Hayat, J.; Trenor, N. M.; Lamm, M. E.; Vlaminck, L.; Billiet, S.; Du Prez, F. E.; Wang, Z. *ACS Macro Lett.* **2016**, *5* (5), 602–606.

(117) Zolfigol, M. A.; Chehardoli, G.; Shirini, F.; Mallakpour, S. E.; Nasr-Isfahani, H. *Synth. Commun.* **2001**, *31* (13), 1965–1970.

(118) Zolfigol, M. A.; Torabi, M.; Mallakpour, S. E. *Tetrahedron* **2001**, *57* (39),

8381–8384.

(119) Zolfigol, M. A.; Nasr-Isfahani, H.; Mallakpour, S.; Safaiee, M. *Synlett* **2005**, *2005* (5), 761–764.

(120) Zolfigol, M. A.; Borazjani, M. K.; Mallakpour, S. E.; Nasr-isfahani, H. *Synth. Commun.* **2000**, *30* (14), 2573–2585.

(121) Hajipour, A. R.; Mallakpour, S. E.; Adibi, H. *Chem. Lett.* **2001**, No. 2, 164–165.

(122) Zolfigol, M. A.; Ghaemi, E.; Madrakian, E.; Niknam, K. *J. Chinese Chem. Soc.* **2008**, *55* (3), 704–711.

(123) Ban, H.; Nagano, M.; Gavrilyuk, J.; Hakamata, W.; Inokuma, T.; Barbas III, C. F. *Bioconjug. Chem.* **2013**, *24* (4), 520–532.

(124) Bauer, D. M.; Ahmed, I.; Vigovskaya, A.; Fruk, L. *Bioconjug. Chem.* **2013**, *24* (6), 1094–1101.

(125) Jones, M. W.; Mantovani, G.; Blindauer, C. A.; Ryan, S. M.; Wang, X.; Brayden, D. J.; Haddleton, D. M. *J. Am. Chem. Soc.* **2012**, *134* (17), 7406–7413.

(126) Werner, S.; Curran, D. P. *Org. Lett.* **2003**, *5* (18), 3293–3296.

(127) Shimizu, M.; Iwasaki, Y.; Yamada, S. *Yakugaku zasshi J. Pharm. Soc. Japan* **1995**, *115* (8), 584–602.

(128) Murao, N.; Ishigai, M.; Sekiguchi, N.; Takahashi, T.; Aso, Y. *Anal. Biochem.* **2005**, *346* (1), 158–166.

Chapter 2
Enzymatic Crosslinking of Polypeptides

Abstract

Horse-radish peroxidase (HRP) and some other enzymes such as myeloperoxidase can convert tyrosine to tyrosyl radical. Reactive tyrosyl radicals combine with each other to form dityrosine and so to crosslink proteins. We have explored this concept for synthetic copolypeptides where the amount of tyrosine, polypeptide length and architecture can be varied. Firstly, tyrosine NCA and other amino acid NCAs were prepared by Fuchs-Farthing method. Then, these monomers were polymerized by hexylamine initiator to obtain statistical and block polypeptides. SEC results showed narrow distribution of polypeptides. Finally, these polypeptides were used in gelation trials. In total, 17 different polypeptides have been tested approximately 45 different conditions each. Concentration of the polypeptide, amount of HRP enzyme and H_2O_2 were varied systematically. However, none of the conditions resulted in gelation.

2.1 Introduction

Peptides derived from natural sources present two challenges. Firstly, their composition varies depending on the source and secondly, synthetic modification is largely limited to side chain modification of the amino acids. On the other hand, NCA polymerization allows researchers to create polypeptides with different lengths, composition and architectures such as random, block or star polymers. Despite being synthetic, the repeating units of NCA polymerization can be completely made of natural amino acids such as glutamic acid, lysine or tyrosine. Additionally, non-natural functional amino acids can also be copolymerized with natural amino acids to widen the scope of the synthetic pathways for functionalization and crosslinking.[1] Natural peptides can be covalently crosslinked using chemical coupling agents[2,3] photocrosslinking[4–8] or simple physically crosslinked through chain interaction[9–17]. In this chapter, we set out to form hydrogel polypeptides by covalent crosslinking. In order to avoid harsh chemicals, we took inspiration from crosslinking reported on natural peptides using specific enzyme. There are several enzymes catalyzing reactions between a pair of the same or different amino acids to form dimers. These kind of enzymes can be used as crosslinking enzyme.[18–24] For example, transglutaminase catalyzes the reaction between lysine and glutamine forming a crosslinked network of gelatin[25,26], short peptide sequences[23] or PEG-peptide hybrids[27] (Figure 2.1). Horse-radish peroxidase and myeloperoxidase enzymes have been shown to crosslink tyrosine via tyrosyl radical formation (Figure 2.2).[20,21,27–32] We hypothesized that the enzymatic crosslinking reaction can be applied to synthetic polypeptides.

Whereas, tyrosinase enzyme oxidizes tyrosine to benzoquinone and this can be exploited to crosslink with amines.[28] Lehrer and Fasman showed that the major

product of the photooxidation of tyrosine (where tyrosyl radical is createad) is o,o'-diytrosine (Figure 2.2).[33]

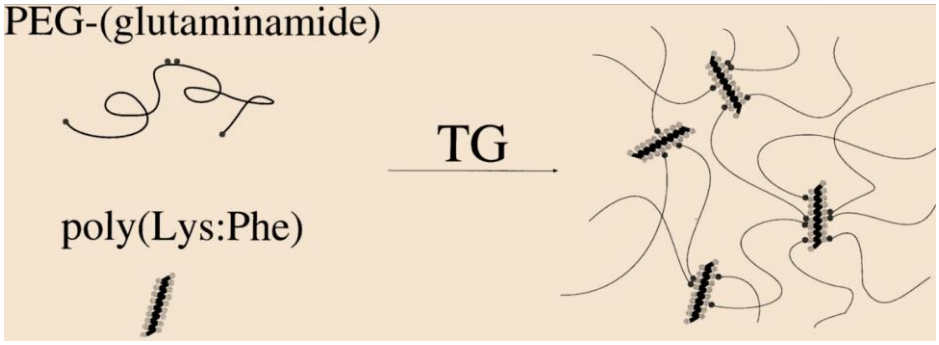

Figure 2.1 Transglutaminase enzyme crosslinked PEG glutamine with lysine containing polypeptide.[27]

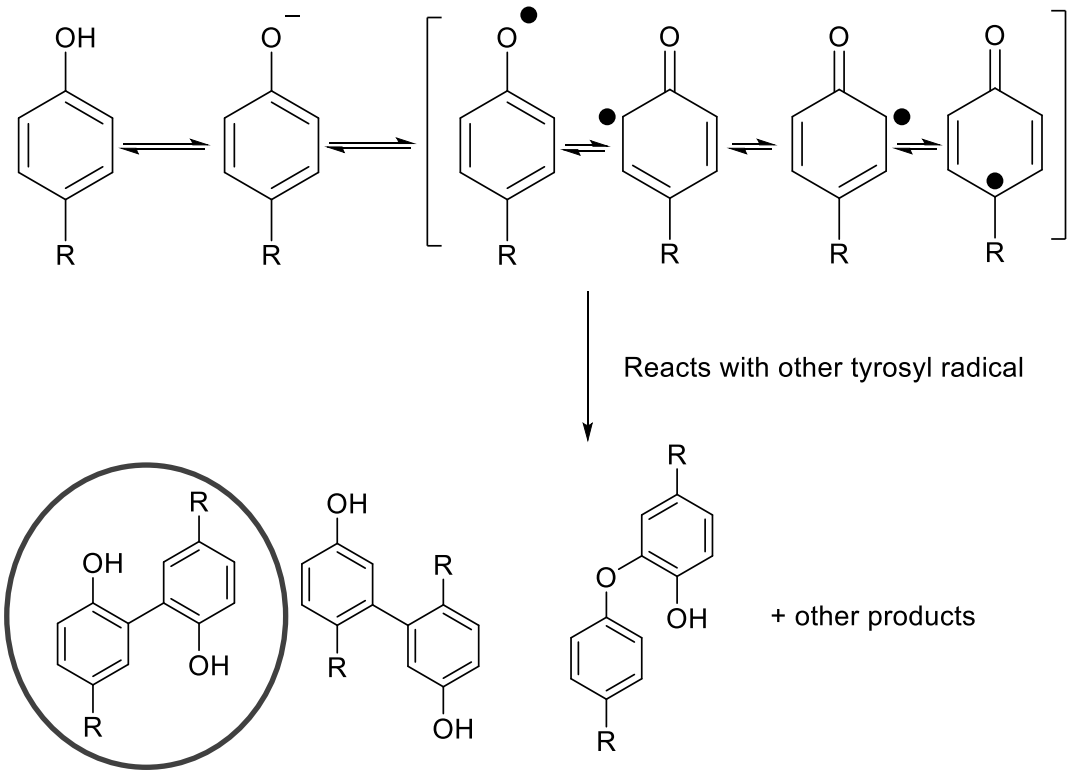

Figure 2.2 Resonance structures of tyrosyl radical. Major product of radical coupling is o-o-dityrosine.[33]

2.2 Results and Discussion

Inspired by the successful reports in the literature, we aimed to crosslink tyrosine containing polypeptides by HRP. For this purpose, we prepared a library of random and block copolypeptides as well as hybrid block copolymers by NCA polymerization (Table 2.1). As monomers benzyl-L-glutamate (BLB), Carbobenzyloxy-L-lysine (ZLL) and O-benzyl-tyrosine NCA (OBT) were synthesized according to literature procedures. The NMR and FTIR spectra were in agreement with the structures as shown in Figure 2.3 and 2.4 for OBT NCA. Ring formation can be seen in ^{1}H-NMR from the proton at 4.4 ppm (Figure 2.3), while carbonyls of the NCA ring can be seen at 1845 cm^{-1} and 1773 cm^{-1} in IR spectrum (Figure 2.5).

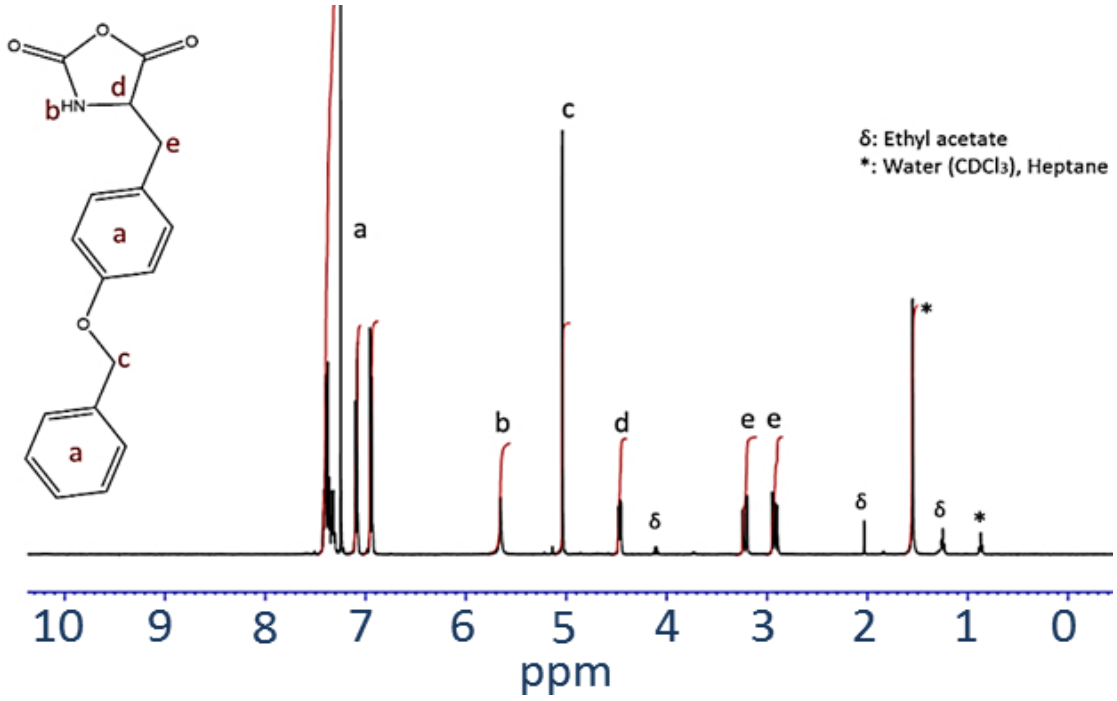

Figure 2.3. NMR spectrum of O-benzyl-tyrosine NCA in chloroform-d.

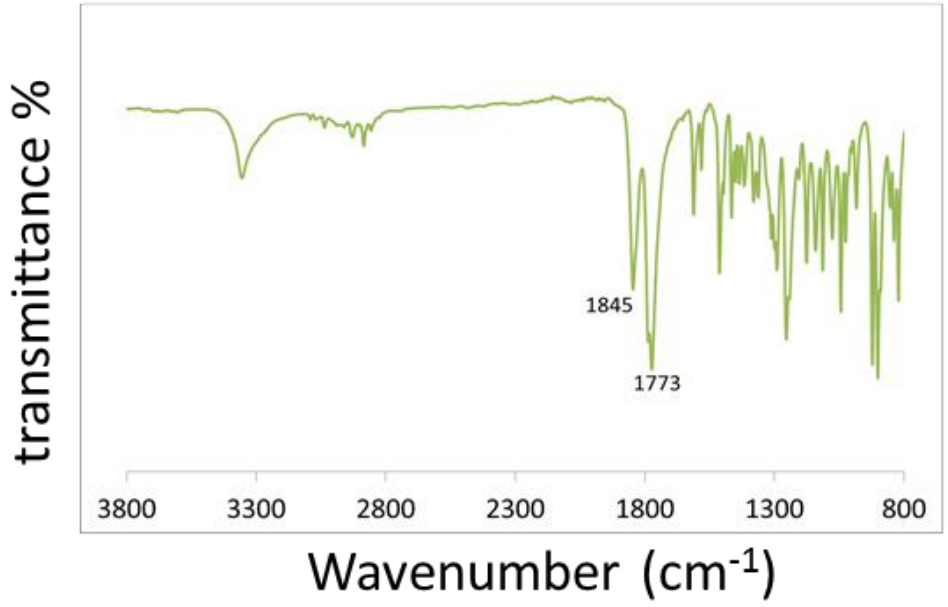

Figure 2.4. IR spectrum of O-benzyl tyrosine NCA (neat). Carbonyl peaks of NCA are at 1845cm^{-1} and 1773cm^{-1}.

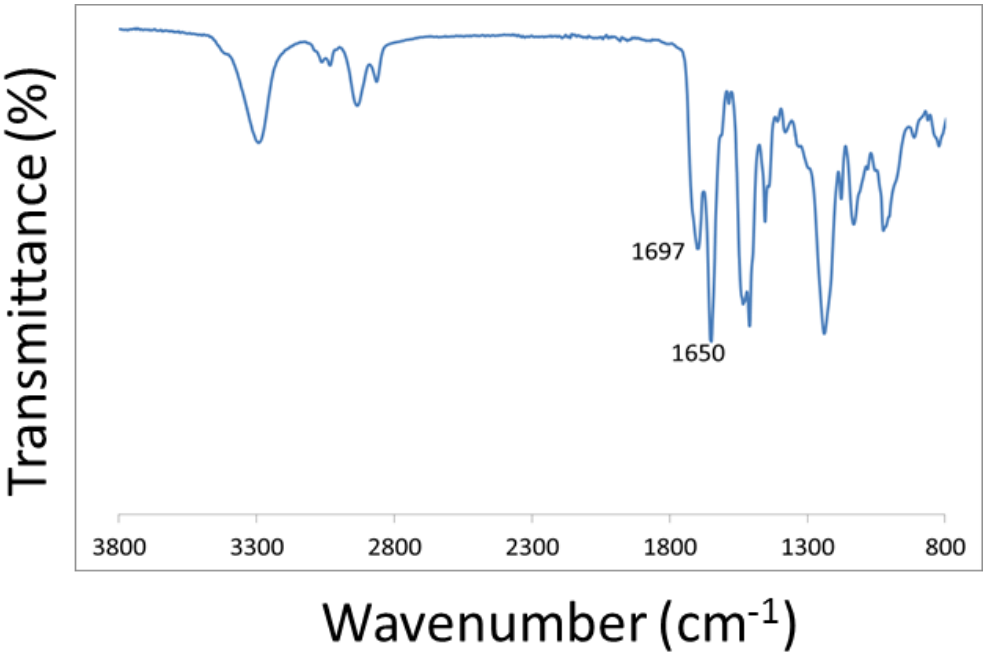

Figure 2.5. IR spectrum of poly(lys-*st*-tyr) (neat).

2.2.1 Tyrosine Containing Polypeptides

Three different groups of polypeptides were prepared. PEG hybrids were prepared by using commercially available PEG mono amines and diamines as initiators. BLB and ZLL containing copolypeptides (statistical and block) were prepared by copolymerization with OBT. Each group of polypeptides was deprotected to obtain main functional groups, phenol of OBT, amine of ZLL and carboxylic acid of BLB. The water insoluble polypeptides become water soluble after deprotection. Removal of protection groups was confirmed by ^{1}H-NMR spectroscopy by examining the aromatic region peaks.

Table 2.1 Summary of synthesized polymers and gelation trials. GPC results for the glutamic acid containing polymers were not added because their data were not reliable.

#	Polymer	Tyr mol ratio	Đ	Mn(NMR)	Gelation
1	$PEG_{2K}Tyr_6$	0.10	1.2	3,5 K	x
2	Tyr_6-block-PEG_{3K}-block-Tyr_6	0.10	1.3	7.5K	x
3	PEG_{5K}-block-co-Gla_{18}-Tyr_6	0.04		9K	x
4	Gla_{12}-block-Tyr_3	0.20		3K	x
5	Gla_{12}-rand-Tyr_5	0.30		3K	x
6	Gla_{16}-rand-Tyr_4	0.25		3.5K	x
7	Gla_{20}-block-Tyr_5	0.20		5K	x
8	Gla_{35}-Tyr_{10}	0.22		10K	x
9	Gla_{40}-rand-Tyr_6	0.13		11K	x
10	Gla_{20} – $Tyramine_5$	0.10		5K	x
11	Lys_{20}-rand-Tyr_5	0.20	1.1	5K	x
12	Lys_{40}-block-Tyr_{10}	0.20	1.05	8K	x
13	Lys_{30}-block-Tyr_{10}	0.25	1.1	8.5K	x
14	Lys_{40}-block-Tyr_{20}	0.33	1.05	10K	x
15	Lys_{40}-rand-Tyr_{10}	0.20	1.11	12K	x
16	Lys_{30}-rand-Tyr_{10}	0.25	1.15	11.5K	x
17	Lys_{40}-rand-Tyr_{20}	0.33	1.05	16K	x

PEG: Polyethylene Glycol **Tyr:** Tyrosine **Gla:** Glutamic acid **Lys:** Lysine

Statistical copolypeptides were synthesized under vacuum at room temperature whereas block copolypeptides were obtained under vacuum at 0^{o}C. For block

polypeptides, the second monomer was added after the consumption of the first monomer which was monitored by IR.

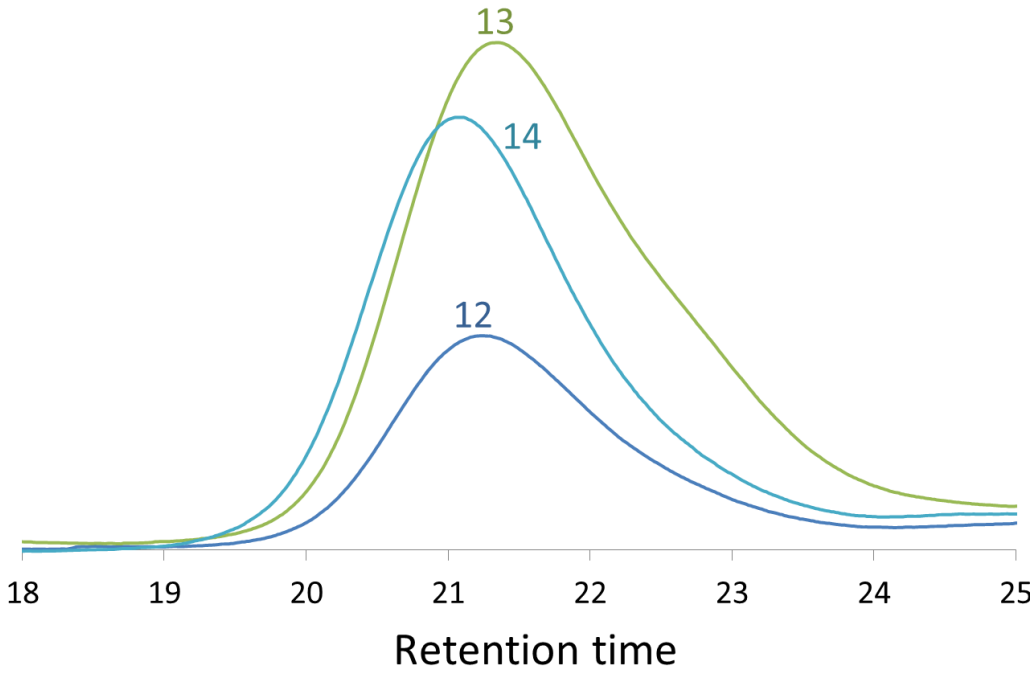

Figure 2.6. GPC chromatogram of lysine containing block copolypeptides (12,13 and 14 from table 1)

2.2.2 Gelation Trials

To test gelation we firstly started with the similar conditions (concentration of polymer, amount of phenol, HRP and H_2O_2 etc.) as reported in literature examples. Then, we varied reaction parameters independently. However, none of the 17 polymers representing many different conditions resulted in gelation. Additionally, no molecular weight change in GPC for the ones soluble in the eluent (#1 and #2) was detected. Unfortunately, we were not able to monitor molecular weight change for all deprotected polypeptides due to their insolubility in SEC solvents (THF & DMF). A couple of fresh batches of HRP enzymes with different types are also tested. The result showed that the tyrosyl radical either does not form or it reacts in different ways not

leading to dityrosine formation. In conclusion, no gelation was observed and no further investigation was done.

Table 2.2. Some conditions to test crosslinking Tyr_6-PEG3K-Tyr_6.

Concentration of Tyr_6-PEG3K-Tyr_6	Amount of HRP/H_2O_2	Result
20mg/mL PBS	10µL/27µL	No gelation
40mg/mL PBS	10µL/27µL	No gelation
80mg/mL PBS	10µL/27µL	No gelation
20mg/mL PBS	20µL/27µL	No gelation
20mg/mL PBS	20µL/54µL	No gelation
20mg/mL PBS	10µL/54µL	No gelation

2.3 Experimental

Materials: Chemicals and reagents: All reagents were purchased from Sigma-Aldrich unless otherwise noted. Protected amino acids were purchased from BACHEM. Triphosgene was purchased from Fluorochem and freshly used. Snake skin dialysis tubing (3.5K MWCO) was obtained from VWR. Silica nitric acid was prepared as described in literature.1 Tris buffer solution was prepared using Trizma® base. Ethyl acetate over moleculer sieves were purchased from Across-Organics .

Methods: ^{1}H and ^{13}C NMR spectra were recorded at room temperature with a Bruker Avance 400 (400 MHz). ATR-FTIR spectra were collected on a Perkin Elmer Spectrum 100 in the spectral region of 650-4000 cm-1, and were obtained from 16 scans with a resolution of 2 cm-1. Background measurements were taken before each analysis.SEC analyses of the protected polypeptides were done using Agilent GPC running on DMF with dn/dc value set to 1.599.

NCA setup: An ideal NCA reaction setup is shown in Figure 2.7. Since NCA is moisture sensitive, all the system should be kept under constant flow of Nitrogen. One end of the system is open to prevent excess pressure and possible explosion due to this

pressure. Additonally, open end of the system is connected to NaOH trap to neutralize HCl (product of the reaction) and possible phosgene gas which is extremely toxic.

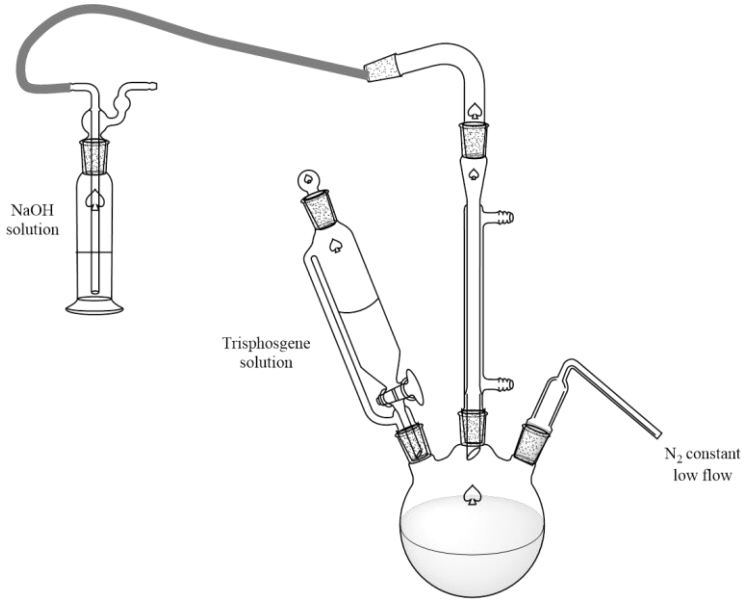

Figure 2.7. Main setup of the NCA polymerization.

Synthesis of O-benzyl-L-tyrosine NCA: 10.0 g (36.9 mmol) of O-benzyl-L-tyrosine placed into oven dried three-neck round-bottomed flask. Then, 80 ml of anhydrous ethyl acetate and 15g (17.5mL, 110mmol) α-pinene added while keeping flask flushed with low flow of N_2. The suspension heated to reflux temperature with keeping N_2 flow continues for whole reaction. 5.5g (18.4 mmol) of triphosgene dissolved in 40mL anhydrous ethyl acetate and added to the suspension dropwise using dropping funnel. Two-thirds of the triphosgene solution was added within approximately 1 hour. Then, addition of triphosgene was stopped for another hour. The remaining triphosgene solution was added dropwise and suspension became clear solution after 2-3 hours. Then, solution was concentrated to approximately half volume by using rotavap. Concentrated solution was precipitated into 150 mL anhydrous heptane. The mixture was kept overnight at -20 for complete crystallization. Then, mixture was brought to room temperature and the solid were collected by vacuum filtration. Solid was

recrystallized four times with 1:2 ethyl acetate:heptane. The final product was white needle shape crystals. Isolated yield: 7.54g , 69%

Synthesis of Lys(Z) NCA: 7g of Lys(Z)-OH were put into oven dried 250mL three neck round bottom flask under constant slow flow of nitrogen. Then 120mL anhydrous ethylacetate added together with 7.5g (8.7mL) a-pinene. The rest of the procedure was same with tyrosine NCA until crsytallization step. Unlike tyrosine NCA, Lysine NCA tends to form wet cake during reaction but it turns into mixable suspension after 1-2 hours and a clear solution after 3-5 hours. The crude was recrystallized two times with 1:1 Ethyl acetate/Heptane mixture. The final product was white fine powder. Isolated yield: 6.3g, 82%

Synthesis of y-Benzyl-l-glutamate NCA: 10g (42.1 mmol) y-benzyl-l-glutamate were put into oven dried 250Ml round bottom flask under constant slow flow of nitrogen. Then 80mL anhydrous ethylacetate added together with 10.4g (12.1mL) a-pinene. The rest of the procedure was same with lysine NCA except that the amount of triphosgene was 6.2g. The crude was recrystallized two times with 1:1 Ethyl acetate/Heptane mixture. The final product was a fluffy white fine solid. Isolated yield: 7.8g, 70,2%

Polymerizations: Hexylamine is used to initiate all polymerizations in this chapter. The repeating units were set by using mol numbers. For synthesizing 20 repeating units (theoretical) polypeptide from, 1g BLG NCA (3.8mmol-20 eq) the amount of hexylamine was set to 0.19 mmol -1eq. Since the amount of initiator is too small to handle, a 50-fold less concentrated stock solution of initiator was used. An exact procedure for poly(BLB_{40}-st-OBT_6) or the entry 9 in table 2.1 is given below.

Synthesis of poly(ZLL_{40}-st-OBT_{10}): 1040 Mg of ZLL-NCA (3.40 mmol) and 252 mg of OBT-NCA (0.85 mmol) were dissolved in 20mL anhydrous DMF under inert atmosphere. The solution was purged with N_2 for 10 minutes. Then, hexylamine (9mg,

0.085 mmol) from stock solution was added fast and moderate vacuum applied. After, 5-6 hours the solution was precipitated into diethyl ether and collected by vacuum filtration. Finally, the product was washed and dried under vacuum. Yield: 972 mg, 88% , NMR shown in figure 2.8.

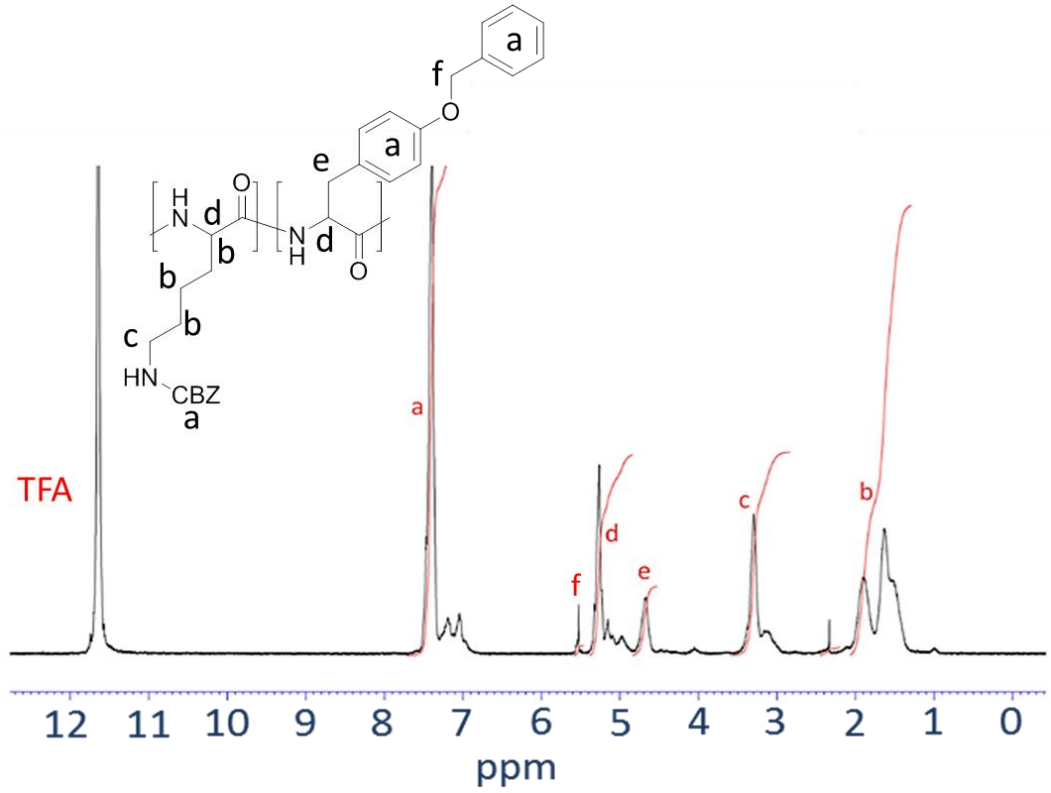

Figure 2.8. ^{1}H-NMR spectrum of poly(ZLL$_{40}$-st-OBT$_{10}$) in TFA-d.

Synthesis of statistical copolymers: The monomers were placed into a oven dried schlenk tube. 7 mL of anhydrous DMF was added for each 1g of monomer (e.g. 21mL DMF for 3 g of monomer mixture). The solution was purged with N_2 for 10 minutes. The initiator was added one time and fast while stirring fast at room temperature. Line vacuum was applied until the end of reaction. The monomer consumption progress was monitored by IR (NCA carbonyls (near 1850cm^{-1} and 1760cm^{-1}) should disappear completely. Generally, the majority of the monomers were consumed in 3-4 hours at room temperature. Then the solution was precipitated into diethyl ether. Product was collected by filtration. DMF was not completely removed even washing with excess

diethyl ether for lysine containing polypeptides. Therefore, these polypeptides were dissolved in chloroform and precipitated in diethyl ether. The process repeated until no more DMF peak was seen in NMR. The solids were collected by filtration and dried in vacuum oven. The yield of the polymerization was generally over 95%.

Synthesis of block copolymers: The first monomer was placed into schelenk tube and anhydrous DMF was added (7mL for 1g of monomer). The solution was purged with N_2 for 10 minutes while cooling solution to 0^oC. The initiator was added one time and fast while stirring solution at 0^oC. The consumption of the first monomer was followed by IR. Generally, it took 2 days for NCA peaks to disappear on IR indicating majority of the monomers were consumed. Then, second monomer was dissolved in anhydrous DMF and added to the polypeptide solution. The consumption of the second monomer was also followed by IR. The resulting solution was precipitated into diethyl ether. The rest of the work up was same with statistical copolymers. The yield of the polymerization was generally over 95%.

Synthesis of PEG polypeptide hybrids: The first monomer was placed into schelenk tube and anhydrous DMF was added (7mL for 1g of monomer). The solution was purged with N_2 for 10 minutes. PEG-amine or PEG-diamine were dissolved in separate flask in DMF (1mL for 0.1g of PEG) and purged with N_2 for 10 minutes. Then PEG solution was added into the monomer solution in one time and fast while stirring the monomer solution. The monomer consumption followed by IR and polypeptide solution was precipitated into diethyl ether. The resulting solid was washed with excess diethyl ether and dried under vacuum oven. The solids were collected by filtration and dried in vacuum oven. The isolated yields of the polymerization were generally over 87%.

Deprotection of the polypeptides: In general, 500mg (approximately 1 equivalent of monomer) of polypeptide dissolved in approximately 5 mL of trifluoroacetic acid. To this solution approximately 1.5 mL HBr (3-4 equivalent) in acetic acid is added slowly. After 4-16h the solution precipitated in diethyl ether and the solid was washed with excess diethyl ether. The resulting solid was dried and dissolved in deionized water. Finally, the solution is placed into 3.5MWCO snake skin dialysis bag and dialyzed for 3-4 days by refreshing dialysis water 4 times a day. An exact procedure is given below;

Synthesis of poly(Lysine$_{40}$-st-Tyrosine$_{10}$): 600mg of poly(ZLL$_{40}$-st-OBT$_{10}$) was dissolved in 12 mL trifluoroacetic acid. 3mL of HBr (33% in acetic acid) was added dropwise and solution stirred. After 4 hours, the mixture was precipitated into diethyl ether. Then, product was washed and collected by vacuum filtration. The dried polypeptide was dissolved in deionized water and placed into 3.5 MWCO snake skin dialysis bag and dialyzed for 3-4 days by refreshing water 4 times a day. Finally, white fluffy product was obtained after freeze-drying. Yield: 445mg.

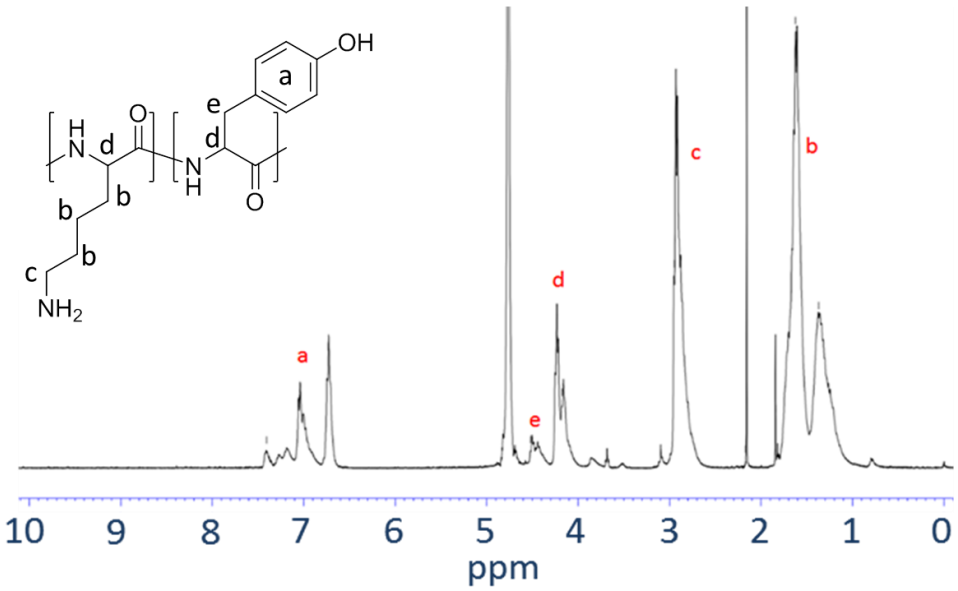

Figure 2.9 ^{1}H-NMR spectrum of poly(Lysine$_{40}$-st-Tyrosine$_{10}$) in D_2O.

Gelation trials: Approximately 45-50 conditions were tested for each polypeptide. Basically, the concentration of the polymer, amount of HRP, H_2O_2 and temperature were varied. Some conditions were shown in table 2-2 to give some insight about the orders of the magnitude.

2.4. References

(1) Quadir, M. A.; Martin, M.; Hammond, P. T. *Chemistry of Materials*. 2014, pp 461–476.

(2) Fan, Z.; Zhang, Y.; Ji, J.; Li, X. *RSC Adv.* **2015**, *5* (22), 16740–16747.

(3) Engler, A. C.; Lee, H.; Hammond, P. T. *Angew. Chemie Int. Ed.* **2009**, *48* (49), 9334–9338.

(4) Mann, B. K.; Gobin, A. S.; Tsai, A. T.; Schmedlen, R. H.; West, J. L. *Biomaterials* **2001**, *22* (22), 3045–3051.

(5) Chen, Y.; Lin, R.; Qi, H.; Yang, Y.; Bae, H.; Melero-Martin, J. M.; Khademhosseini, A. *Adv. Funct. Mater.* **2012**, *22* (10), 2027–2039.

(6) Krannig, K.-S.; Huang, J.; Heise, A.; Schlaad, H. *Polym. Chem.* **2013**, *4* (14), 3981–3986.

(7) Sun, J.; Schlaad, H. *Macromolecules* **2010**, *43* (10), 4445–4448.

(8) Nichol, J. W.; Koshy, S. T.; Bae, H.; Hwang, C. M.; Yamanlar, S.; Khademhosseini, A. *Biomaterials* **2010**, *31* (21), 5536–5544.

(9) Schneider, J. P.; Pochan, D. J.; Ozbas, B.; Rajagopal, K.; Pakstis, L.; Kretsinger, J. *J. Am. Chem. Soc.* **2002**, *124* (50), 15030–15037.

(10) Pochan, D. J.; Pakstis, L.; Ozbas, B.; Nowak, A. P.; Deming, T. J.

Macromolecules **2002**, *35* (14), 5358–5360.

(11) Breedveld, V.; Nowak, A. P.; Sato, J.; Deming, T. J.; Pine, D. J. *Macromolecules* **2004**, *37* (10), 3943–3953.

(12) Nowak, A. P.; Breedveld, V.; Pine, D. J.; Deming, T. J. *J. Am. Chem. Soc.* **2003**, *125* (50), 15666–15670.

(13) Chen, Y.; Pang, X.; Dong, C. *Adv. Funct. Mater.* **2010**, *20* (4), 579–586.

(14) Deming, T. J. *Soft Matter* **2005**, *1* (1), 28–35.

(15) Markland, P.; Zhang, Y.; Amidon, G. L.; Yang, V. C. *J. Biomed. Mater. Res.* **1999**, *47* (4), 595–602.

(16) Zhang, Z.; Chen, L.; Deng, M.; Bai, Y.; Chen, X.; Jing, X. *J. Polym. Sci. Part A Polym. Chem.* **2011**, *49* (13), 2941–2951.

(17) Pakstis, L. M.; Ozbas, B.; Hales, K. D.; Nowak, A. P.; Deming, T. J.; Pochan, D. *Biomacromolecules* **2004**, *5* (2), 312–318.

(18) Jin, R.; Moreira Teixeira, L. S.; Dijkstra, P. J.; Karperien, M.; van Blitterswijk, C. A.; Zhong, Z. Y.; Feijen, J. *Biomaterials* **2009**, *30* (13), 2544–2551.

(19) Jin, R.; Lin, C.; Cao, A. *Polym. Chem.* **2014**, *5* (2), 391–398.

(20) Wu, C.; Strehmel, C.; Achazi, K.; Chiappisi, L.; Dernedde, J.; Lensen, M. C.; Gradzielski, M.; Ansorge-Schumacher, M. B.; Haag, R. *Biomacromolecules* **2014**, *15* (11), 3881–3890.

(21) Lee, F.; Chung, J. E.; Xu, K.; Kurisawa, M. *ACS Macro Lett.* **2015**, *4* (9), 957–960.

(22) Lee, F.; Chung, J. E.; Kurisawa, M. *Soft Matter* **2008**, *4* (4), 880–887.

(23) Hu, B.-H.; Messersmith, P. B. *J. Am. Chem. Soc.* **2003**, *125* (47), 14298–14299.

(24) Hu, B.; Messersmith, P. B. *Orthod. Craniofac. Res.* **2005**, *8* (3), 145–149.

(25) McDermott, M. K.; Chen, T.; Williams, C. M.; Markley, K. M.; Payne, G. F. *Biomacromolecules* **2004**, *5* (4), 1270–1279.

(26) Yung, C. W.; Wu, L. Q.; Tullman, J. A.; Payne, G. F.; Bentley, W. E.; Barbari, T. A. *J. Biomed. Mater. Res. Part A* **2007**, *83* (4), 1039–1046.

(27) Sperinde, J. J.; Griffith, L. G. *Macromolecules* **1997**, *30* (18), 5255–5264.

(28) Teixeira, L. S. M.; Feijen, J.; van Blitterswijk, C. A.; Dijkstra, P. J.; Karperien, M. *Biomaterials* **2012**, *33* (5), 1281–1290.

(29) Jin, R.; Lin, C.; Cao, A. *Polym. Chem.* **2014**, *5* (2), 391–398.

(30) Ren, K.; He, C.; Cheng, Y.; Li, G.; Chen, X. *Polym. Chem.* **2014**, *5* (17), 5069–5076.

(31) Zhang, Y.; Fan, Z.; Xu, C.; Fang, S.; Liu, X.; Li, X. *Eur. Polym. J.* **2015**, *72*, 717–725.

(32) Oudgenoeg, G.; Hilhorst, R.; Piersma, S. R.; Boeriu, C. G.; Gruppen, H.; Hessing, M.; Voragen, A. G. J.; Laane, C. *J. Agric. Food Chem.* **2001**, *49* (5), 2503–2510.

(33) Lehrer, S. S.; Fasman, G. D. *Biochemistry* **1967**, *6* (3), 757–767.

(34) Sealy, R. C.; Harman, L.; West, P. R.; Mason, R. P. *J. Am. Chem. Soc.* **1985**, *107* (12), 3401–3406.

(35) Joschek, H.-I.; Miller, S. I. *J. Am. Chem. Soc.* **1966**, *88* (14), 3273–3281.

(36) Wang, L. S.; Chung, J. E.; Pui-Yik Chan, P.; Kurisawa, M. *Biomaterials* **2010**, *31* (6), 1148–1157.

(37) Tran, N. Q.; Joung, Y. K.; Lih, E.; Park, K. M.; Park, K. D. *Biomacromolecules* **2010**, *11* (3), 617–625.

(38) Menzies, D. J.; Cameron, A.; Munro, T.; Wolvetang, E.; Grøndahl, L.; Cooper-White, J. J. *Biomacromolecules* **2013**, *14* (2), 413–423.

(39) Wu, C.; Böttcher, C.; Haag, R. *Soft Matter* **2015**, *11* (5), 972–980.

Chapter 3
TAD-Tyrosine Functionalization

Abstract

Highly efficient functionalization and cross-linking of polypeptides was achieved via tyrosine-triazolinedione (TAD) conjugation chemistry. The feasibility of the reaction is demonstrated by the reaction of 4-phenyl-1,2,4-triazoline-3,5-dione (PTAD) with tyrosine containing block copolymer PEG-Tyr as well as a random copolymer of tyrosine and lysine (poly(Lys_{40}-*st*-Tyr_{10})) prepared form N-carboxyanhydride (NCA) polymerisation. Selective reaction of PTAD with the tyrosine units was obtained verified by Size-Exclusion Chromatography (SEC) and NMR spectroscopy. Moreover, two monofunctional and two difunctional TAD molecules were synthesized. It was found that their stability in the aqueous reaction media significantly varied. Under optimized reaction conditions selective functionalization and cross-linking, yielding polypeptide hydrogels, could be achieved. TAD-mediated conjugation could offer an interesting addition in the toolbox of selective (click-like) polypeptide conjugation methodologies for NCA polymerization as it does not require functional non-natural amino acids.

3.1 Introduction

Synthetic polypeptides derived from the polymerisation of amino acid N-carboxyanhydrides (NCA) are highly promising biomimetic materials for biomedical applications.[1, 2] Advanced polymerisation techniques in tandem with recently developed orthogonal functionalization approaches have enabled a large structural and functional diversity with the potential to design bespoke polypeptide biomaterials.[3, 4] Lately, researchers focused on the facile orthogonal functionalization of synthetic polypeptides by 'click' chemistry, for example azide-alkyne[5-8] , thiol-ene[9] (click-like) and thiol-yne[10, 11] reactions. While these techniques are highly efficient, selective and readily applicable for synthetic polypeptides, all of them require special non-natural amino acid monomers. Numerous strategies have also been devised for the functionalization of natural amino acids in polypeptides, for example of lysine, glutamic acid and cysteine.[12, 13] However, these reactions lack the selectivity and efficiency of 'click' chemistry.

We are interested in developing routes for the selective functionalization and cross-linking of synthetic polypeptides by 'click'-like chemistry on natural amino acids and identified tyrosine as a potential candidate. There have been several reports on the selective modification of tyrosine, such as Mannich-type reactions, conjugation via diazonium salts or cyclic imines, among others.[14-17] Haddleton and co-workers reported the first time of PEGylation of tyrosine by using diazonium salt-terminated PEGs (Figure 3.1). Unfortunately, all these techniques have certain limitations: Mannich-type reactions are relatively slow, diazonium salts have poor selectivity (unless carried out at a defined and narrow pH range) and cyclic imines have low yields.

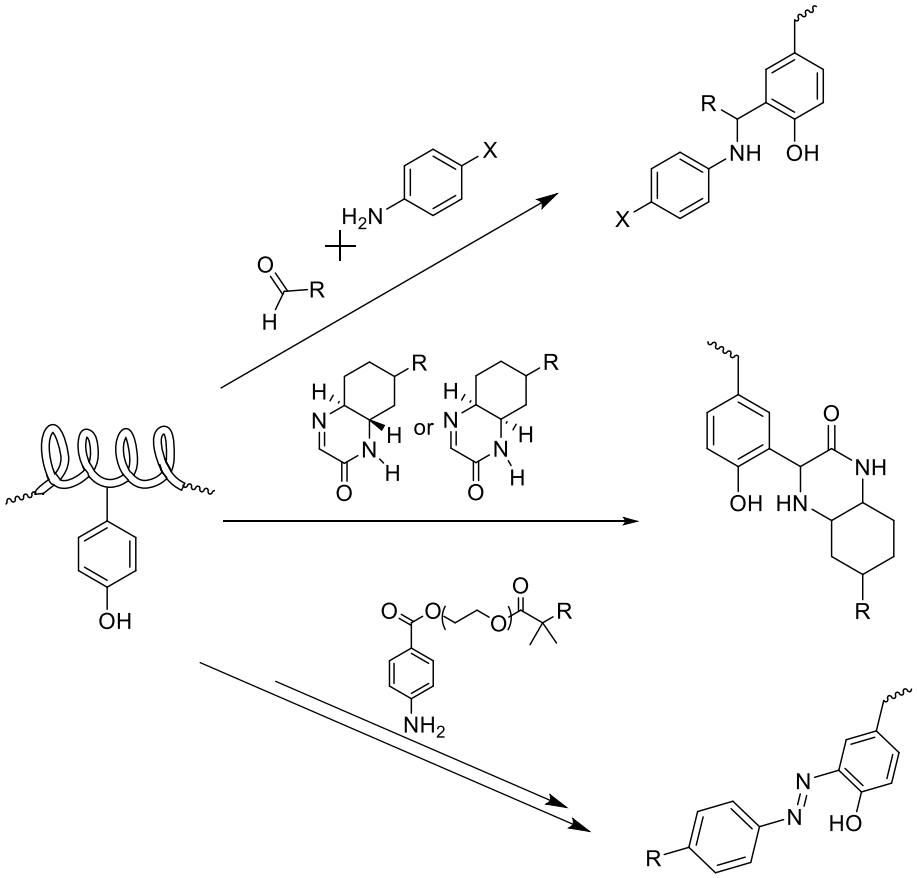

Figure 3.1. Tyrosine functionalization by Mannich-type reaction, cyclic imines and diazonium salt coupling, (top to bottom)[14-17].

Recently Ban *et. al.* reported a click-like reaction for tyrosine, which uses a class of cyclic azodicarbonyl compounds such as 4-phenyl-1,2,4-triazoline-3,5-dione (PTAD).[18, 19] The authors demonstrated that conjugation is fast, selective and efficient on short amino acid sequences as well as larger natural proteins, and can be combined with other conjugation techniques (Figure 3.2).

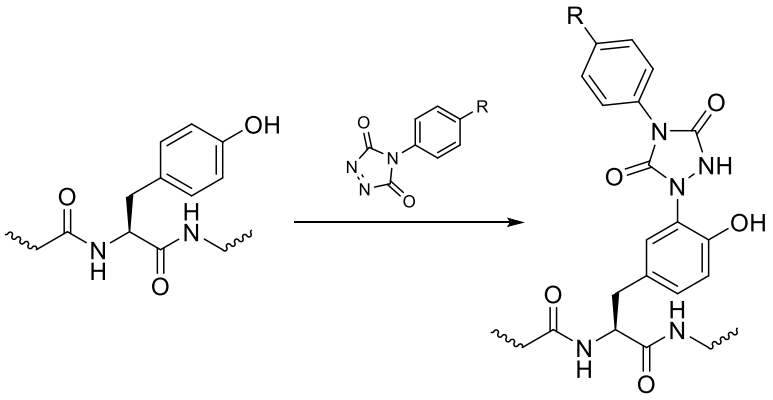

Figure 3.2. Click-like tyrosine conjugation by TAD.

The latter was effectively utilized by Hu to prepare well-defined glycoconjugated vaccine for treatment of candidiasis.[20, 21] The synthetic strategy involved the alkynylation of tyrosine units of the nontoxic mutant diphtheria toxin CRM197, a protein carrier in many licensed vaccines, via protein 1,2,4-triazoline-3,5-dione (TAD) chemistry followed by the attachment of glucan chain onto it via azide-alkyne click chemistry. They also showed that use of tris buffer can scavenge isocyanate decomposition product of TAD[22] which lowers the selectivity. TAD functionalization was also recently used to radiolabel tyrosine of natural proteins using [18F]4-(4-fluorophenyl)-1,2,4-triazole-3,5-dione.[23] In another example, Bauer et. al. prepared bifunctional TAD linkers and showed protein-DNA conjugation (Figure 3.3).[24]

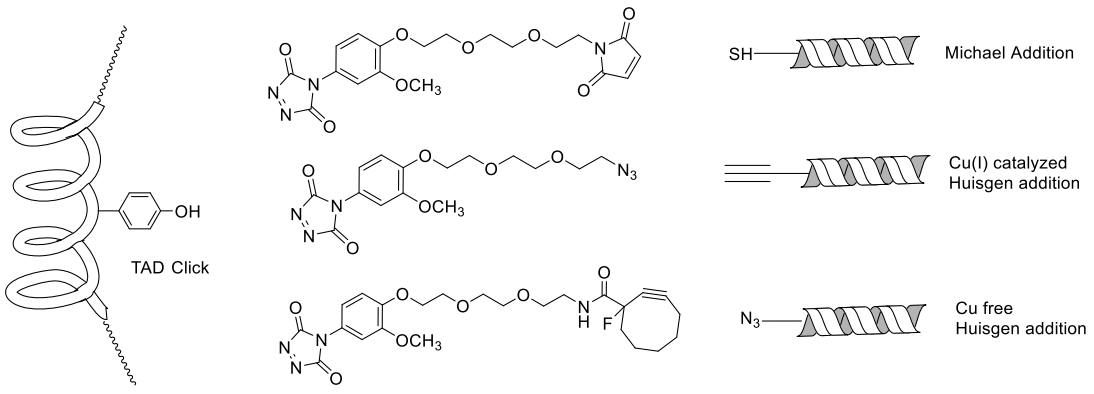

Figure 3.3. Preparation of protein DNA conjugates by bifunctional TAD linkers.[24]

TAD chemistry was also recently exploited in fully synthetic polyacrylates by Du Prez *et. al.* to enable ultrafast reversible click reaction with indole groups to create dynamic polymer networks.[25, 26] Very recently, Nakamura and coworkers have published a method for tyrosine-specific modification. They modified bovine serum albumin using in situ activated luminol derivative under under oxidative conditions (Figure 3.4).[27]

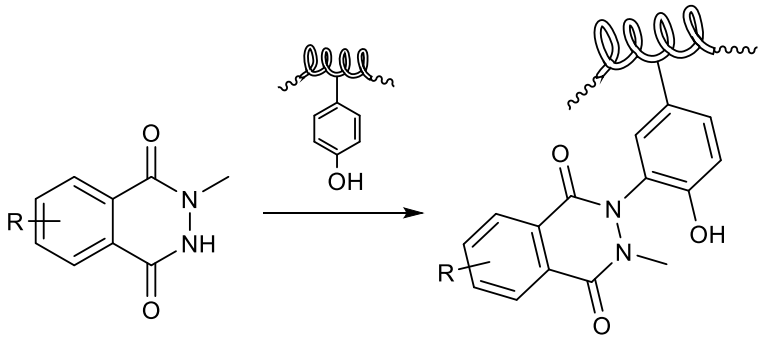

Figure 3.4. Tyrosine functionalization by Luminol derivatives.

3.2 Results and Discussion

Inspired by these reports we have explored the TAD-tyrosine reaction for the conjugation and cross-linking of synthetic polypeptides. A specific focus was on the demonstration of the selectivity in the presence of an excess lysine in the polypeptide. Lysine is a facile monomer to introduce hydrophilicity and cationic charges for the preparation of hydrogels and complexation of pharmacologically active nucleic acids (e.g. RNA).[28-30]

3.2.1 Testing TAD-Tyrosine reaction

In order to demonstrate the versatility of the reaction, PTAD conjugation was first carried out on a poly(ethylene glycol) (PEG)-Tyr block copolymer. This model system was selected as the PEG chain improves the polypeptide solubility in organic solvents permitting convenient reaction analysis. Amine functional PEG (5000 g/mol) was used to initiate the polymerisation of benzyl-L-Tyr NCA targeting an average of 3-4 tyrosine units.[31] A clear increase in molecular weight was apparent in Size Exclusion Chromatography (SEC) analysis upon macroinitiation (Figure 3.5). Quantitative deprotection of the benzyl ether groups in TFA/HBr/acetic acid yielded the PEG-Tyr_4 block copolymer confirmed by ^1H NMR spectroscopy. Initially, conjugation with commercially available PTAD was tested in acetonitrile/Tris buffer 1:1 mixture (Figure 3.5). The reaction was monitored by the change of PTAD's distinct red colour. Firstly, the colour turned into maroon, followed by brown, orange and finally pale yellow during the reaction. PTAD conjugation to the block copolymer took around 1.5 hours with a functionalization yield of about 83%. The increase in molecular weight after PTAD conjugation is clearly evident in the SEC traces (Figure 3.5).

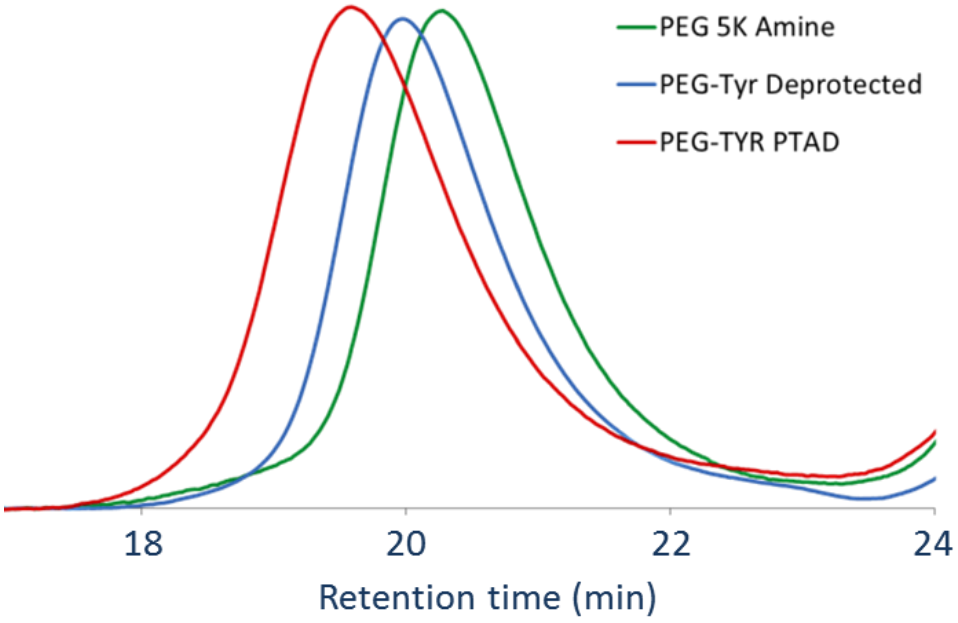

Figure 3.5. SEC chromatograms of PEG-amine (5000 g/mol), PEG-Tyr5 block copolymer before and after PTAD functionalization.

3.2.2 Selectivity of the TAD-Tyrosine reaction

To further test the selectivity of tyrosine ligation, a statistical copolymer of ZLL-lysine and benzyl-L-tyrosine (4:1) was prepared using hexylamine as initiator (Scheme 1). SEC of the copolymer resulted in a M_w of 11,500 g/mol (dispersity index, Đ=1.1). Subsequent quantitative deprotection of the polypeptide, monitored by ^{1}H NMR spectroscopy (Figure 3.6), in TFA/HBr/acetic acid yielded poly(Lys_{40}-*st*-Tyr_{10}). Conjugation with PTAD was carried out in acetonitrile/Tris buffer 1:1 mixture and the distinct colour change was observed during the reaction. PTAD functionalization of poly(lys_{40}-*st*-tyr_{10}) took approximately 7-8 minutes for 25 mg/mL polymer concentration and a feed ratio Tyr/PTAD of 1.2. From ^{1}H NMR spectra it was calculated that at least 85% of the tyrosine units in the copolymer were functionalized with PTAD (Figure 3.6). No evidence of PTAD reacting with lysine was seen in ^{1}H-NMR spectrum.

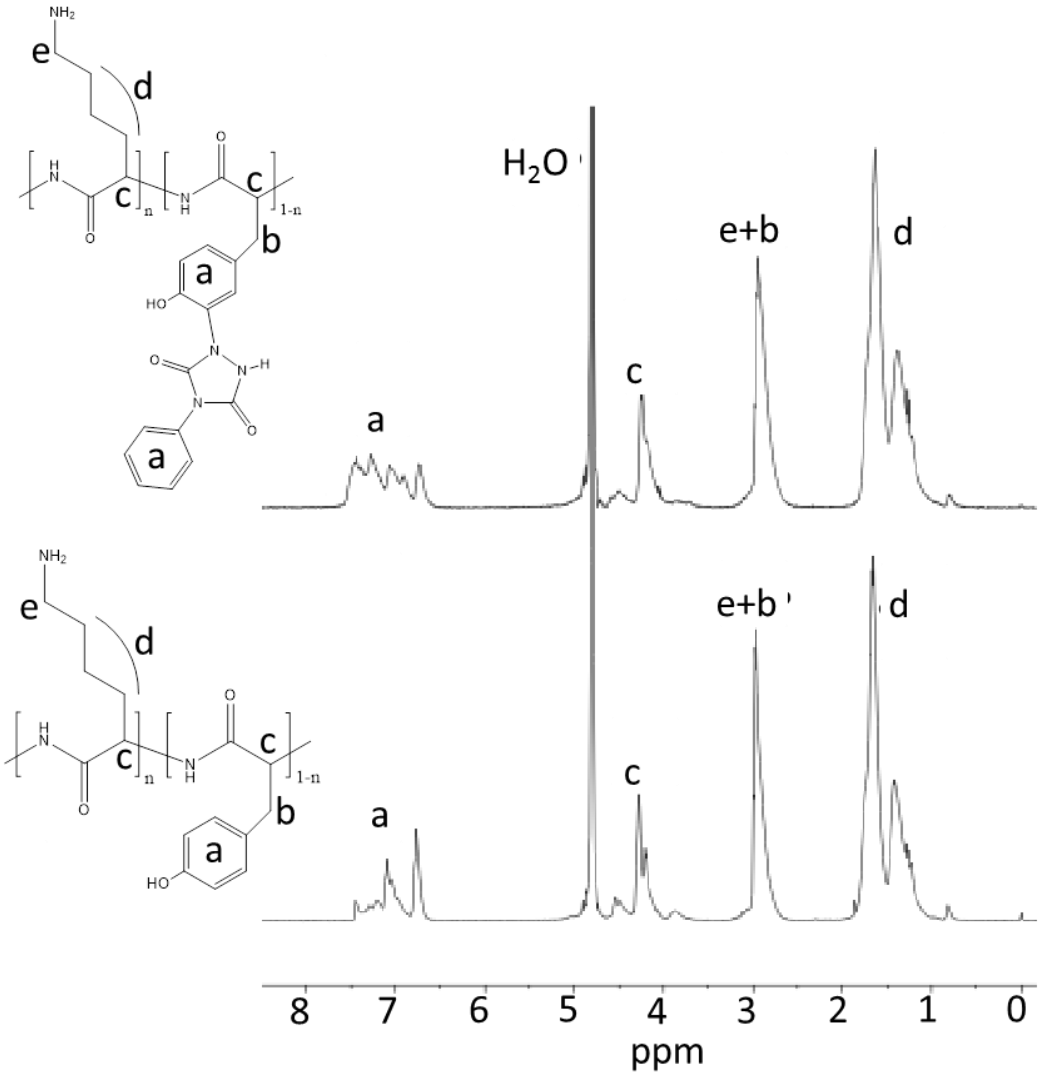

Figure 3.6. ^{1}H-NMR spectrum of poly(Lys_{40}-st-Tyr_{10}) (at bottom) and after PTAD conjugation (top) in D_2O.

The results obtained with the model compound PTAD highlight the ability to selectively functionalise tyrosine units by TAD chemistry in the presence of an excess of lysine. While the reaction was not quantitative under the tested conditions, it should allow the formation of cross-linked polypeptides and hydrogels.

3.2.3 Functionalization of Tyrosine with other TADs

A series of four mono and difunctional TAD molecules (figure 3.7) were investigated in the cross-linking of poly(lys_{40}-*st*-tyr_{10}). The precursors of difunctional TAD compounds were prepared from the corresponding diisocyanates as described in

literature. Firstly, hydrazine carboxylates of each compound were prepared by reaction of corresponding isocyanate with ethyl carbazate. Then, urazole ring formation was achieved under basic aqueous conditions or ethanol/K_2CO_3. For the final oxidation step from urazole to TAD two different methods were employed. Firstly, commercially available 1,3-dibromo-5,5-dimethylhydantoin (DBMH) was used in acetonitrile. During the process the insoluble urazole compounds became soluble and gave characteristic red colour. However, the product contained two side products, i.e. HBr and dimethyl hyndantoin. We observed that the presence of HBr in the subsequent conjugation step had a negative effect on the reaction yield. Reduced yields at low pH was also reported by Ban.[18] Additionally, the presence of acid may cause polypeptide hydrolysis. Neutralizing the HBr in a basic workup resulted in immediate decomposition of the product. Alternatively, urazole compounds were oxidized to the corresponding TADs by using silica supported nitric acid, which gave cleaner products in good yields. By this method all TAD derivatives 1-4 were successfully obtained as confirmed by ^{1}H NMR spectroscopy yet their stability significantly varied.

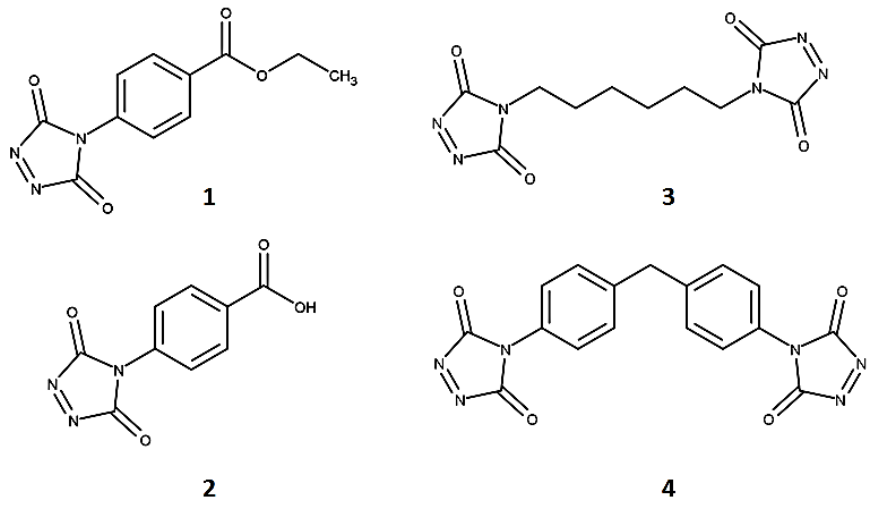

Figure 3.7. TAD derivatives for functionalization and crosslinking.

MDP-TAD (**2**) was obtained as a red powder but turn into brown within 1-2 hours indicating that oxidation method was not compatible with the compound. Crosslinking trials with **2** failed and resulted in a brown precipitate in acetonitrile/tris (1:1) conditions. HM-bisTAD (**3**), benzoate and benzoic acid TAD derivatives were stable as powders. However, 4-ethyl benzoate TAD (**1**) and TAD benzoic acid (**4**) immediately decomposed in 1:1 acetonitrile/Tris buffer conditions. Lowering the aqueous ratio of the mixture retarded the decomposition and conjugation yields of 30% with benzoate TAD and up to 81% with TAD-Benzoic acid in DMF/tris buffer (9:1) was achieved. These results underline that the success of TAD-Tyr functionalization depends on the stability of TAD in the aqueous mixture.

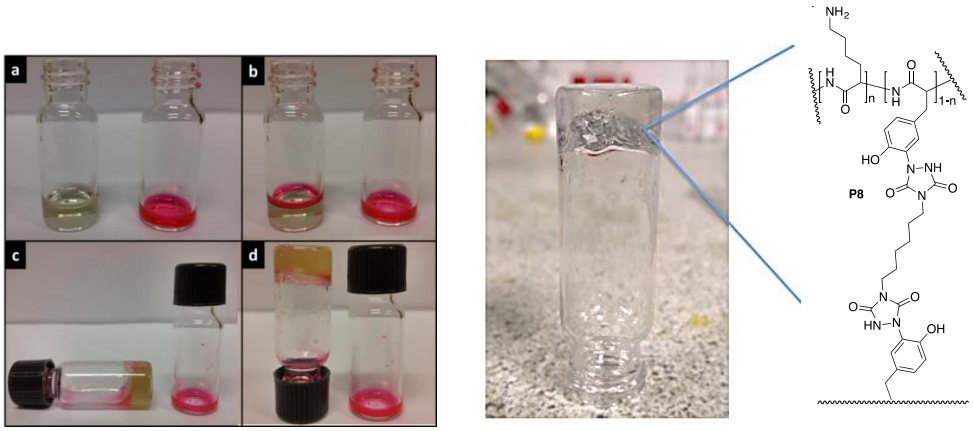

Figure 3.8. Poly(lys-ran-tyr) hydrogel crosslinked by HM-TAD.

The difunctional HM-bisTAD reacted well with poly(lys_{40}-*st*-tyr_{10}). Cross-linking of the polymer and formation of a stable hydrogel occurred in less than 2 min. at room temperature. When HM-bisTAD was added to the polypeptide solution it resulted in phase separation because of hydrophobic nature of HM-TAD. After 1 min. of stirring the reaction mixture became viscous and the hydrogel formed as evident from the vial tilting method (Figure 3.8). Unreacted HM-bisTAD could be washed out by THF and the previously pale yellow hydrogel became completely clear. Swelling test were done

after freeze drying of the hydrogel. The hydrogel is capable of absorbing 38 times its own weight i.e. 97,43% of the material is water.

3.2.4 Orthogonal Functionalization of Lysine and Tyrosine

We have tested the orthogonal functionalization of tyrosine and lysine with TAD and a sugar. Firstly, we modified Poly(lys-ran-tyr) with PTAD and then sugar (Figure 3.9). We succesfully functionalized both with this order. Then we reverse the functionalization order. In this case, sugar functionalized Poly(lys-ran-tyr) was not soluble anymore in ideal PTAD functionalization conditions. Therefore, we have tried non ideal conditions where tris buffer was missing. We saw that PTAD was decomposed and reacted with other groups (probably OH of sugar). Finally, we solved the problem by partial functionalization of lysine in which Poly(lys-ran-tyr) was soluble in ideal PTAD conjugaton conditions (1:1 Acetonitrile/Tris Buffer).

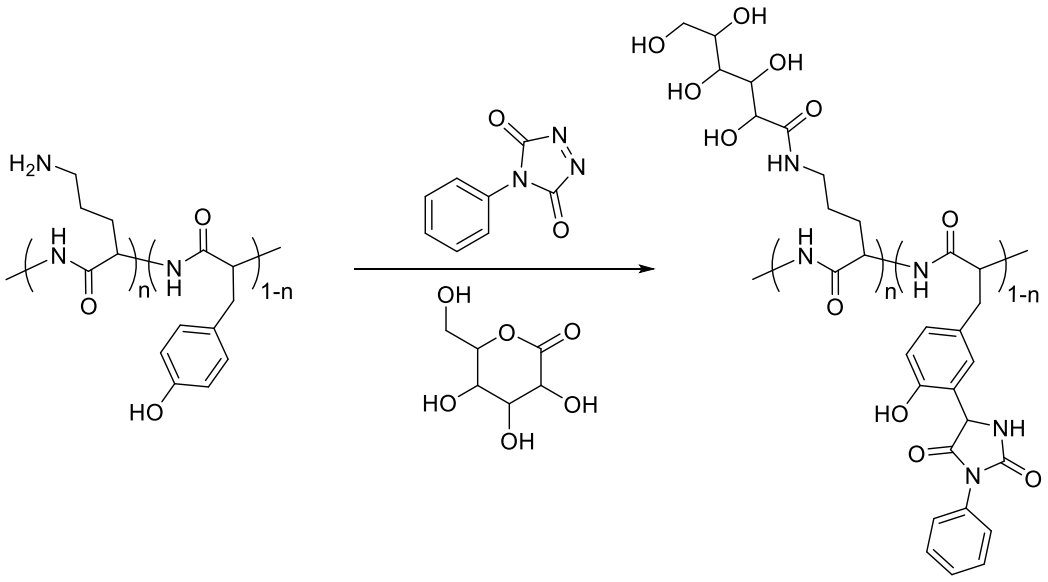

Figure 3.9. Orthogonal functionalization of tyrosine and lysine with PTAD and D-(+)-gluconic acid δ-lactone.

3.3 Experimental

Materials: Chemicals and reagents: All reagents were purchased from Sigma-Aldrich unless otherwise noted. Protected amino acids were purchased from BACHEM. Triphosgene was purchased from Fluorochem and freshly used. Snake skin dialysis tubing (3.5K MWCO) was obtained from VWR. Silica nitric acid was prepared as described in literature. Tris buffer solution was prepared using Trizma® base. Ethyl acetate over moleculer sieves were purchased from Across-Organics .

Methods: ^{1}H and ^{13}C NMR spectra were recorded at room temperature with a Bruker Avance

400 (400 MHz). ATR-FTIR spectra were collected on a Perkin Elmer Spectrum 100 in the spectral region of 650-4000 cm^{-1}, were obtained from 16 scans with a resolution of 2 cm^{-1}. Background measurements were taken before each analysis.SEC analyses of the protected polypeptides were done using Agilent GPC running on DMF with dn/dc value set to 1.599.

Synthesis of poly(Z-Lys40-st-O-benzyl-Tyr10): 1090 mg (3.56mmol) Lysine NCA and 267mg (0.89mmol) of tyrosine NCA were dissolved in 10 mL anhydrous DMF and the solution was purged with nitrogen for 10 minutes. 9 mg Hexylamine (1.8 mL of 50mg/ml stock solution in DMF – 0.089 mmol) was added fast to the solution and stirred at room temperature. The reaction was monitored by IR spectroscopy until all monomer was consumed (6-8 hours). Then the polypeptide solution was precipitated dropwise into 200 mL diethyl ether. After decanting the solvent, fresh diethyl ether was added and stirred for 20 min and repeated one more time. The product was then collected and dried under vacuum. Isolated Yield: 1075mg, 93%.

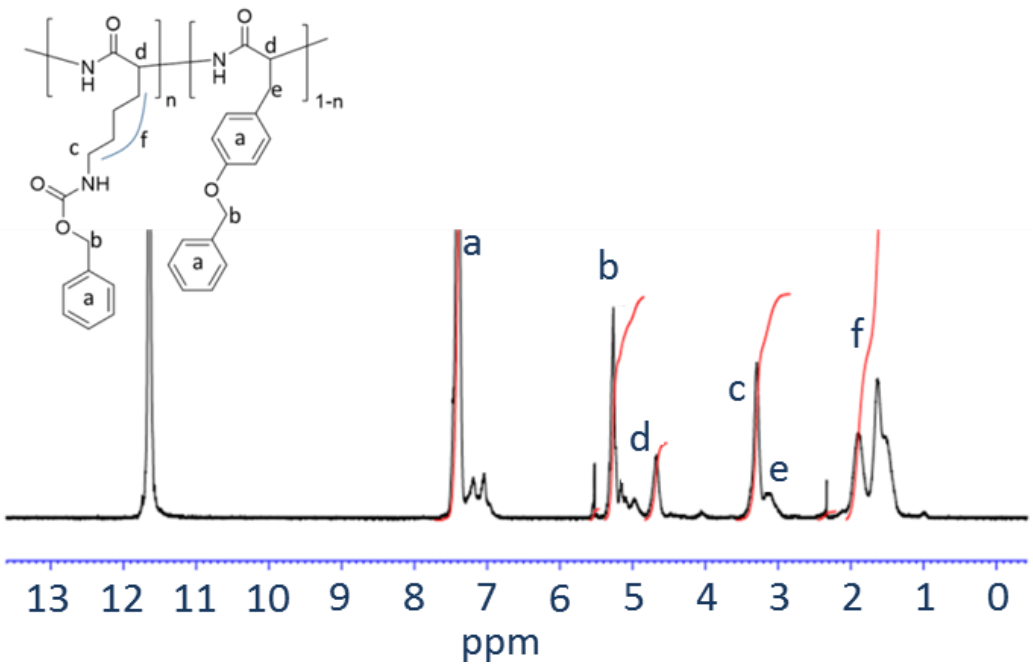

Figure 3.10. NMR spectrum of poly(Z-Lys$_{40}$-*st*-O-benzyl-Tyr$_{10}$) in TFA-d.

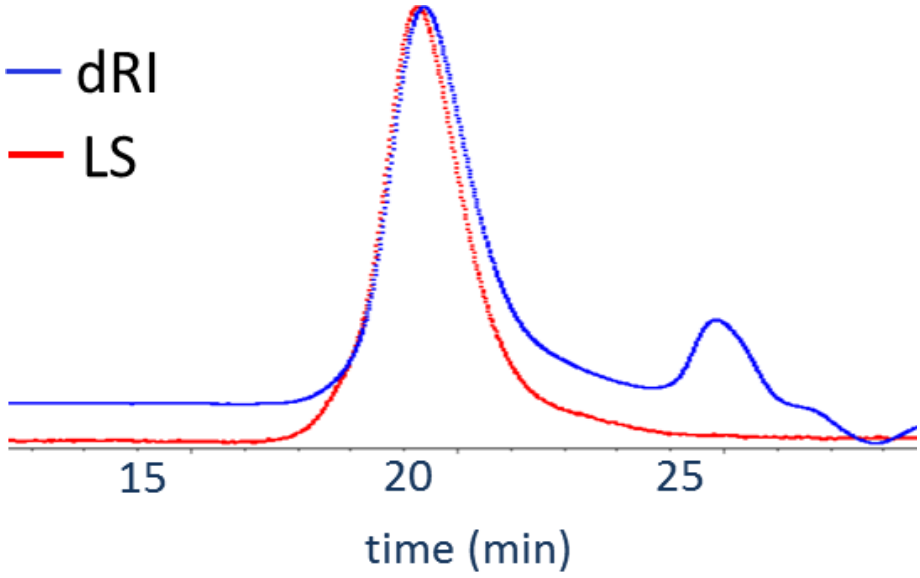

Figure 3.11. GPC chromatogram of poly(Z-Lys$_{40}$-*st*-O-benzyl-Tyr$_{10}$)

Synthesis of poly(Lys$_{40}$-*st*-Tyr$_{10}$): 600 mg of protected polymer was dissolved in 5-6 ml trifluoroacetic acid. To this solution, 0.5 mL of HBr (33% in acetic acid) solution was added dropwise and stirred overnight. Then the solution was precipitated in 100 mL diethyl ether. After the product was collected, it was washed with an excess diethyl ether and dried under vacuum. The dried polymer was dissolved in water and placed

into a 3.5 MWCO snake skin dialysis tubing and dialyzed against water for 3 days (refreshing water 4-5 times a day). Finally, solution was freeze dried and white fluffy product collected. Yield: 410mg - 89%

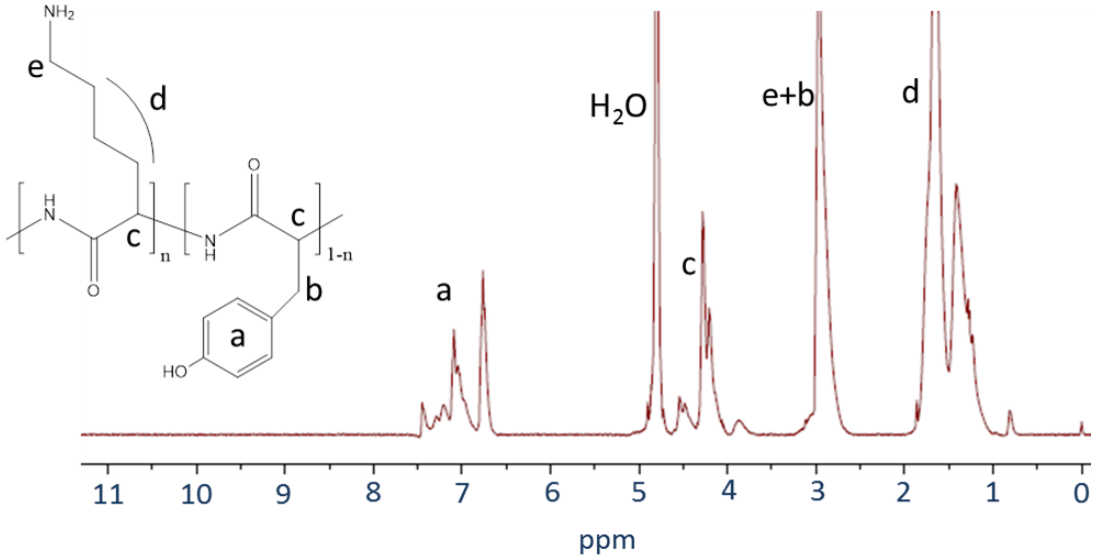

Figure 3.12. NMR spectrum of poly(Lys_{40}-*st*-Tyr_{10}) in D_2O.

Synthesis of Urazoles

Little et. al. reported high scale synthesis of urazoles starting from isocyanates, amines and carboxylic acid.[32] We used isocyanates as precursors since it was the most practical (no column, simple washing to remove unreacted material). However, using amines makes more sense where purity of the isocyanate is questionable or the isocyanate is too reactive to handle such as PEG-isocyanate.

Hexamethylene bisurazole

Step 1 (Hexamethylene bishydrazine carboxylate): Ethyl carbazate (5,02 g; 48 mmol) was dissolved in 30 mL of anhydrous THF under inert atmoshphere. Then a solution of hexamethylene diisocyanate (4,03 g; 24 mmol) in anhydrous THF (30 mL) was added to this solution dropwise at 0^o C. After 2-3 min. precipitation of the product was observed. The mixture was stirred for 2 hours and the collected product washed

with an excess THF. The final product was dried under vacuum to give a white material (8,7 g, 23 mmol, 96%).

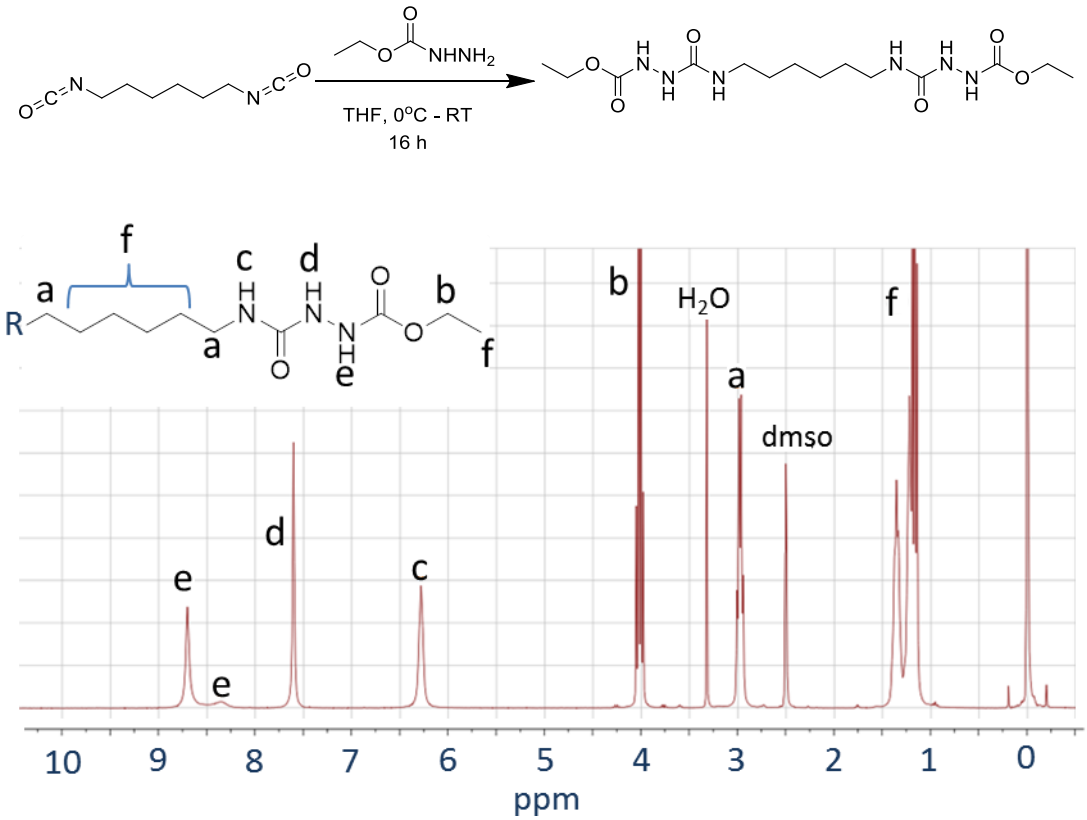

Figure 3.13. ^{1}H-NMR spectrum of hexamethylene bishydrazine carboxylate in dmso-d^{6}.

Step 2 (hexamethylne bisurazole 6): 5 grams(13,21mmol) of hexamethylene bishydrazine carboxylate was suspended in 150 mL absolute ethanol. 6.2g (45mmol) of anhydrous potassium carbonate was added to this solution and heated to reflux for one day. Then the ethanol was evaporated and the crude material dissolved in deionized water/ice. Afterwards concentrated HCl was added dropwise at 0^{o}C until the pH of the solution became 1-2. Then the product was collected by filtration and washed with an excess of deionized water. Finally, the product was dried under vacuum (2,01 g, 7.08mmol, 53%)

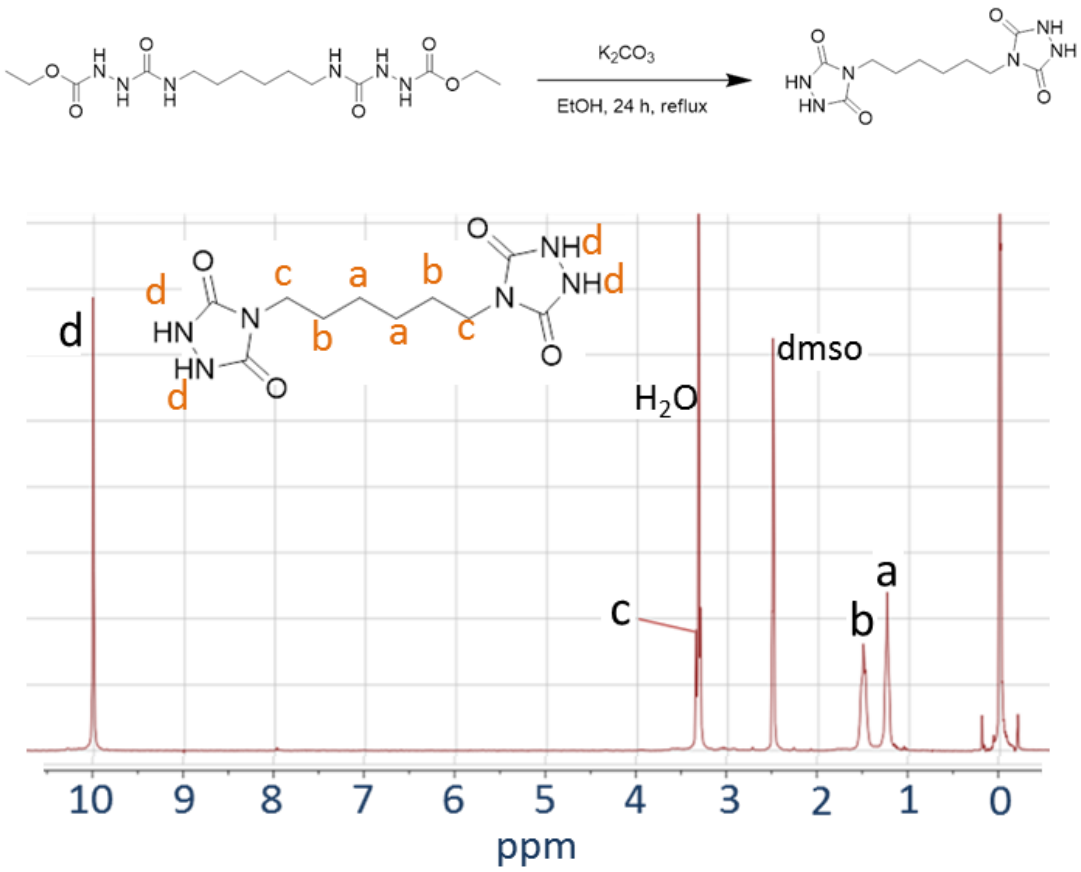

Figure 3.14. ^{1}H-NMR spectrum of hexamethylene bisurazole in dmso-d^{6}.

Methylene diphenyl bisurazole 5

Step 1 (methylene diphenyl bishydrazine carboxylate): Ethyl carbazate (5,02 g; 48 mmol) was dissolved in 30 mL of anhydrous THF under an inert atmoshphere. Then a solution of methylenediphenyl diisocyanate (6.06 g; 24 mmol) in anhydrous 30 mL THF was added dropwise to this solution at 0^{o} C. The reaction was stirred for one hour and all solvent evaporated under vacuum. Yield: 100 %.

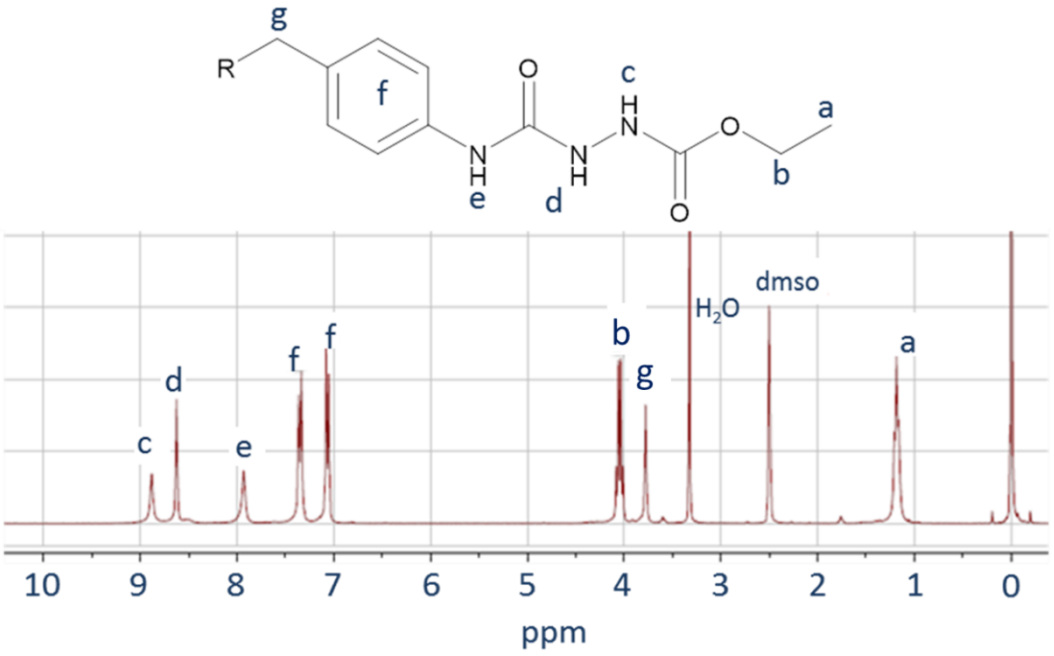

Figure 3.15. NMR spectrum of Methylene diphenyl bishydrazine carboxylate in dmso-d6.

Step 2 (methylene diphenyl bisurazole 5): 5 g (10,83mmol) of methylene diphenyl bishydrazine carboxylate refluxed in 4N KOH (12 mL) solution overnight. After reaction cooled down and concentrated HCl is added dropwise at 0^{o}C until pH of the solution becomes 1-2. Then, product was collected by filtration and washed with excess deionized water. Finally, product was dried under vacuum to give white powder. (Yield: 2.57g, 7.03mmol, 65%)

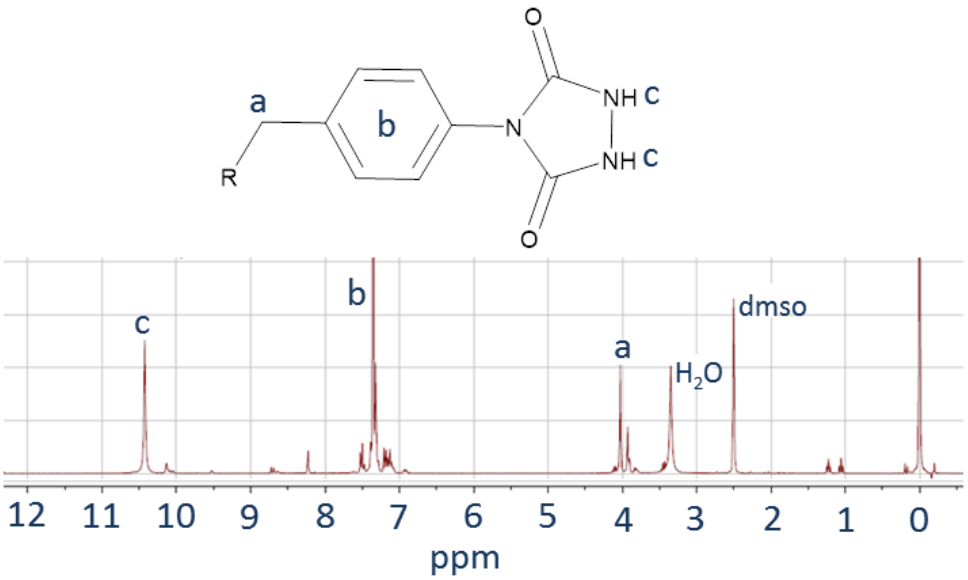

Figure 3.16. NMR spectrum of Methylene diphenyl bisurazole in dmso-d6.

Ethyl 4-urazole benzoate

Step 1 (ethyl 4-hydrazine carboxylate benzoate): Ethyl carbazate 2.08g (20mmol) was dissolved in 15 mL anhydrous THF under inert atmosphere. Then solution of ethyl 4-isocyanatobenzoate 3.82g (20 mmol) in 15 mL anhydrous THF was added to this solution dropwise at 0^{o} C. The reaction was stirred for 1 hour and the product collected by filtration. Isolated yield: 5.42g, 92%

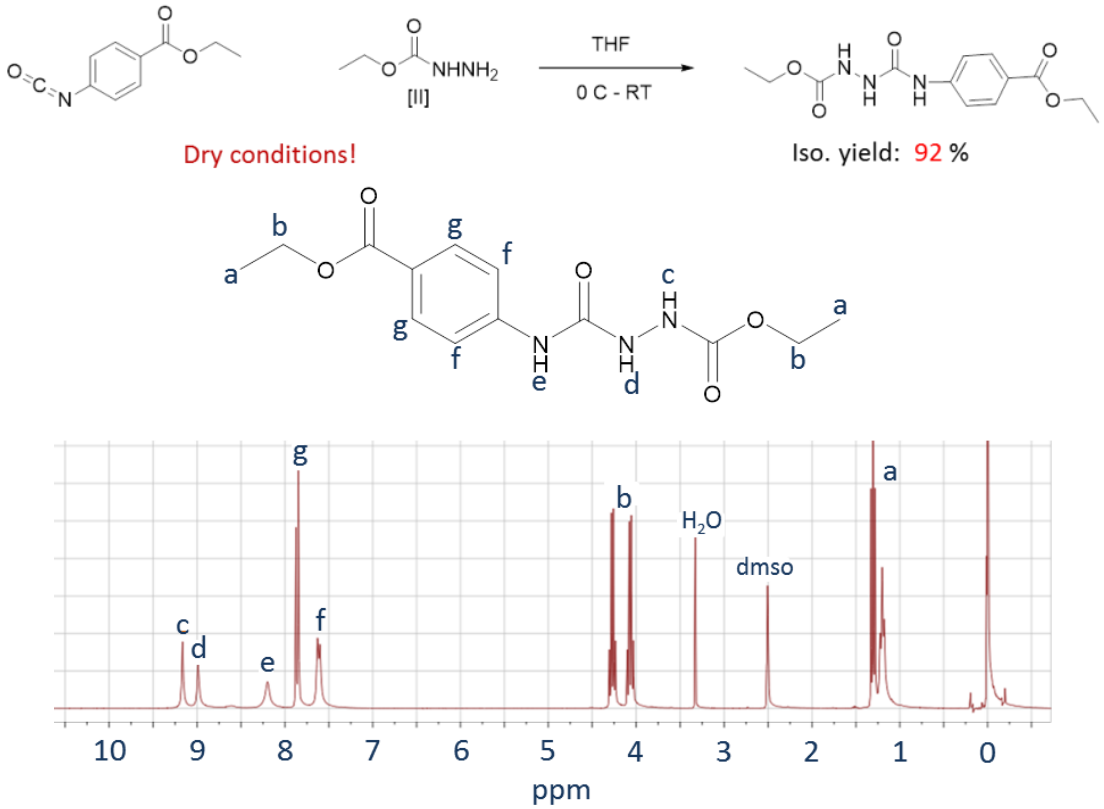

Figure 3.17. NMR spectrum of Ethyl 4-Hydrazine Carboxylate Benzoate.

Step 2 (ethyl 4-urazole benzoate): 5g (17 mmol) of 4-Ethylbenzoate hydrazine carboxylate was suspended in 150 mL absolute ethanol. 3 g (21 mmol) of anhydrous potassium carbonate was added to this solution and heated to reflux for 16 hours. Then, ethanol was evaporated completely and the crude product dissolved in deionized water/ice mixture. Afterwards, concentrated HCl was added dropwise at 0^{o}C until pH of the solution became 5-6. Then, the product was collected by filtration and washed with an excess of deionized water. Isolated yield: 3.34g, 79%

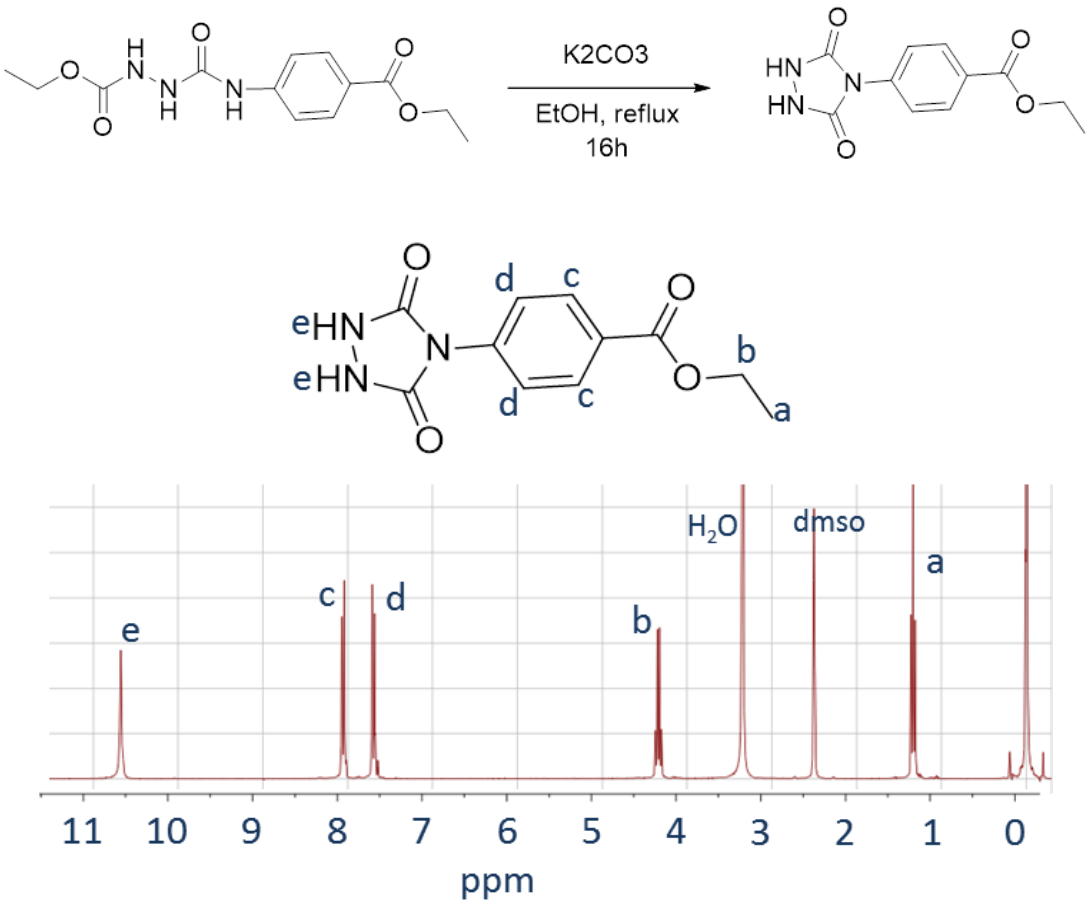

Figure 3.18. NMR spectrum of Ethyl 4-urazole benzoate.

Urazole benzoic acid: 4-Ethyl urazole benzoate 2 g (8 mmol) was suspended in 20 mL H_2O. To this solution 2,2g (16 mmol) of KOH was added and stirred at 80^oC for 30 min. The solution was cool down to 0^o C and acidified to pH 1-2. The product was collected by filtration. Yield: Quantitative

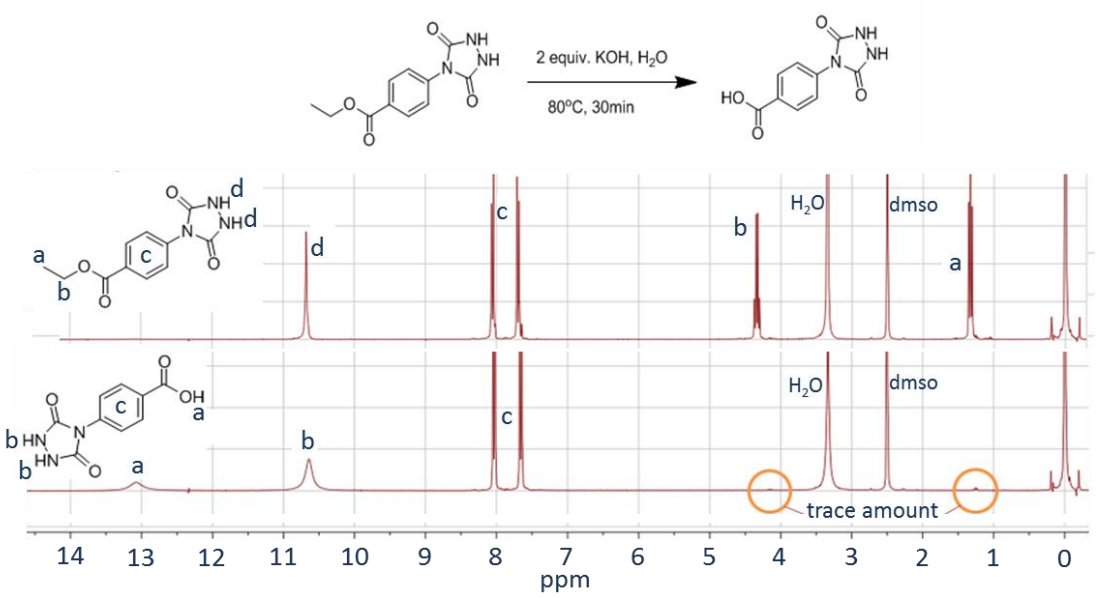

Figure 3.19. NMR spectrum of ethyl 4-urazole benzoic acid in dmso-d[6].

Oxidation of Urazoles

Oxidation of urazoles to corresponding TADs has been extensively studied since 1960 when Cookson's first isolation of TAD.[33, 34] Especially by Mallakpour and Zolfigol.[35-43] We have tried some of these conditions to oxidize our urazoles. Using commercially available 1,3-dibromo-5,5-dimethylhydantoin looked practical.[35] However, we observed that oxidized product contains side product of oxidizing agent (dimethyl hydantion) and 2 or 4 mole equivalent of HBr (Figure 3.20). Therefore, we focused on the procedures with less side products. It is important because TADs are generally too reactive to purify. Using freshly prepared silica nitric acid as described in literature. The latter method gave slightly cleaner products free of side product of the oxidizer (methyl hyndantoin) but it still contains residual HNO_3 which can be removed by rotavap. The drawback of silica nitric acid is the water coming from the aqeous nitric acid may decompose the TAD. However, using dichloromethane as a solvent and drying the oxidized solution over anhydrous $MgSO_4$ before rotavap solves the problem.

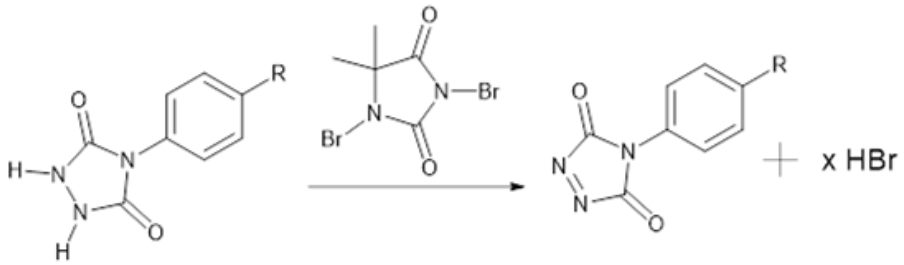

Figure 3.20. Oxidation of Urazoles by commercially available DBDMH.

In general, 100mg of urazole compound suspended in 6mL anhydrous acetonitrile or dichloromethane. 1.1 mole equivalent DBDMH dissolved 4mL of same solvent and added slowly in 1-2 minutes while string. The suspension turns into solution after 5-60 min depending on the urazole. Then all the solvent evaporated by rotavap and pink or red compounds were collected. The yields will be misleading since product contains Methyl hydantoin side products

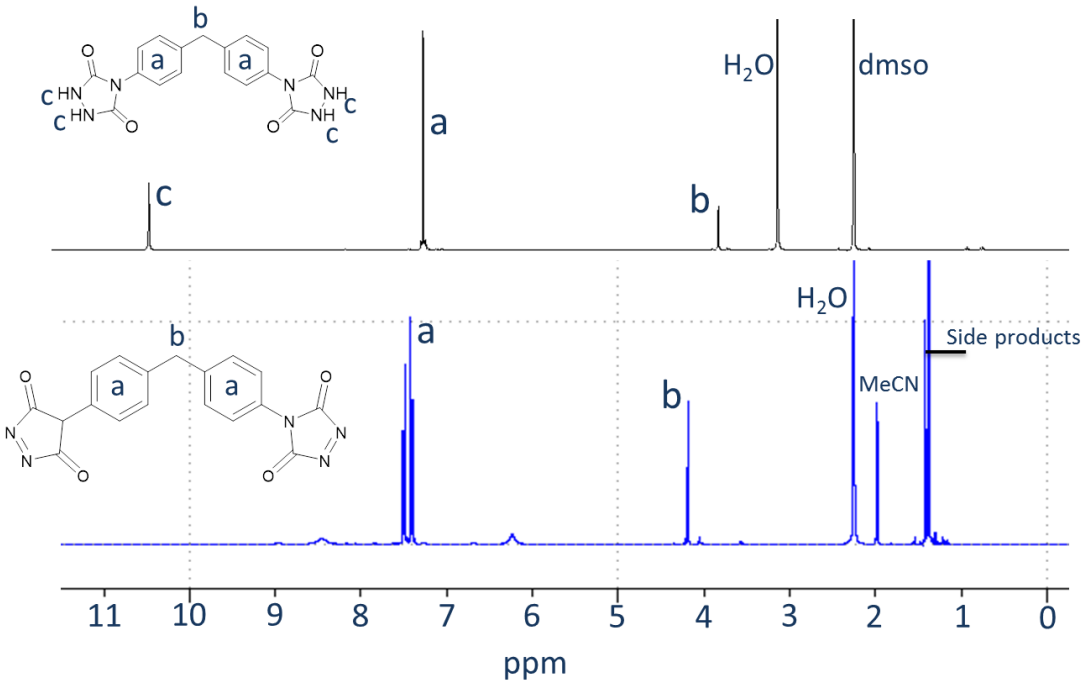

.**Figure 3.21.** NMR spectrum of MDP urazole in DMSO-d6 (top) and MDP-bisTAD in acetonitrile-d3(bottom).

Figure 3.22. Stability of TAD derivatives in acetonitrile oxidized by DMBH.

For silica nitric acid oxidation, we observed that using dichloromethane as solvent gives much cleaner product than acetonitrile. For oxidation, three times amount in grams of silica nitric acid was added to urazole solution slowly in 5 minutes while stirring. The mixture was stirred for 2-3 hours and filtered. Then anhydrous $MgSO_4$ was added and stirred for 10 min. Finally, product was collected after filtering and evaporating all the solvents by rotavap. The isolated yields were generally 80-95%.

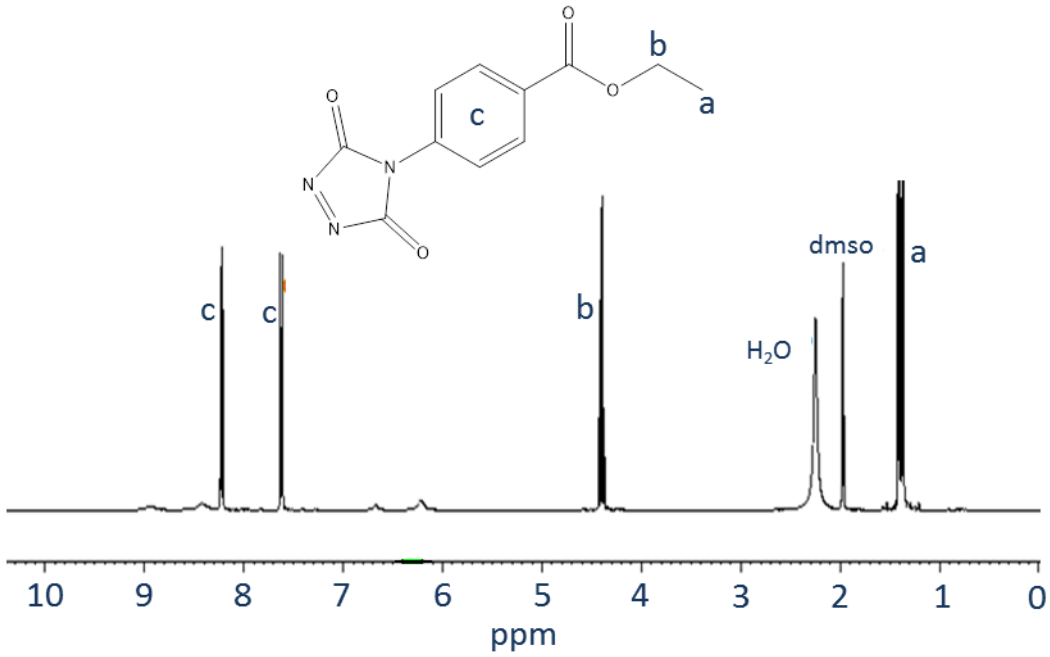

Figure 3.23. NMR spectrum of Ethyl 4-TAD benzoic acid in dmso-d6.

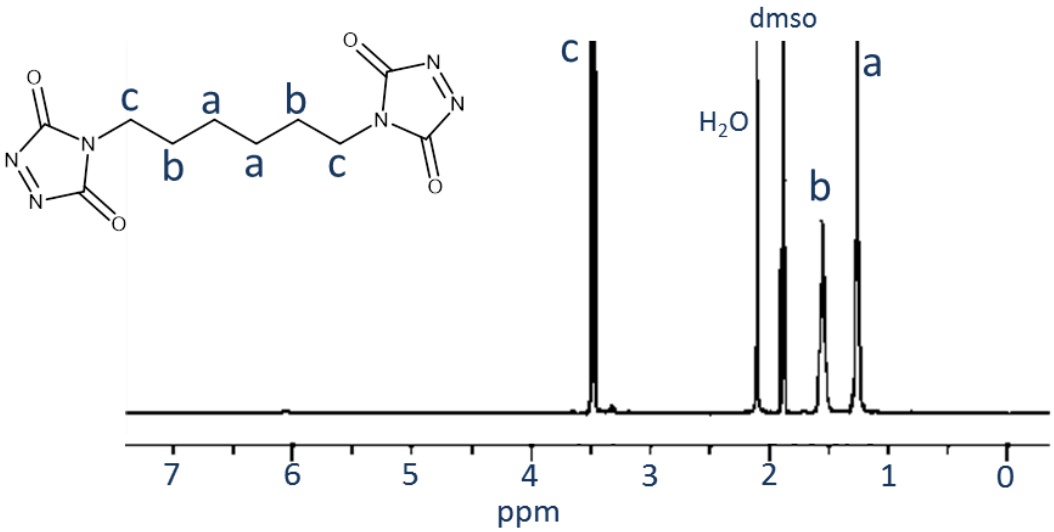

Figure 3.24. NMR spectrum of hexamethylene bisTADs in acetonitrile-d3.

Crosslinking of poly(Lys_{40}-*st*-Tyr_{10}) by HM-TAD 6: 30 mg of polypeptide was dissolved in a 0.2 mL acetonitrile/tris (1:1) mixture. To this solution 50 µL HM-bisTAD stock solution was added (100 mg/mL, freshly prepared by silica nitric acid method) while stirring the solution. After 60-70 s the pink colour completely disappeared and gel formation was observed. The pale yellow gel was washed with THF to produce a clear gel.

Conjugation of TAD derivatives: Unlike PTAD conjugation, TAD benzoic acid and Ethyl 4-benzoate TAD conjugations were not successful in 1:1 acetonitrile and tris buffer mixture. These compounds were immediately decomposed in these conditions. A brown precipitate formed and isolated polypeptide remained same with no conjugation. Therefore, we lowered aqeous part to slow down decomposition.

COOH-PTAD conjugation: 30mg (approx. 7.2mg, 0.043mmol Tyr) of poly(Lys_{40}-st-Tyr_{10}) was dissolved in 0.3mL DMF and 0.03mL DI water. To this solution 12mg (0.054 mmol) of COOH-PTAD in 0.15mL DMF is added dropwise. Red color of TAD-benzoic acid disappeared instantly. The solution stirred for 2 min more and

diluted with 3 mL DI water and placed into 3.5 MWCO dialysis bag. After 4 days, dialysis product was collected by freeze dryer and characterized by NMR (Figure 3.25). Conjugation yield was calculated as 81% from NMR integration.

Ethyl 4-benzoate TAD conjugation: The same procedure was followed. However, the resulting polymer was not soluble in water anymore. Additionally, side products were observed indicating that TAD was decomposed and reacted with lysine.

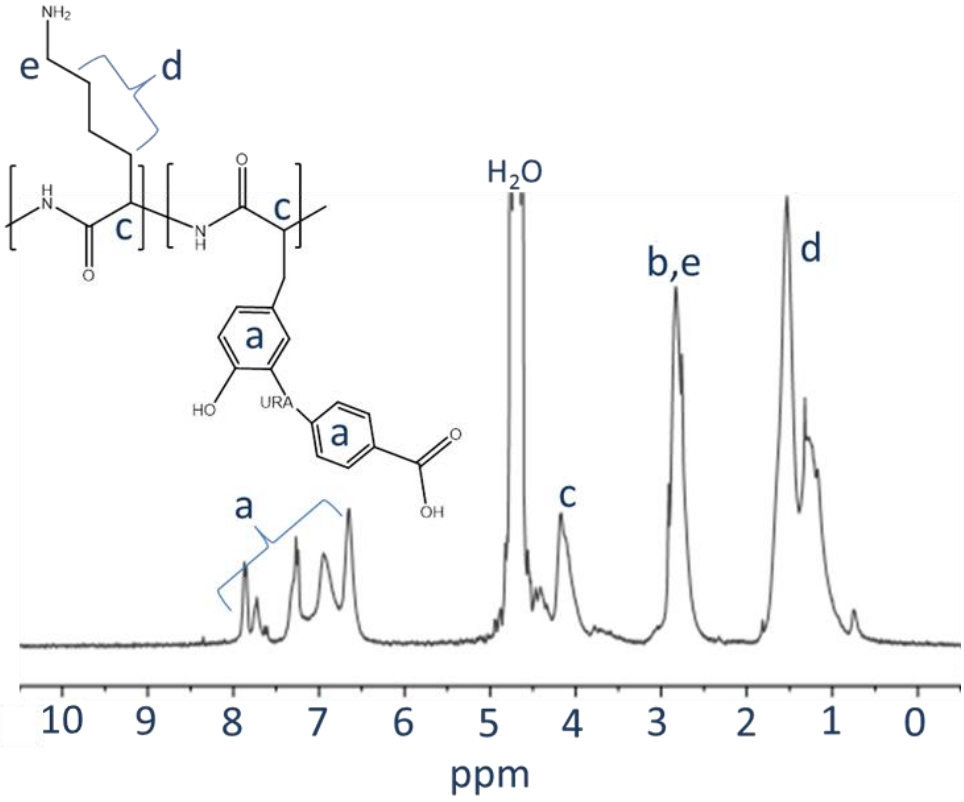

Figure 3.25. NMR spectrum of COOH-PTAD attached poly(Lys_{40}-st-Tyr_{10}) in D_2O.

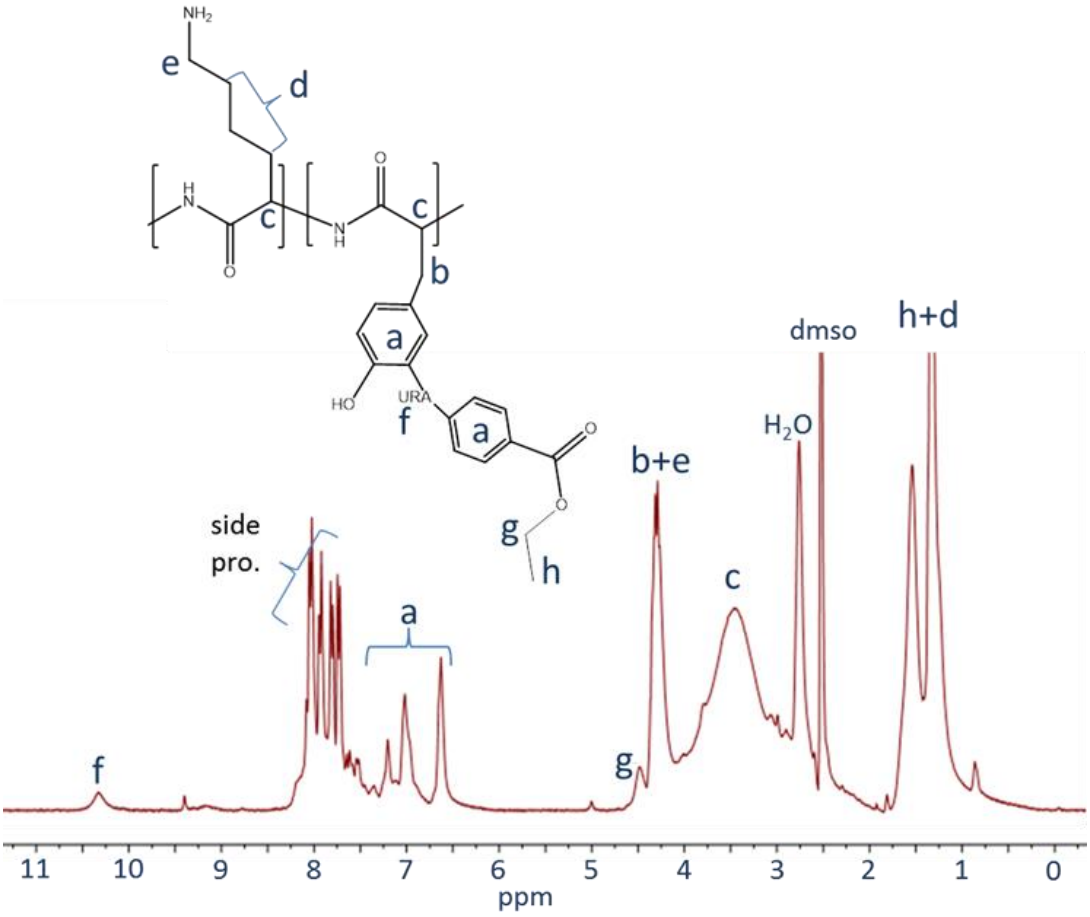

Figure 3.26. NMR spectrum of Benzoate-PTAD attached poly(Lys_{40}-ran-Tyr_{10}) in dmso-d6.

Glucosylation of poly(Lys_{40}-ran-Tyr_{10}) followed by PTAD: 300 mg of poly(Lys_{40}-ran-Tyr_{10}) was dissolved in 3 mL DMSO and 0.3 mL water. To this solution 30mg (0.15mmol) of D-(+)-gluconic acid δ-lactone was added and stirred for 24 hours (Figure 3.27). Then the solution was placed into a 3.5 MWCO snake skin dialysis bag and dialyzed against DI water for 3 days. The polypeptide was obtained by freeze drying. Then, 50 mg of this polypeptide was dissolved in 1 mL of MeCN/0.1M tris buffer (1:1). To this solution 8 mg (0.04mmol) of PTAD (in 0.1 mL MeCN) was added together with 0.1 ml tris buffer. The red solution turned into orange and pale brown in 3-4 min. After 30 min, the solution was put into 3.5 MWCO dialysis bag and dialysed for 3 days. Finally, the solution was freeze dried and characterized by NMR (Fig 3.28).

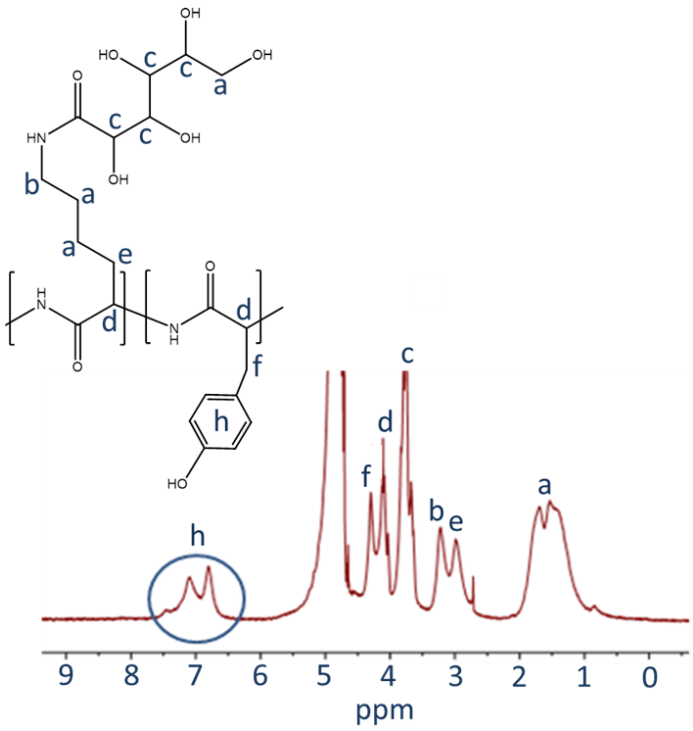

Figure 3.27. NMR spectrum of sugar functionalized poly(Lys_{40}-ran-Tyr_{10}) in dmso-d6.

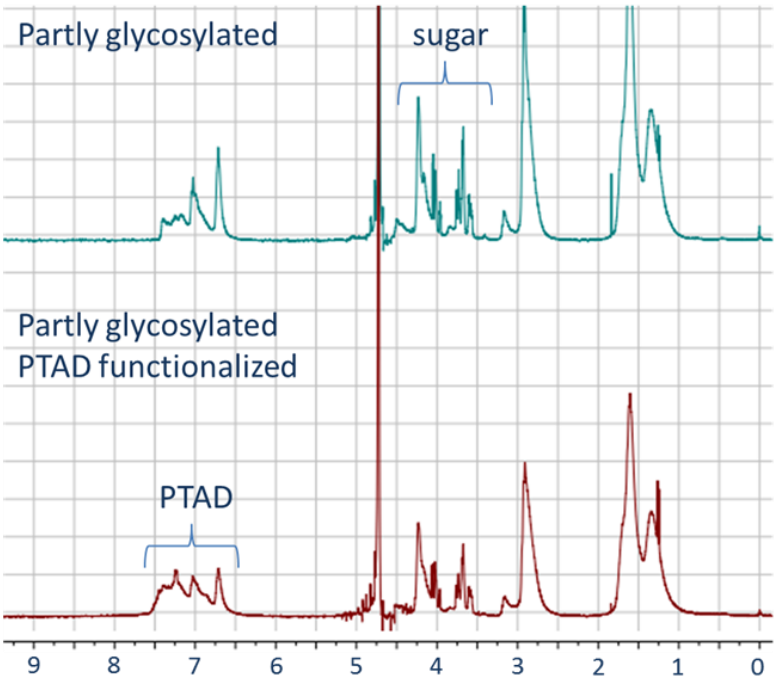

Figure 3.28. Orthogonal functionalization of partially glucosylated lysine. PTAD functionalization carried out in 1:1 MeCN/Tris buffer.

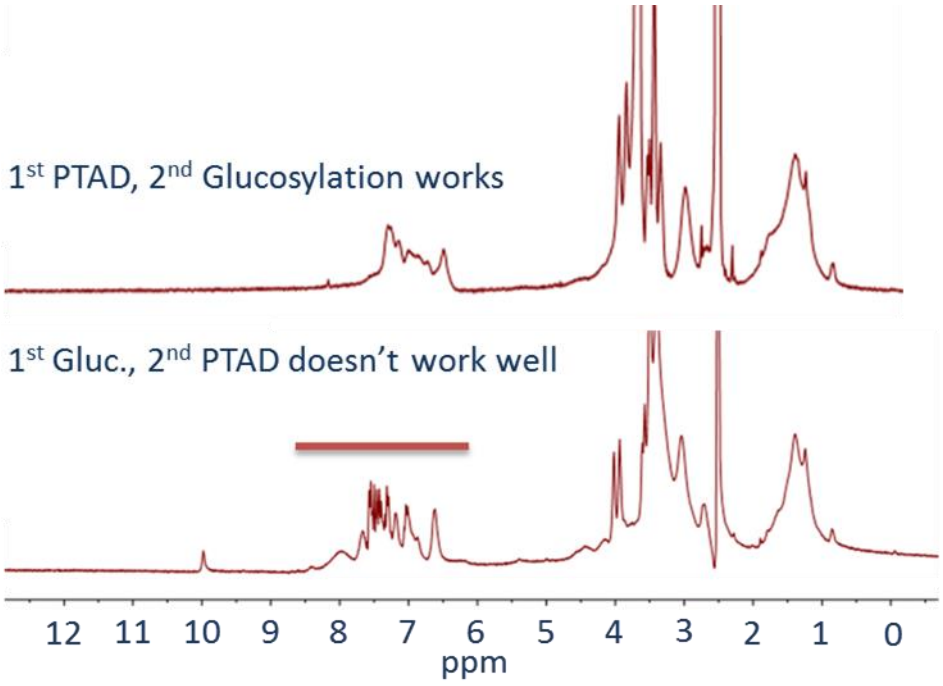

Figure 3.29. [1]H-NMR of rrthogonal functionalization of fully glucosylated lysine in dmso-d6.

When polypeptides were fully glycosylated, it became insoluble in acetonitrile/tris buffer. PTAD functionalization was tested in DMF but it was unsuccessful (Figure 3.29).

3.4 Conclusion

In conclusion, combination of NCA polymerization with tyrosine-TAD reaction has shown to be a very efficient method to prepare well defined functionalized polypeptides and polypeptide based hydrogels. Further functionalization of tyrosine can be done with novel TAD compounds such as PEG-TAD or glucose-TAD. However, the stability of these compounds in aqueous media will determine the functionalization efficiency. Interestingly, stable bifunctional TAD compounds will enable researchers to prepare novel polypeptide hydrogels where amino acids such as lysine, glutamic acid or cysteine remain unaffected or free for functionalization.

3.5 References

(1) Byrne, M.; Murphy, R.; Kapetanakis, A.; Ramsey, J.; Cryan, S. A.; Heise, A. *Macromolecular rapid communications*, 2015.

(2) Bonduelle, C.; Lecommandoux, S. B. *Biomacromolecules*, 2013, **14**, 2973-2983.

(3) Hadjichristidis, N.; Iatrou, H.; Pitsikalis, M.; Sakellariou, G. *Chemical reviews*, 2009, **109**, 5528-5578.

(4) Deming, T. J. *Chemical reviews*, 2015, **116**, 786-808.

(5) Engler, A. C.; Lee, H. I.; Hammond, P. T. *Angewandte Chemie International Edition*, 2009, **48**, 9334-9338.

(6) Huang, J.; Habraken, G.; Audouin, F.; Heise, A. *Macromolecules*, 2010, **43**, 6050-6057.

(7) Tang, H.; Zhang, D. *Biomacromolecules*, 2010, **11**, 1585-1592.

(8) Borase, T.; Ninjbadgar, T.; Kapetanakis, A.; Roche, S.; O'Connor, R.; Kerskens, C.; Heise, A.; Brougham, D. F. *Angewandte Chemie International Edition*, 2013, **52**, 3164-3167.

(9) Sun, J.; Schlaad, H. *Macromolecules*, 2010, **43**, 4445-4448.

(10) Krannig, K. S.; Schlaad, H. *Journal of the American Chemical Society*, 2012, **134**, 18542-18545.

(11) Krannig, K. S.; Huang, J.; Heise, A.; Schlaad, H. *Polymer Chemistry*, 2013, **4**, 3981-3986.

(12) Mildner, R.; Menzel, H. *Journal of Polymer Science Part A: Polymer Chemistry*, 2013, **51**, 3925-3931.

(13) Habraken, G. J.; Koning, C. E.; Heuts, J. P.; Heise, A. *Chemical Communications*, 2009, 3612-3614.

(14) Joshi, N. S.; Whitaker, L. R.; Francis, M. B. *Journal of the American Chemical Society*, 2004, **126**, 15942-15943.

(15) Minakawa, M.; Guo, H. M.; Tanaka, F. *The Journal of organic chemistry*, 2008, **73**, 8669-8672.

(16) Kodadek, T.; Duroux-Richard, I.; Bonnafous, J. C. *Trends in pharmacological sciences*, 2005, **26**, 210-217.

(17) Jones, M. W.; Mantovani, G.; Blindauer, C. A.; Ryan, S. M.; Wang, X.; Brayden, D. J.; Haddleton, D. M. *Journal of the American Chemical Society*, 2012, **134**, 7406-7413.

(18) Ban, H.; Gavrilyuk, J.; Barbas III, C. F.; *Journal of the American Chemical Society*, 2010, **132**, 1523-1525.

(19) Ban, H.; Nagano, M.; Gavrilyuk, J.; Hakamata, W.; Inokuma, T.; Barbas III, C. F. *Bioconjugate chemistry*, 2013, **24**, 520-532.

(20) Hu, Q. Y.; Allan, M.; Adamo, R.; Quinn, D.; Zhai, H.; Wu, G.; Clark, K.; Zhou, J.; Ortiz, S.; Wang, B. *Chemical Science*, 2013, **4**, 3827-3832.

(21) Adamo, R.; Allen, M.; Berti, F.; Danieli, E.; Hu, Q.Y. *Patent*, **2012**., US 9149541 B2

(22) Dao, L. H.; Mackay, D. *Canadian Journal of Chemistry*, 1979, **57**, 2727-2733.

(23) Jessica, F.; Corentin, W.; Sylvestre, D.; Christian, L.; André, L. *RSC Advances*, 2013, **3**, 24936-24940.

(24) Bauer, D. M.; Ahmed, I.; Vigovskaya, A.; Fruk, L. *Bioconjugate chemistry*, 2013, **24**, 1094-1101.

(25) Billiet, S.; De Bruycker, K.; Driessen, F.; Goossens, H.; Van Speybroeck, V.; Winne, J. M.; Du Prez, F. E. *Nature chemistry*, 2014, **6**, 815-821.

(26) Roling, O.; De Bruycker, K.; Vonhören, B.; Stricker, L.; Körsgen, M.; Arlinghaus, H.F.; Ravoo, B. J.; Du Prez, F. E. *Angewandte Chemie International Edition*, 2015.

(27) Sato, S.; Nakamura, K.; Nakamura, H.; *ACS chemical biology*, 2015.

(28) Männistö, M.; Vanderkerken, S.; Toncheva, V.; Elomaa, M.; Ruponen, M.;Schacht, E.; Urtti, A. *Journal of controlled release*, 2002, **83**, 169-182.

(29) Byrne, M.; Victory, D.; Hibbitts, A.; Lanigan, M.; Heise, A.; Cryan, S.A. *Biomaterials Science*, 2013, **1**, 1223-1234.

(30) Kadlecova, Z.; Rajendra, Y.; Matasci, M.; Baldi, L.; Hacker, D.L.; Wurm, F. M.; Klok, H. A. *Journal of Controlled Release*, 2013, **169**, 276-288.

(31) Huang, J.; Hastings, C. L.; Duffy, G. P.; Kelly, H. M.; Raeburn, J.; Adams, D. J.; Heise, A. *Biomacromolecules*, 2012, **14**, 200-206.

(32) Little, T.; Meara, J.; Ruan, F.; Nguyen, M.; Qabar, M. *Synthetic communications*, 2002, **32**, 1741-1749.

(33) Cookson, R.; Gilani, S.; Stevens, I. *Tetrahedron Letters*, 1962, **3**, 615-618.

(34) Cookson, R.;Gilani, S.; Stevens, I. *Journal of the Chemical Society C: Organic*, 1967, 1905-1909.

(35) Zolfigol, M. A.; Nasr-Isfahani, H.; Mallakpour, S.; Safaiee, M. *Synlett*, 2005, **2005**, 0761-0764.

(36) Zolfigol, M. A.; Torabi, M.; Mallakpour, S. E. *Tetrahedron*, 2001, **57**, 8381-8384.

(37) Zolfigol, M. A.; Ghorbani-Vaghei, R.; Mallakpour, S.; Chehardoli, G.; Choghamarani, A. G.; Yazdi, A. H. *Synthesis*, 2006, **2006**, 1631-1634.

(38) Zolfigol, M. A.; Madrakian, E.; Ghaemi, E.; Mallakpour, S. *Synlett*, 2002, **2002**, 1633-1636.

(39) Hajipour, A. R.; Mallakpour, S. E.; Adibi, H. *Chemistry Letters*, 2001, 164-165.

(40) Zolfigol, M. A.; Mallakpour, S. E. *Synthetic communications*, 1999, **29**, 4061-4069.

(41) Zolfigol, M. A.; Borazjani, M. K.; Mallakpour, S. E.; Nasr-isfahani, H. *Synthetic Communications*, 2000, **30**, 2573-2585.

(42) Zolfigol, M. A.; Bagherzadeh, M.; Mallakpour, S.; Chehardoli, G.; Kolvari, E.; Choghamarani, A. G.; Koukabi, N. *Catalysis Communications*, 2007, **8**, 256-260.

(43) Ghorbani-Choghamarani, A.; Chenani, Z.; Mallakpour, S. *Synthetic Communications*, 2009, **39**, 4264-4270.

Chapter 4
Tryptophan-TAD Functionalization

Abstract

In the previous chapter, it was demonstrated that the TAD-tyrosine functionalization is challenging due to the decomposition of TAD in aqueous conditions. Therefore, there is a limited synthetic window in terms of reaction parameters for the TAD-tyrosine reaction. On the other hand, tryptophan readily reacts with TAD in organic solvents such as chloroform, DMF, acetonitrile, and their mixtures where TADs are stable. In order to investigate tryptophan-TAD reaction, a library of tryptophan-containing copolypeptides was prepared. The copolypeptides were then functionalized with PTAD, TAD Benzoate, PEG-bisTAD and PEG-monoTAD (PEGylation). Finally, we explored secondary functionalization on those polypeptides with thiol-ene and copper catalyzed azide-alkyne cycloaddition.

4.1. Introduction

An ideal functionalization reaction (such as a click reaction) should be selective, highly efficient, and ideally be free of impurities.[1] For polymer modifications, there are also other requirements to fulfill, such as equimolar functionalization and complete removal of side products by an easy work up, e.g. precipitation (Figure 4.1). Click reactions such as azide-alkyne cycloaddition or Diels-Alder reactions generally meet these requirements.[2] On the other hand, a copper-catalyzed azide-alkyne click reaction might not be suitable for polymer modifications targeting biological applications unless copper (I) is completely removed or converted into copper (II).[3] Click-like thiol-ene reactions seem more suitable in those cases as they are either catalyzed or triggered by light irradiation.[4] Light irradiation has the advantage of not requiring additional chemical activators and as such finds applications in the biomaterials sector.[5]

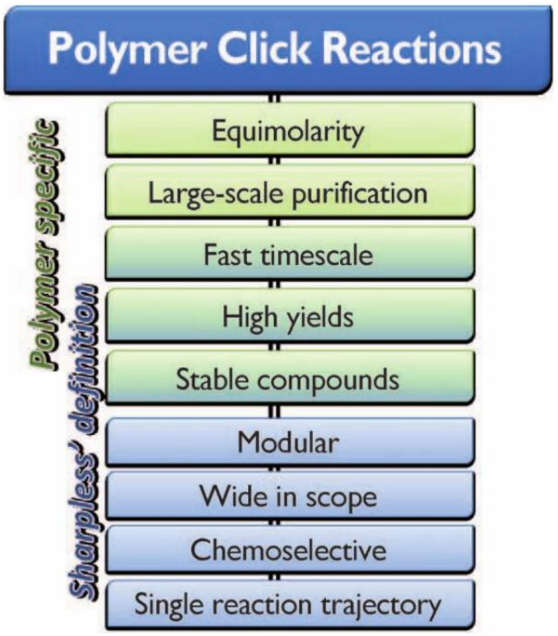

Figure 4.1. Proposed definition of small molecule click reactions and polymer specific click reactions.[2]

Diels-Alder reactions do not necessarily require a catalyst but the adduct formation depends on the reaction temperature.[6] Some dienes or dienophiles are so reactive that they readily react at -78^{o}C whereas others may require higher temperatures and several hours to be completed. A Diels-Alder reaction that fulfills the requirements of high efficiency and fast reaction rate was introduced in 1962 by Cookson *et al*., who synthesized a very reactive dienophile known as 4-phenyl-TAD (PTAD).[7] They showed that PTAD quantitatively reacts with cyclopentadiene at -78^{o}C.[8] Although PTAD is highly reactive towards dienes, it is reasonably easy to handle and storable as a powder.[9] Additionally, TADs are also reactive towards vinyl ethers[10], styrene, or β-diketones.[11] In 1980, G. B. Butler mentioned the importance of TADs in his review paper by stating that "TADs are low-temperature modifiers with exceptional versatility".[11] In the past, TAD functionalization was studied for the modification as well as crosslinking of polymers in order to tune their mechanical properties. However, they did not receive much attention as an alternative click reaction. TAD became popular in biology for fluorescence labeling of vitamin D, vitamin A and some other biologically important molecules by DMEQ-TAD (Figure 4.2).[12,13,14] In 2003 Corey *et al*. reported for the first time that indole can be protected and deprotected by TAD (Figure 4.3).[15] They demonstrated that the TAD-indole reaction is catalyst and side product free as well as reversible at high temperature. Compared to other click reactions, TAD chemistry is much easier to carry out. Simple mixing of TAD with the indole-containing product in open air and room temperature is generally sufficient for completion of the reaction.

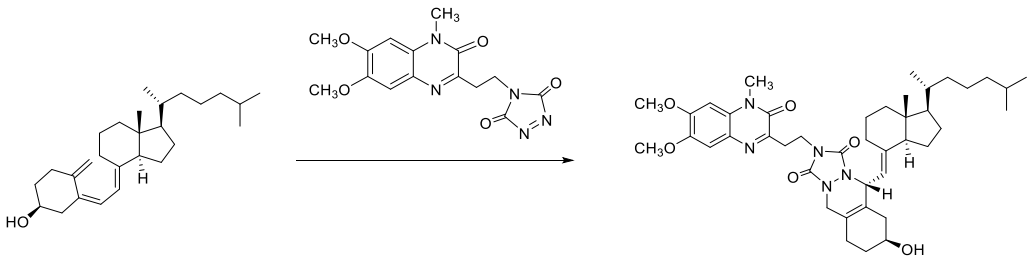

Figure 4.2. DMEQ-TAD labeling of vitamin D.[12]

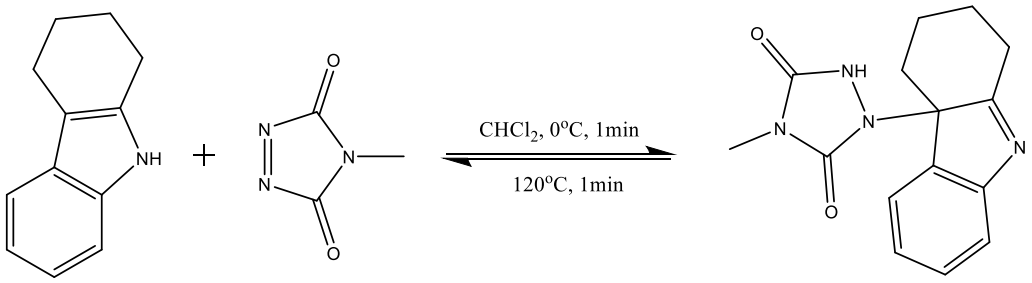

Figure 4.3. Protection-deprotection method of indole 2,3-π bond.[15]

Recently, TAD chemistry was rejuvenated and now receives increasing attention highlighted in a number of examples. The Du Prez *et. al.* demonstrated that thermal reversibility and ultrafast kinetic of TAD-indole reaction can be exploited to create a dynamic polymeric system for potential self-healing, recyclable, reshapeable and rewritable materials (Figure 4.4).[16,17] The same group also showed the practicability of TAD-diene reactions by preparing 58 layer organic films in 20 minutes.[18] Zhang, Du Prez and their coworkers further demonstrated that polymer-polymer coupling can efficiently be done by TAD-diene chemistry.[19,20] This additive free coupling process can be monitored by the disappearance of the distinct red color of the TAD upon reaction. Fabrication of highly elastic sustainable materials by crosslinking plant oils by TAD was reported by Wang *et al*.[21,22] Firstly, they synthesized triblock oil based copolymer, namely poly(styrene-b-soybean oil acrylate-b-styrene), via ATRP polymerization. Then, these polymers were crosslinked from their middle block by

4,4′-(1,4-phenylene)-bis(1,2,4-triazoline-3,5-dione). The crosslinking helped to achieve excellent mechanical properties where oil based polymers generally fall short.

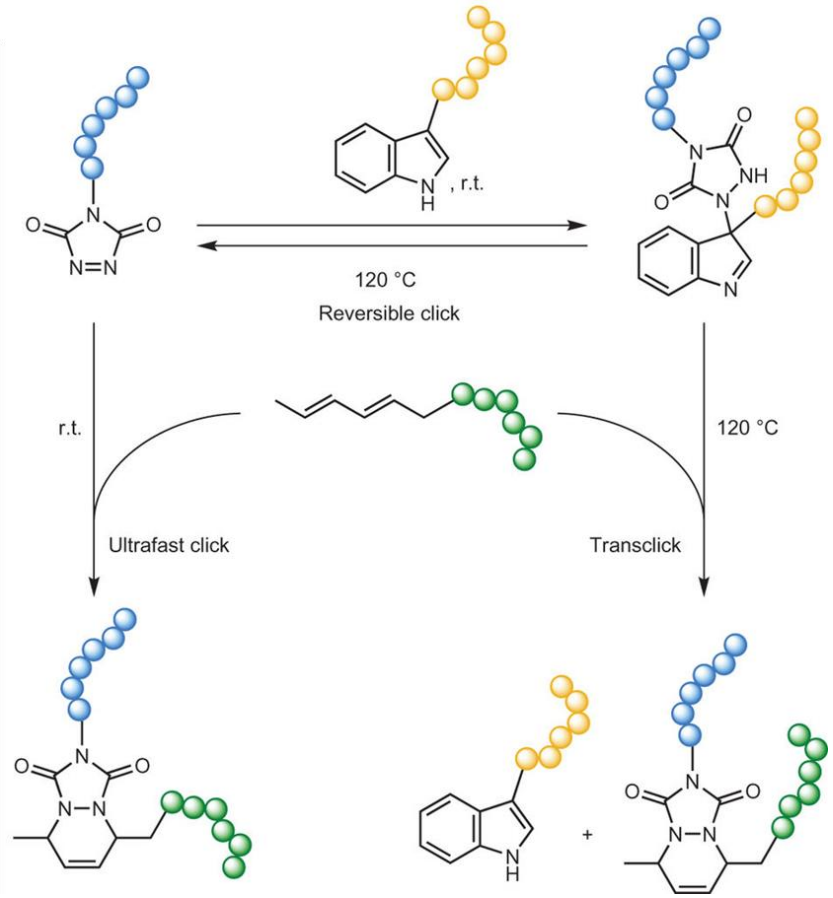

Figure 4.4. At high temperature, TAD gives a retro reaction with indole while it binds to conjugated diene irreversibly.[16]

TAD-furan reactions are less explored compare to the other TAD reaction. This reaction also constitutes a click reaction. To date, there are only two reports on TAD-furan reactions. In 2007, the Gleason group showed deposition of PTAD onto furan containing film. The film was cast from commercially available furfuryl methacrylate.[23] The second example was developed in the Madder group showing orthogonal peptide labeling by the PTAD-furan reaction (Figure 4.5).[24] Furan containing peptide was prepared using commercially available synthetic amino acid furylalanine via SPPS.

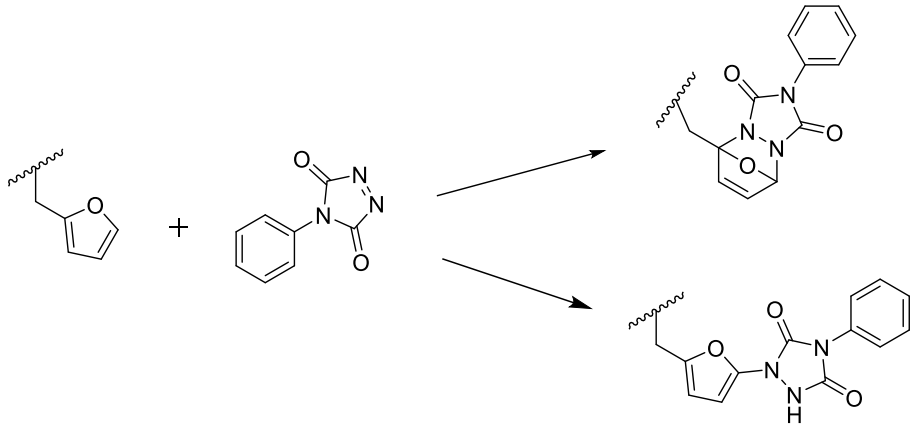

Figure 4.5. Furan group reacts with TAD either in Diels-Alder reaction or electrophilic aromatic substition.[24]

The natural amino acid tryptophan contains an indole group which can be used for TAD functionalization. In this chapter, TAD-tryptophan functionalization was investigated for copolypeptides prepared by NCA polymerization. This strategy offers significant advantages over established (click) conjugation approaches on synthetic polypeptides. While thiol-ene[25–27], thiol-yne[28–31] as well as azide alkyne[32–36] click reaction have been exploited for synthetic polypeptides, they are all based on non-natural amino acids, which need to be specially synthesized.[37,38] Even though conjugation approaches on natural amino acids have been reported such as thiol reaction on cysteine,[39,40] TAD reactions on tyrosine and various chemistries on glutamic acid,[41–45] aspartic acid[46] as well as lysine,[47–49] the incompatibility of their functional groups with the NCA ring demands the protection and polymer analogous deprotection of these amino acids prior to their conjugation. A successful tryptophan-TAD reaction would overcome these additional steps.

4.2. Results and Discussion

4.2.1 The TADs for Functionalization and Crosslinking

The list of TADs used in this chapter is shown in Figure 4.6. Syntheses of HM-bisTAD and ethyl 4-TAD benzoate were described in Chapter 3. PEG-bisTAD and PEG-monoTAD were synthesized from PEG-bisamine and PEG-monoamine in three steps as shown in figure 4.7.

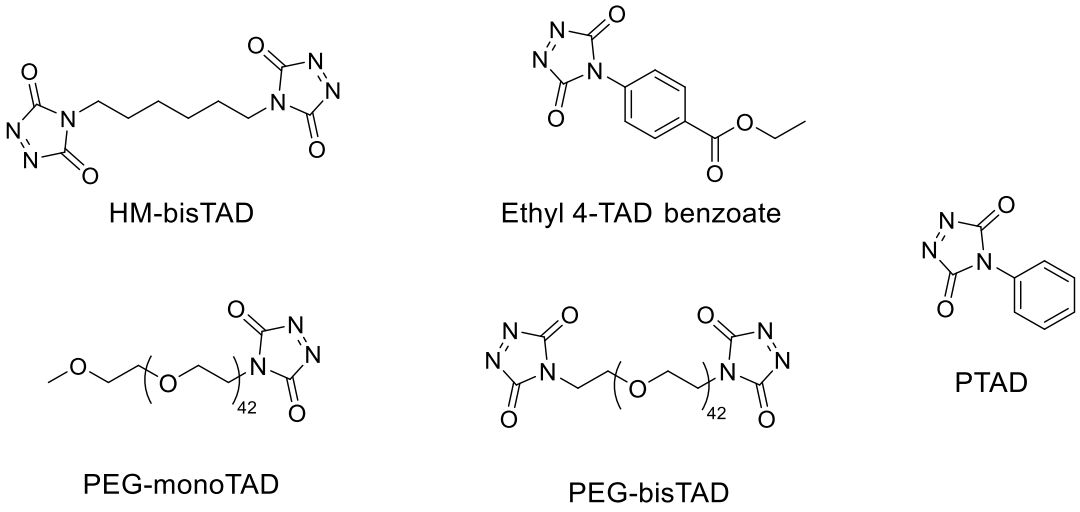

Figure 4.6: TAD derivatives for tryptophan functionalization.

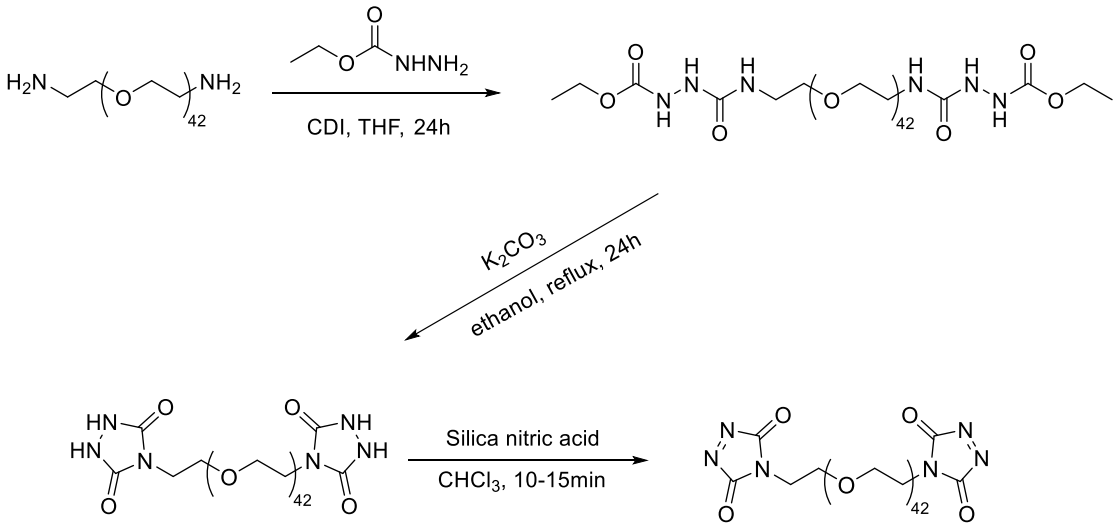

Figure 4.7: Synthesis of PEG-bisTAD

Synthesis of PEG-TAD

In the first step, the PEG-bisamine was reacted with CDI and ethyl carbazate to form the PEG-hydrazinecarboxylate. The CDI impurities from this step could easily be removed by dialysis (Appendix Figure 1). For an efficient dialysis, all THF must be evaporated and the remaining solid dissolved in DI water. In the second step, PEG-hydrazinecarboxylate was converted to PEG-urazole under basic conditions (K_2CO_3, ethanol) and the product was purified by dialysis. In this step, all the ethanol must be evaporated and the solid be dissolved in DI water, while the pH should be set to 7 to prevent damage to the dialysis tubing from acid or base. Unless sufficient time was given for urazole formation, a mixture of PEG-hydrazinecarboxylate and PEG-urazole might be obtained (Appendix Figure 2). After dialysis, the product was recovered by freeze drying, which helped to obtain an extremely dry PEG-urazole. PEG-hydrazinecarboxylate and PEG-urazole formation were confirmed by ^{1}H-NMR (Figure 4.8 and Figure 4.9).

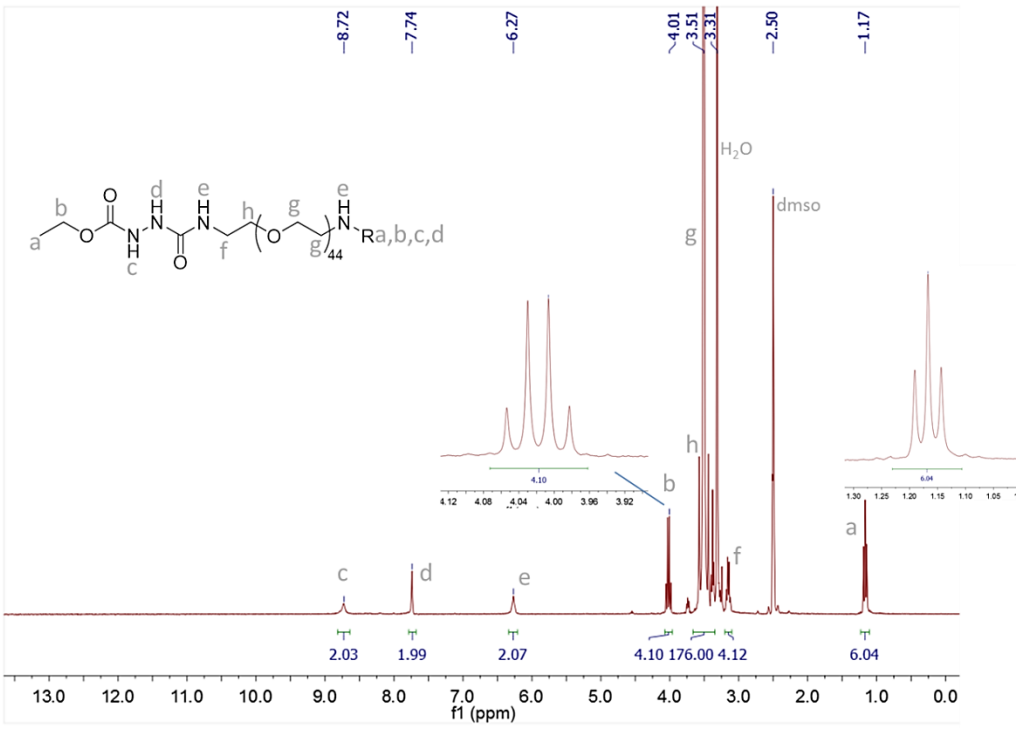

Figure 4.8: ^{1}H-NMR spectrum of PEG-bishydrazinecarboxylate in dmso-d6.

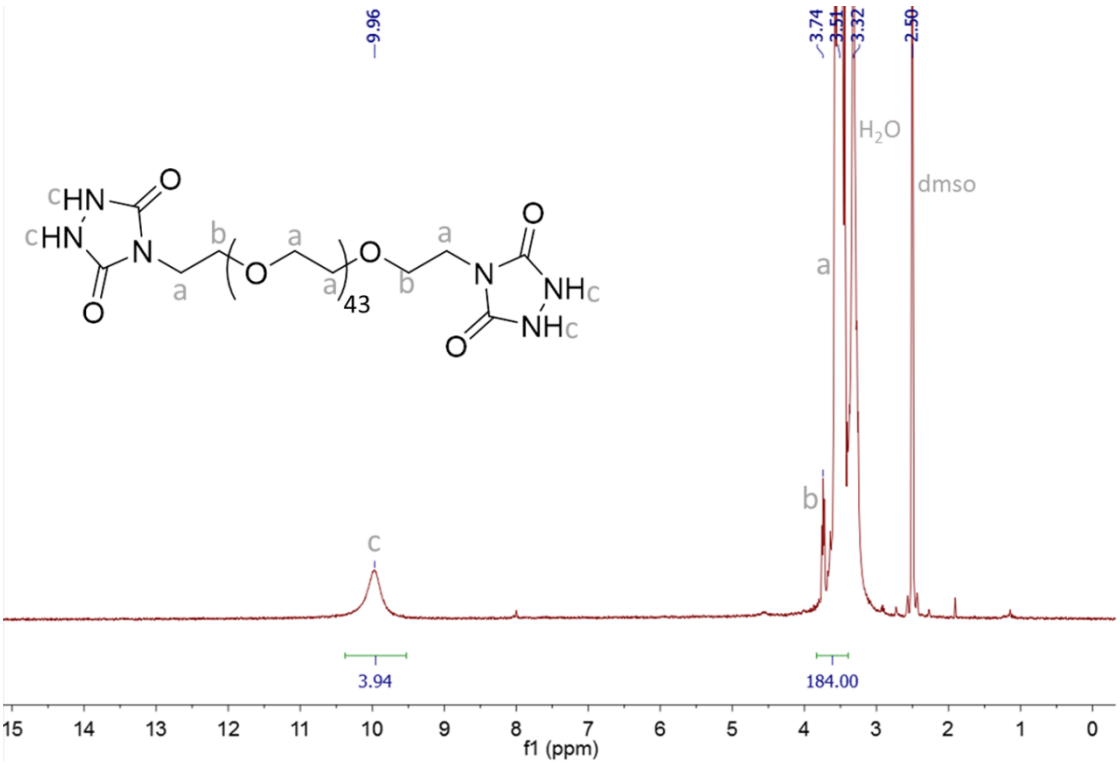

Figure 4.9: ^{1}H-NMR spectrum of PEG-bisurazole in dmso-d6.

The oxidation of PEG-urazole was done with silica nitric acid. It was observed that the oxidation in DMF, THF or acetonitrile was very slow (very faint pink solution – almost transparent). Additionally, the low-intensity color disappeared within 1-2 hours indicating PEG-TAD decomposition. On the other hand, oxidation in chloroform and dichloromethane resulted in a dark pink solution and the color was preserved for at least 24 hours at room temperature. The success of the oxidation step is evident from IR and NMR spectra. The infrared spectra (Figure 4.10) show that the peaks at carbonyl region at 1698 cm^{-1} disappeared and new peaks were observed between 1707 and 1785 cm^{-1}. Additionally, a new peak at 1394 cm^{-1} appeared, probably due to a change in C-N stretching (or N=N). From the ^{1}H-NMR spectrum (Figure 4.11), it was calculated from the integration of NH peak at 10 ppm, that 95% of the urazole groups were converted into TAD within 15 minutes (15% w/w silica nitric acid). Full conversion as evident from the disappearance of the NH peak at 10 ppm, can be

achieved by increasing reaction time or silica nitric acid amount. The PEG-monoTAD was obtained following the same procedure starting from PEG-amine.

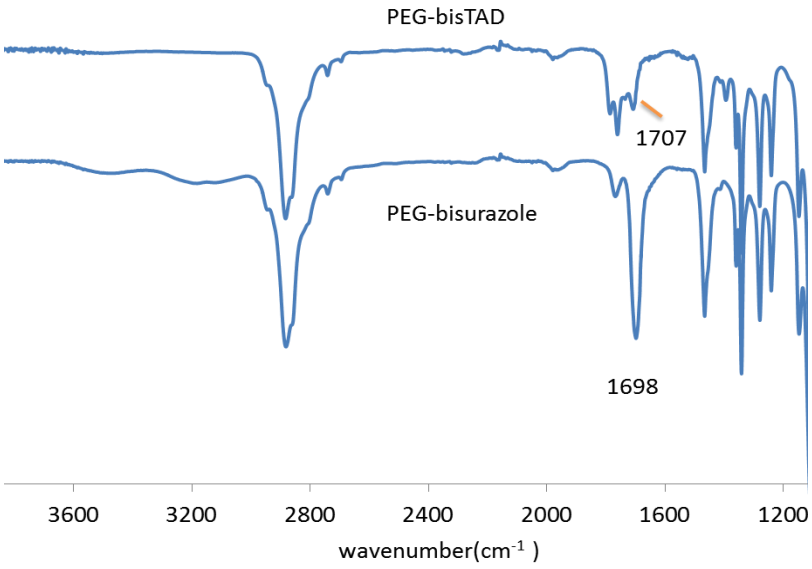

Figure 4.10: IR spectrum of PEG-bisurazole (blue-neat) and PEG-bisTAD (red-neat).

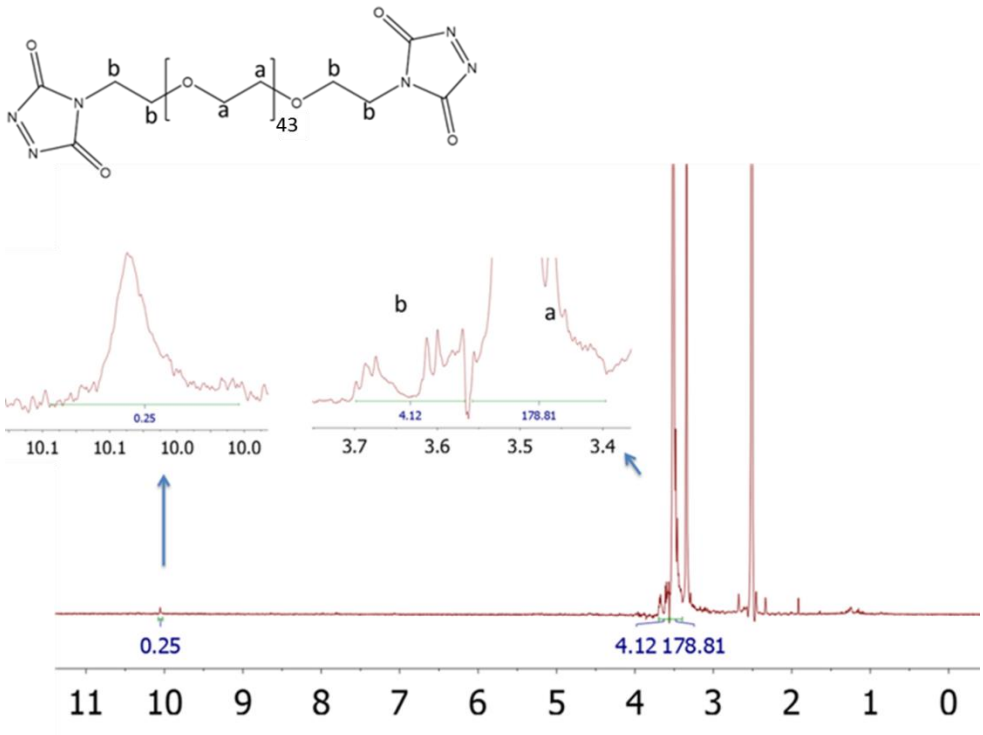

Figure 4.11: ^{1}H-NMR spectrum of PEG2K- bisTAD in dmso-d6. The peak at 10 ppm represents the H-N of non-oxidized urazole.

4.2.2 Synthesis of the Monomer: Tryptophan NCA

Tryptophan NCA was reported in the literature by direct phosgenation of L-tryptophan with triphosgene (Figure 4.12).[50–52] We optimized the reported procedure by adding triphosgene dropwise over a longer period (instead of adding at once as reported) and crystallizing the obtained NCA with heptane/ethyl acetate mixture (instead of only ethyl acetate). Evidence of ring formation can be obtained from the ^{1}H-NMR spectrum (Figure 4.13), specifically from characteristic protons 5 and 6. This is supported by ^{13}C-NMR (Figure 4.14) displaying NCA specific signals from carbons 2, 11 and 12. The IR spectrum (Figure 4.15) shows the typical NCA carbonyls 1842 cm^{-1} and 1773 cm^{-1}. Those peaks also disappear after polymerization allowing easy monitoring of the reaction progress.

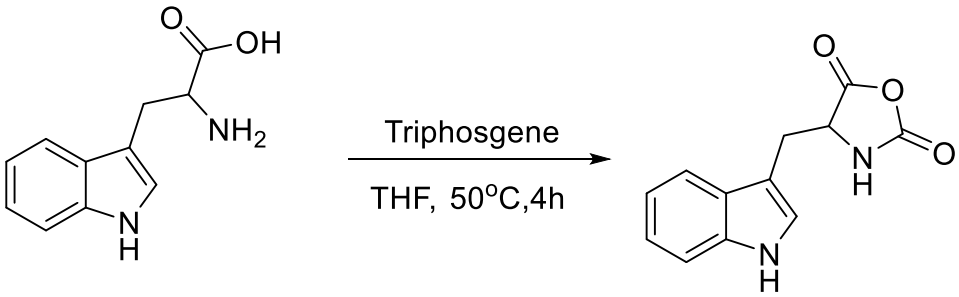

Figure 4.12: Synthesis of tryptophan NCA

Upscaling of the tryptophan NCA synthesis (>10 g) enabled the preparation of large amounts of tryptophan containing polypeptides, which were used for the synthesis of hydrogels by the tryptophan-TAD reaction for biocompatibility studies and mechanical analyses (Chapter 5).

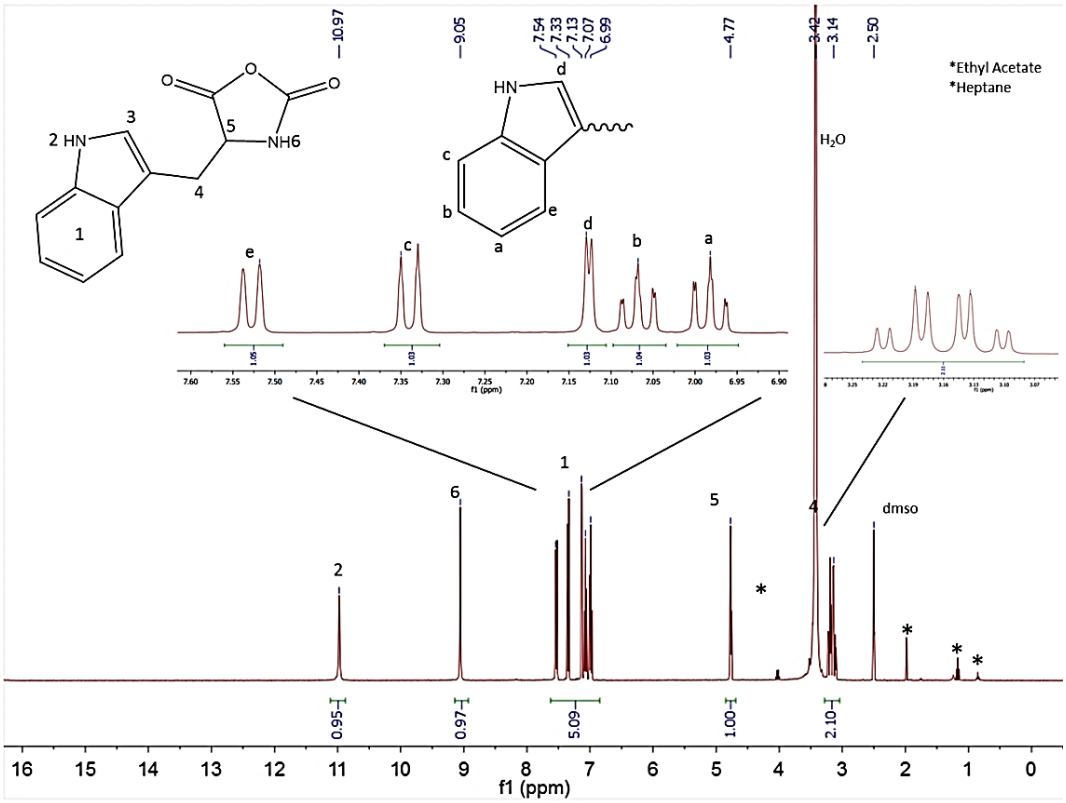

Figure 4.13:[1]H-NMR of tryptophan NCA in dmso-d6.

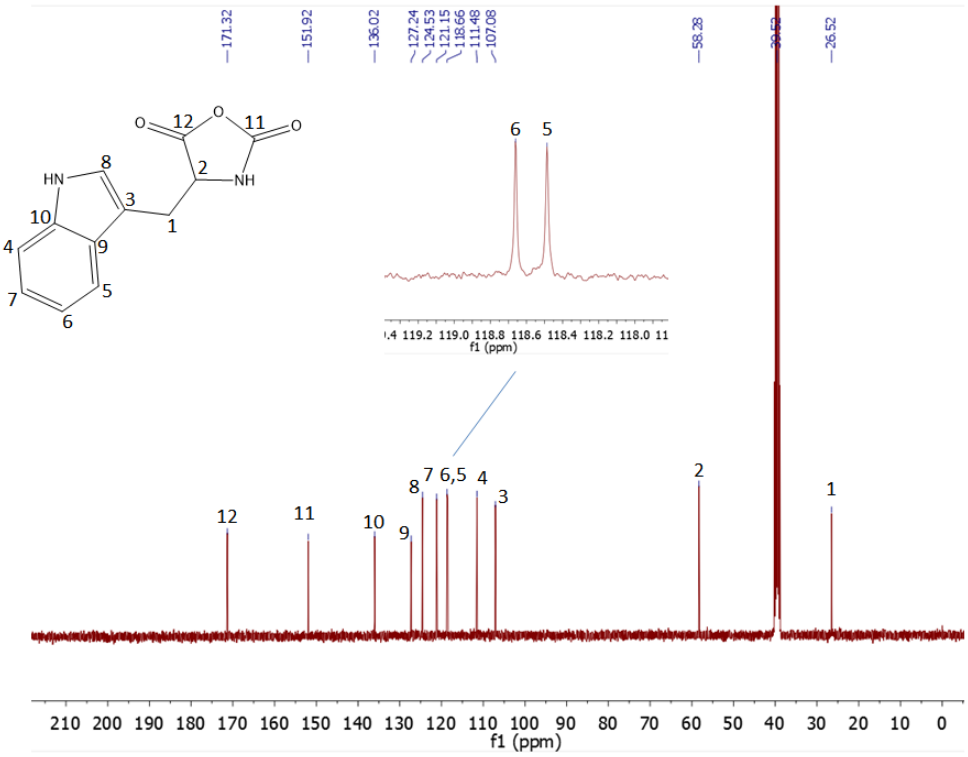

Figure 4.14: [13]C-NMR of tryptophan NCA in dmso-d6.

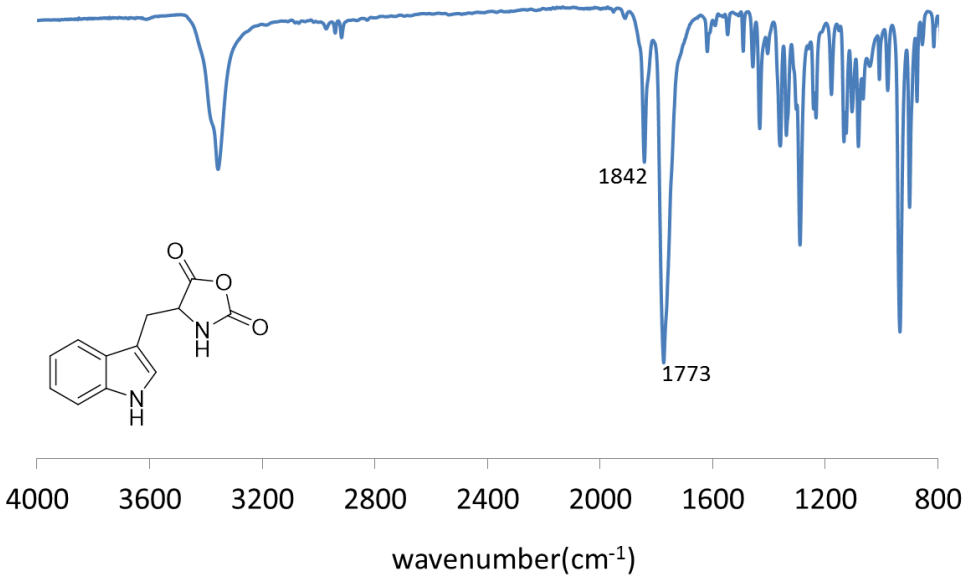

Figure 4.15: IR spectrum of tryptophan NCA (neat). The NCA carbonyl peaks are seen at 1842 cm^{-1} and 1773 cm^{-1}.

4.2.3 TAD-Tryptophan Functionalization and Crosslinking

4.2.3.1 Reaction with PEG-Trp block copolymers

We observed that the PEG-TAD derivatives were stable in chloroform and dichloromethane but not in DMF. Polypeptides are generally soluble in DMF, sometimes in chloroform and mixtures of these solvents or with other solvents such as acetonitrile. Therefore, to test the PEG-TAD reaction with polypeptides, we aimed to prepare a tryptophan polypeptide initiated from PEG2K-amine as PEG would facilitate the polypeptide solubility. The success of this reaction is evident from the ^{1}H-NMR spectrum yielding a tryptophan block length of 5-6 units (Figure 4.16). This polymer was soluble in dichloromethane and when mixed with PEG-bisTAD (Trp:TAD 1:1), a hydrogel was obtained within 5-10 seconds (Figure 4.18 and 4.19). When the reaction was carried out in chloroform an instantaneous reaction was observed, in some cases leading to inhomogeneous gels.

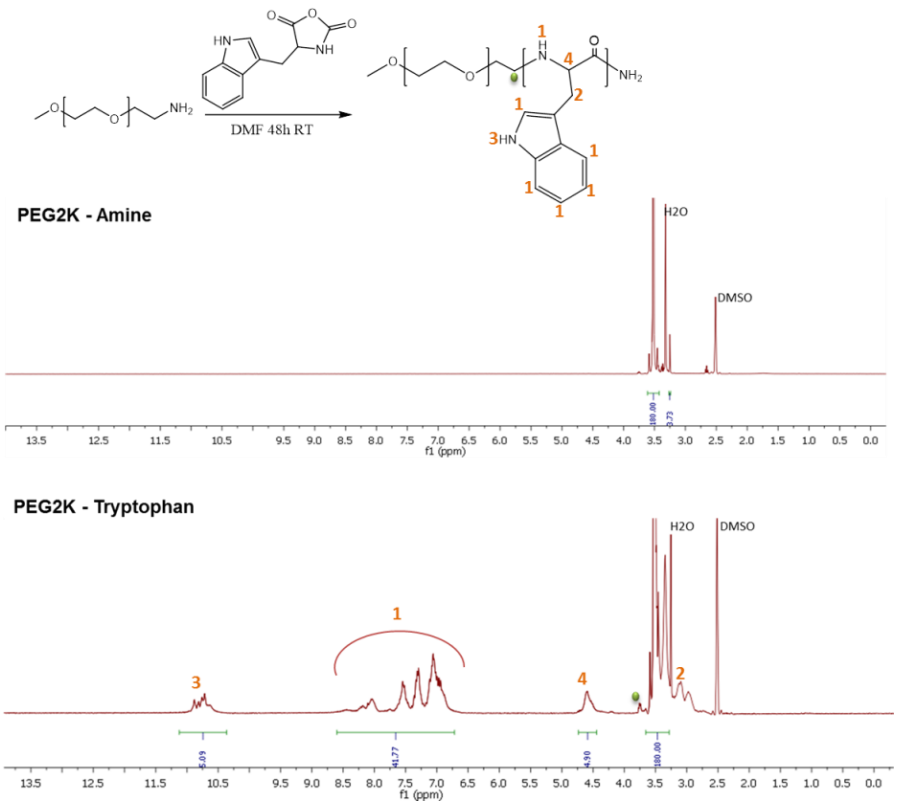

Figure 4.16. ^{1}H-NMR spectrum of PEG2K-amine and PEG2K-tryptophan in dmso-d6.

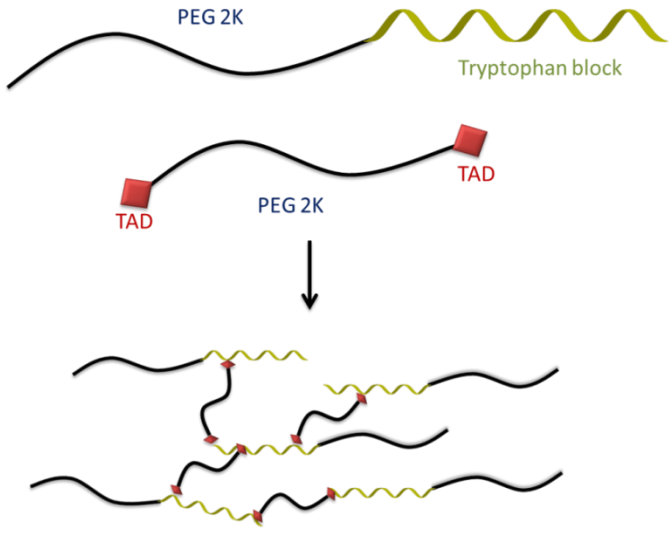

Figure 4.17. Hybrid polypeptide hydrogel made by tryptophan-TAD click.

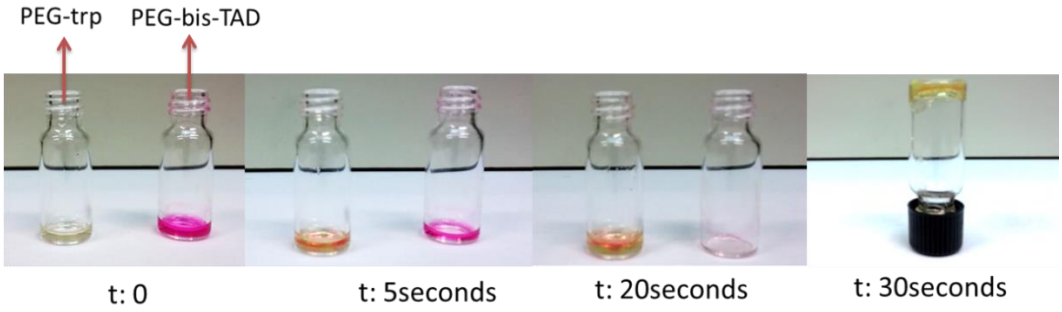

Figure 4.18. Crosslinking PEG-Trp polypeptide with PEG-bisTAD in dichloromethane. The reaction was fast and the color disappears within 5-10 s if shaken vigorously.

Figure 4.19. Crosslinking poly(z-Lys-*st*-Trp) with PEG-bisTAD in chloroform. Instantaneous reaction prevents proper mixing and resulted in a precipitate like gelation.

4.2.3.2 Reaction with Poly(Z-Lys-st-Trp) Copolypeptides

For further tests of TAD functionalization, a statistical copolymer of tryptophan and Z-lysine (denoted P6) was prepared by hexyl amine initiator with tryptophan NCA to Z-lysine NCA ratio of 15:85 (Figure 4.20). Quantitative copolymerization was monitored with the help of FTIR spectroscopy by the disappearance of the NCA carbonyl peaks at 1842 cm^{-1} and 1773 cm^{-1} (Figure 4.15) and appearance of polypeptide backbone amide peaks at 1696 cm^{-1} and 1648 cm^{-1} (Figure 4.21). ^{1}H-NMR analysis (Figure 4.22) of the copolymer largely confirmed agreement of the polymer composition, poly(Z-

Lys_{85}-*st*-Trp_{15}), with the monomer feed ratio, although overlapping peaks result in a somewhat reduced accuracy of the peak integration.

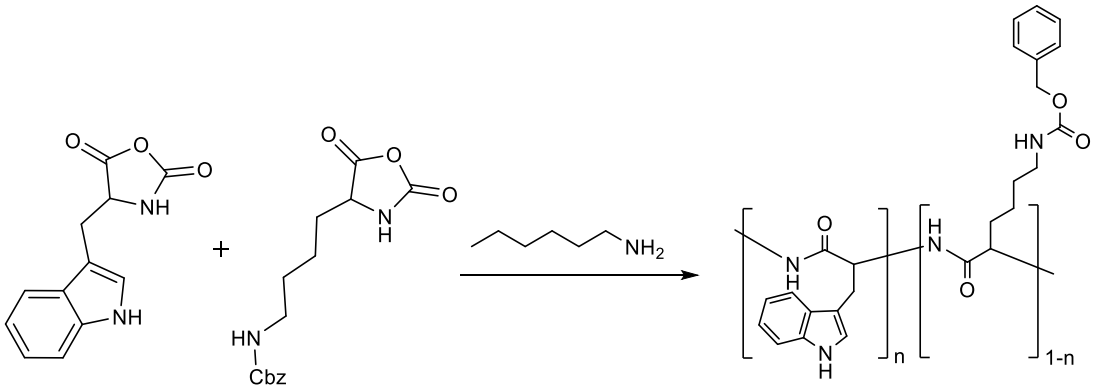

Figure 4.20: Synthesis of poly(Z-Lys-*st*-Trp)

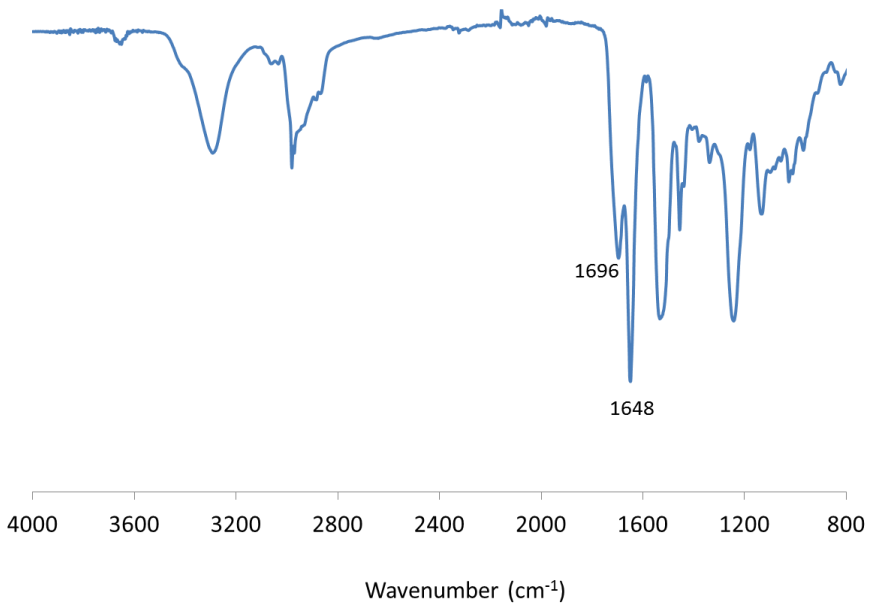

Figure 4.21: FTIR spectrum of poly(Z-Lys-*st*-Trp). Characteristic polypeptide amide peaks can be seen at 1696 cm^{-1} and 1648 cm^{-1}.

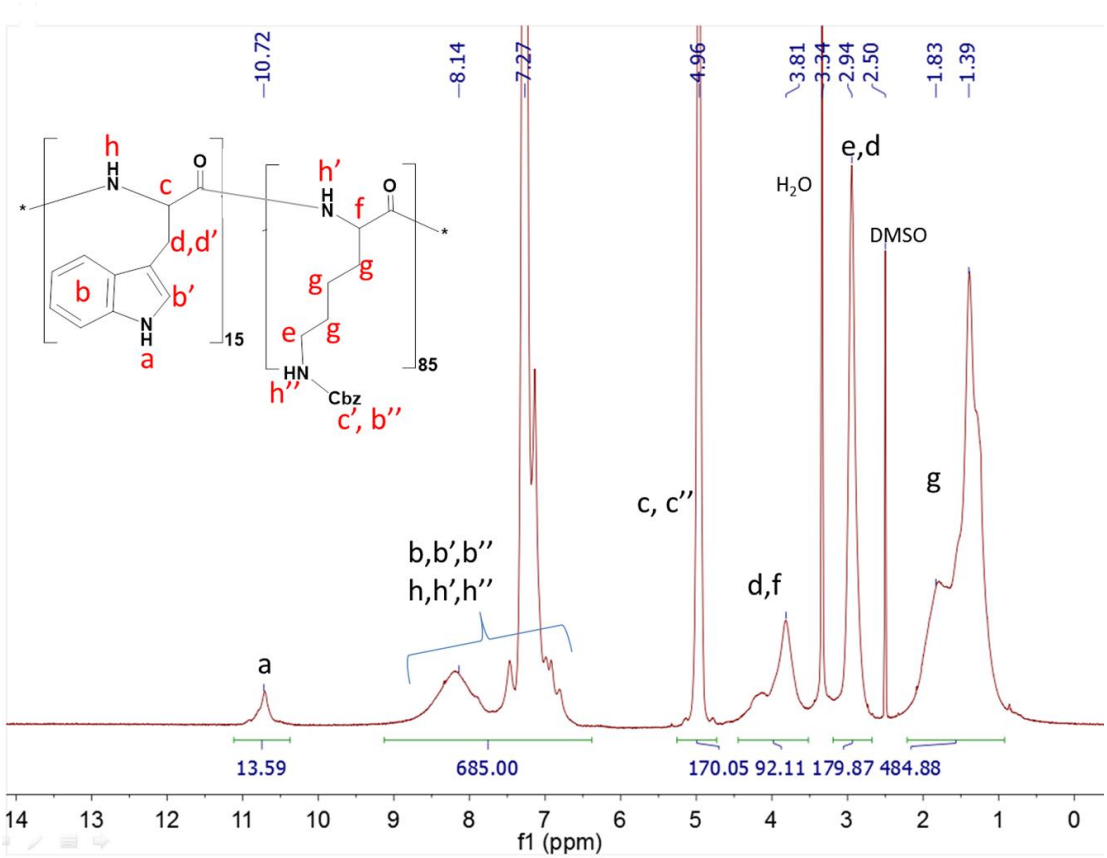

Figure 4.22: ^{1}H-NMR of poly(Z-Lys$_{85}$-*st*-Trp$_{15}$) in DMSO-d6.

TAD-tryptophan reaction may take place at C2 or C3 of indole group as shown in figure 4.23. However, the main product is more likely C2 adduct due to enhanced carbocation stability and less steric hindrance at intermediate step. In the following only the C2 adduct is presented since spectroscopically no conclusive evidence for the C3 adduct was found.

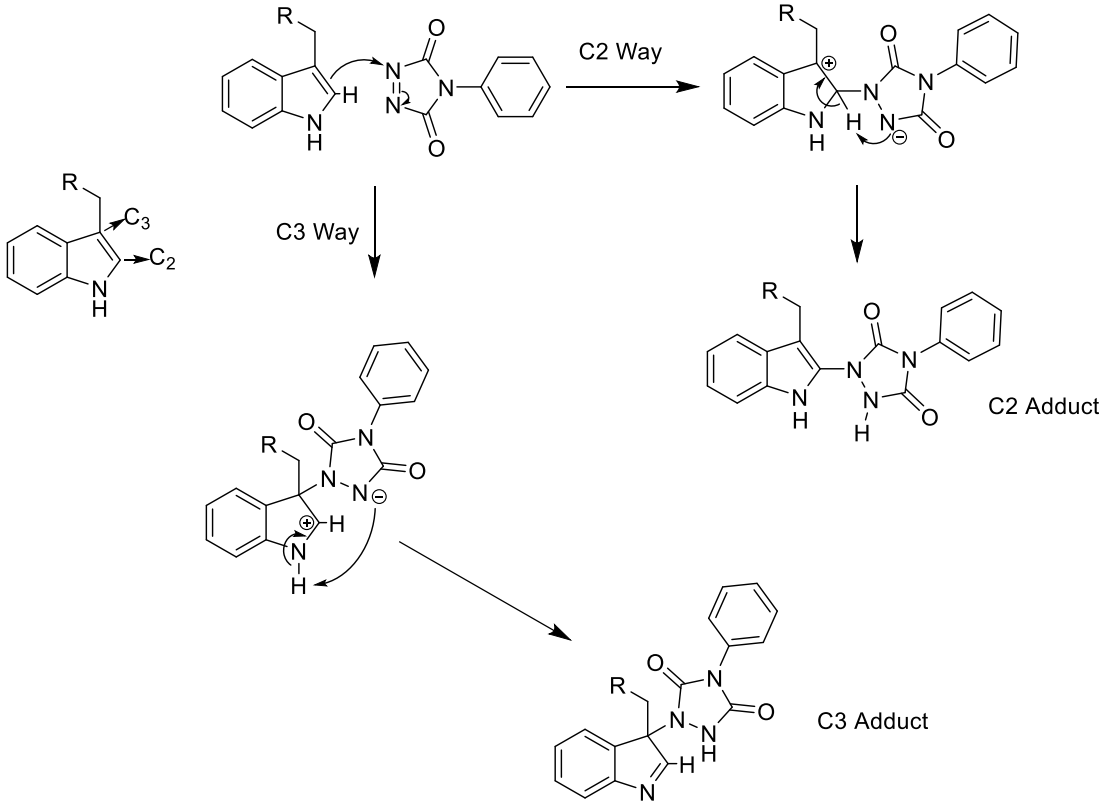

Figure 4.23. PTAD-Tryptophan reaction mechanism.

Initially, poly(Z-Lys$_{85}$-*st*-Trp$_{15}$) was reacted with PTAD at a ratio of PTAD to Trp of 1.1:1 in acetonitrile/chlorofom (1:1) mixture. ^{1}H-NMR confirmed the success of the reaction from the presence of NH protons **a** and b in Figure 4.24.

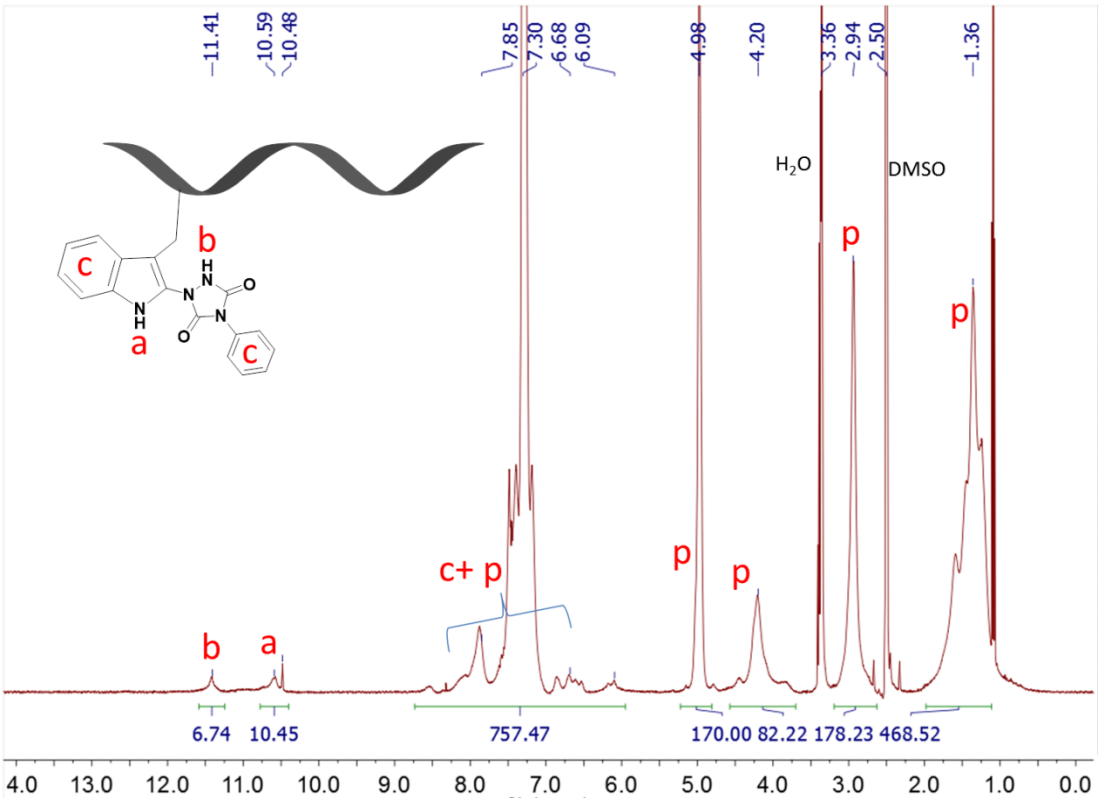

Figure 4.24: ^{1}H-NMR spectrum of poly(Z-lys$_{85}$-st-trp-PTAD$_{15}$).

The IR spectrum of the reaction product shows that the additional carbonyl groups of the TAD moiety change the pattern in the carbonyl region after functionalization. Additional peaks at 1773 cm^{-1} and 1770 cm^{-1} were assigned to the carbonyls of PTAD (Figure 4.25). As a second TAD derivative, TAD-benzoate was investigated in this reaction and it was found that it reacts with tryptophan similar to PTAD. Simple mixing of the copolypeptide with the TAD solution at room temperature is sufficient and the reaction can be monitored by the color change. Although N-H protons of the copolypeptide backbone and the attached TADs were not identifiable in the ^{1}H-NMR spectrum of TAD-benzoate product, the protons of the ethyl ester groups of TAD-benzoate were clearly distinguishable (Figure 4.26).

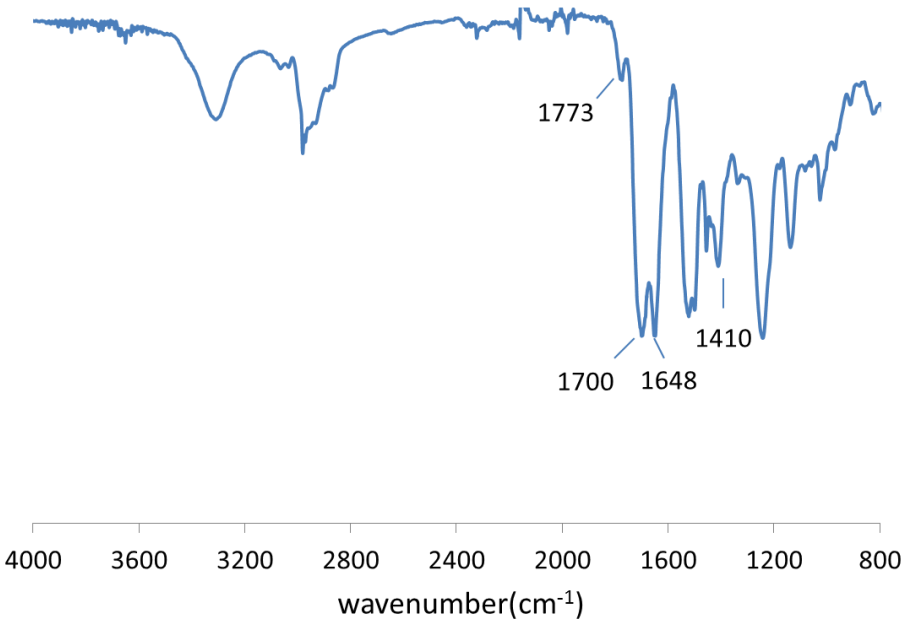

Figure 4.25: IR spectrum of PTAD functionalized poly(Z-Lys$_{90}$-st-Trp$_{10}$). The carbonyl peaks pattern changed due to extra carbonyl peaks from PTAD.

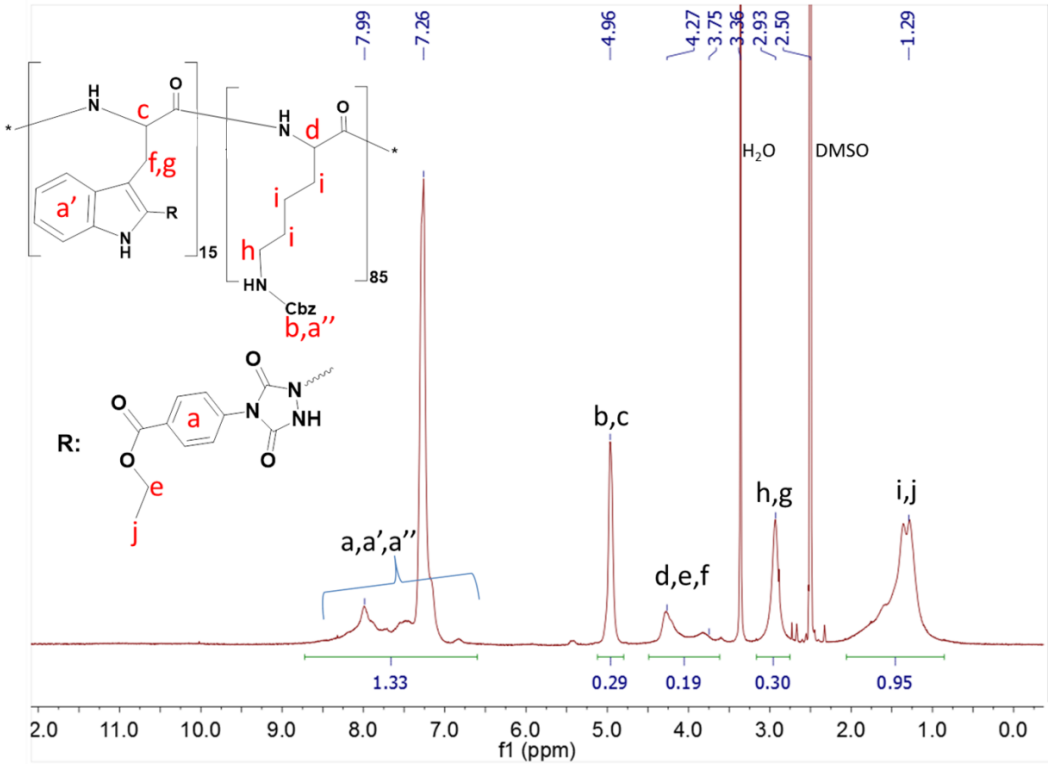

Figure 4.26: ^{1}H-NMR of TAD-benzoate functionalized poly(Z-Lys$_{85}$-*st*-Trp$_{15}$) in dmso-d6.

GPC chromatograms show that the hydrodynamic volume has clearly shifted after copolypeptide functionalization. P6 (M_w: 9.66 kg/mol, PDI: 1.11) had the lowest elution time in DMF, while both P6-PTAD (M_w: 15.54 kg/mol, PDI: 1.18) and P6-TADbenzoate (M_w: 15.89 kg/mol, PDI:1.28) eluted at a lower retention time (Figure 4.27).

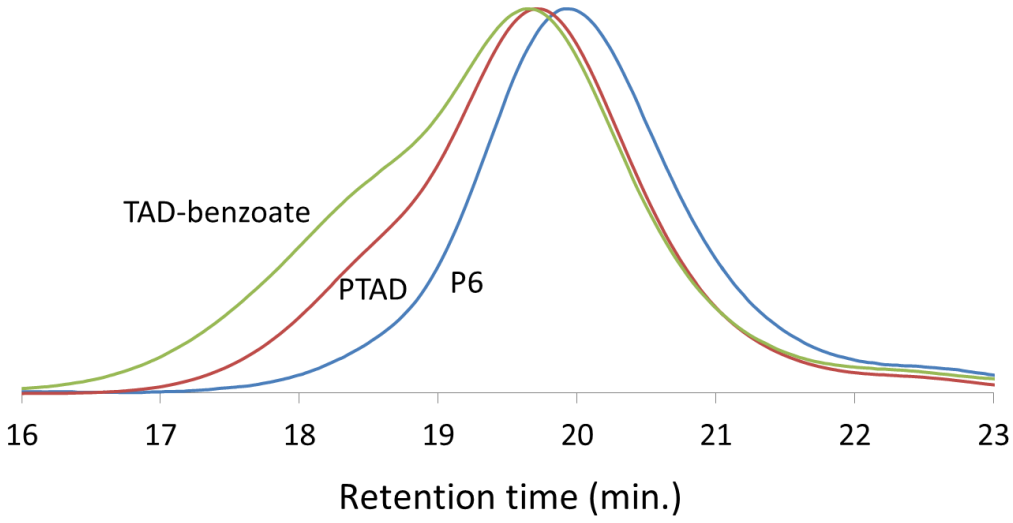

Figure 4.27. GPC chromatogram of P6 (blue), P6 PTAD (red) and TAD-Benzoate functionalized P6 (green).

The instantaneous reaction of P6 with PEG-monoTAD (1:1.1 eq. Trp: PEG-monoTAD) was carried out in chloroform and the obtained copolymer analyzed by GPC. Comparison of the chromatograms before and after PEGylation highlights a clear shift to higher molecular weights evident of a successful PEGylation of the polypeptide (Figure 4.28). As an excess of PEG-TAD was used, a signal representing unreacted PEG-TAD can also be seen in the chromatogram.

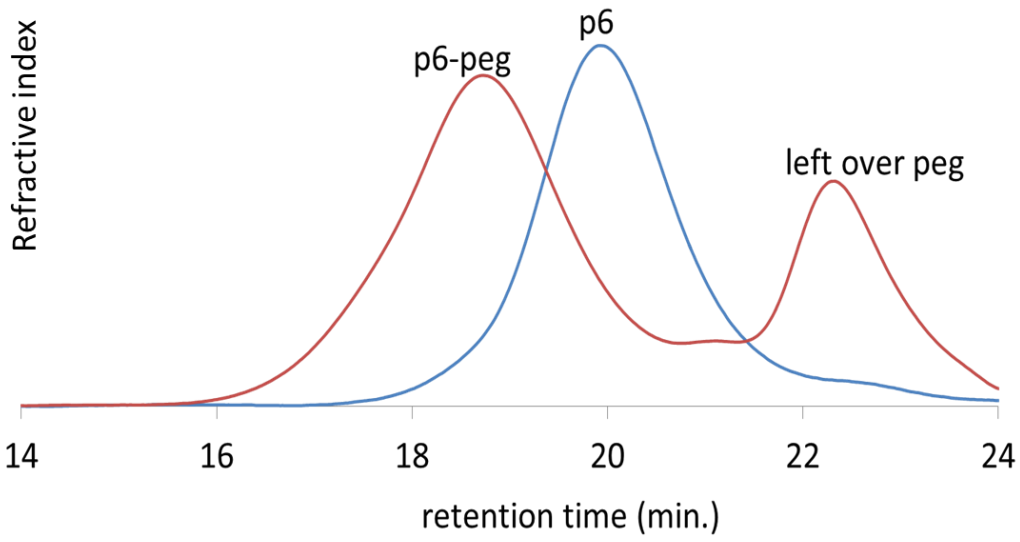

Figure 4.28. SEC analysis of P6 before and after reaction with PEG-TAD.

The TAD functionalizations with tryptophan are highly valuable because tryptophan NCA does not require protection-deprotection chemistry like other amino acids. Additionally, tryptophan is a natural amino acid that can be commercially obtained at a very affordable price and at high quality. The reaction is highly selective (because other amino acids are on protected form) so that other amino acids such as lysine, glutamic acid or cysteine can be used with tryptophan without concerns about their protecting groups or orthogonal deprotection strategies. Therefore, tryptophan-TAD functionalization is probably the easiest and most convenient modification method for the NCA-derived polypeptides to date.

4.2.4 Co-Click Functionalization of Poly(Z-lys-st-trp)

In this part, we explored how well TAD-tryptophan functionalization integrates with other common click reactions, i.e. thiol-ene and azide-alkyne cycloaddition. A similar copolypeptide of CBZ-lysine and tryptophan was synthesized using propargylamine and allylamine as initiators (poly($Lysine_{50}$-st-Trp_{20}). This adds alkene and alkyne end groups to polypeptides (Figure 4.29).

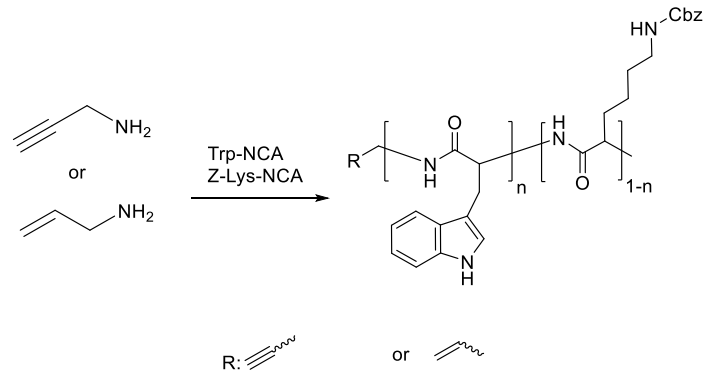

Figure 4.29 NCA polymerization initiated by propargyl amine or allylamine

4.2.4.1 Thiol-ene Functionalization Following PTAD

PTAD functionalization of both copolymers was successfully done using the functionalization conditions described above. ^{1}H-NMR spectra show that the alkene endgroups of the copolypeptides were still intact. The presence of alkene group can be seen at 5.70 ppm after polymerization (proton –i- in figure 4.31) and after PTAD functionalization (proton –i- in figure 4.32).

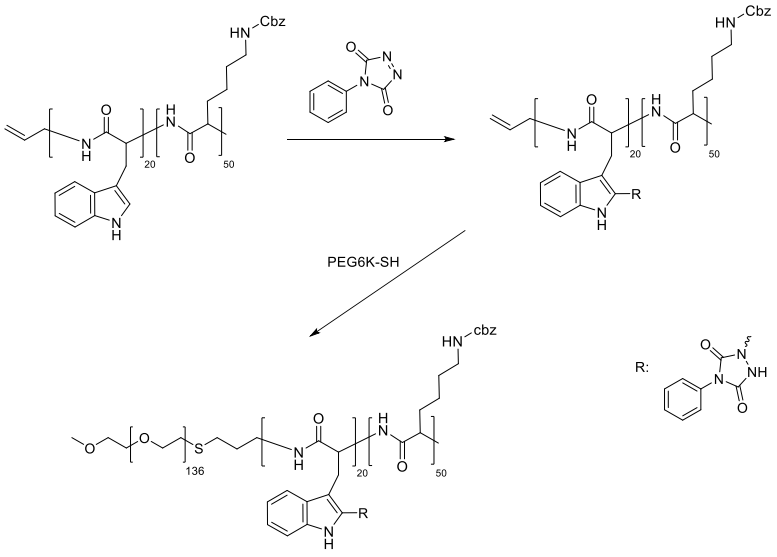

Figure 4.30 Thiolene click reactions following TAD click on poly(Lys_{50}-*st*-Trp_{20}).

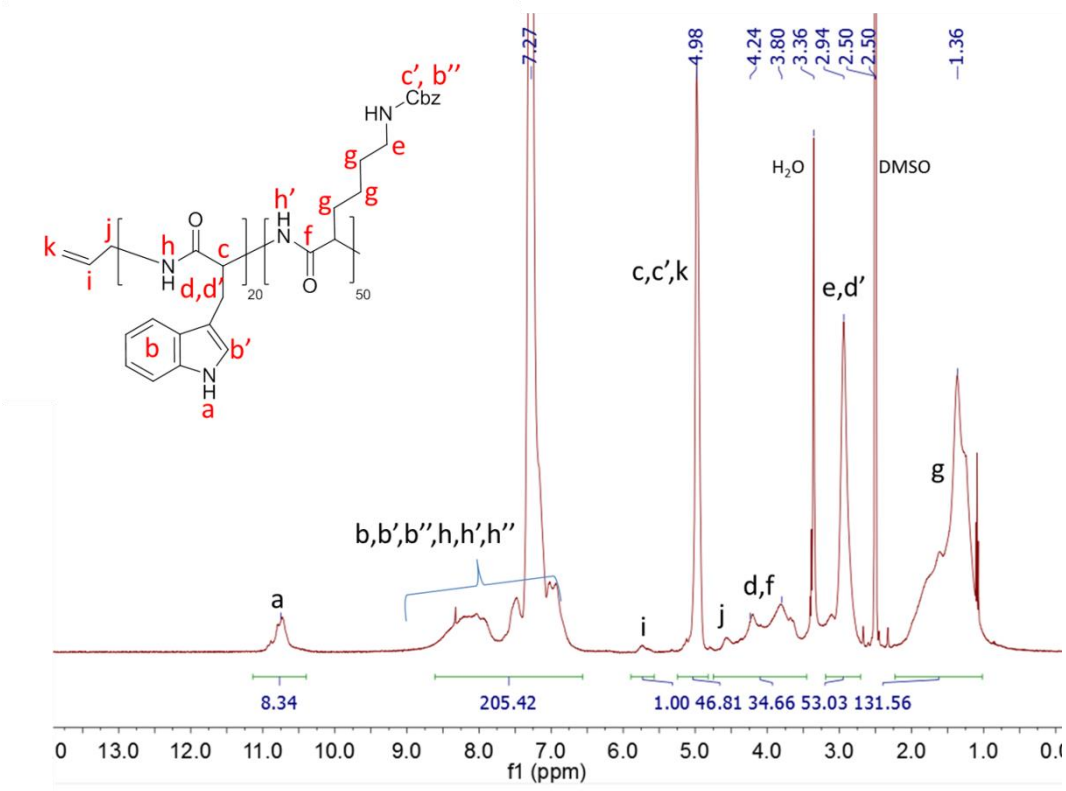

Figure 4.31: ^{1}H-NMR of allylamine initiated poly(Z-Lys$_{50}$-*st*-Trp$_{20}$) in dmso-d6.

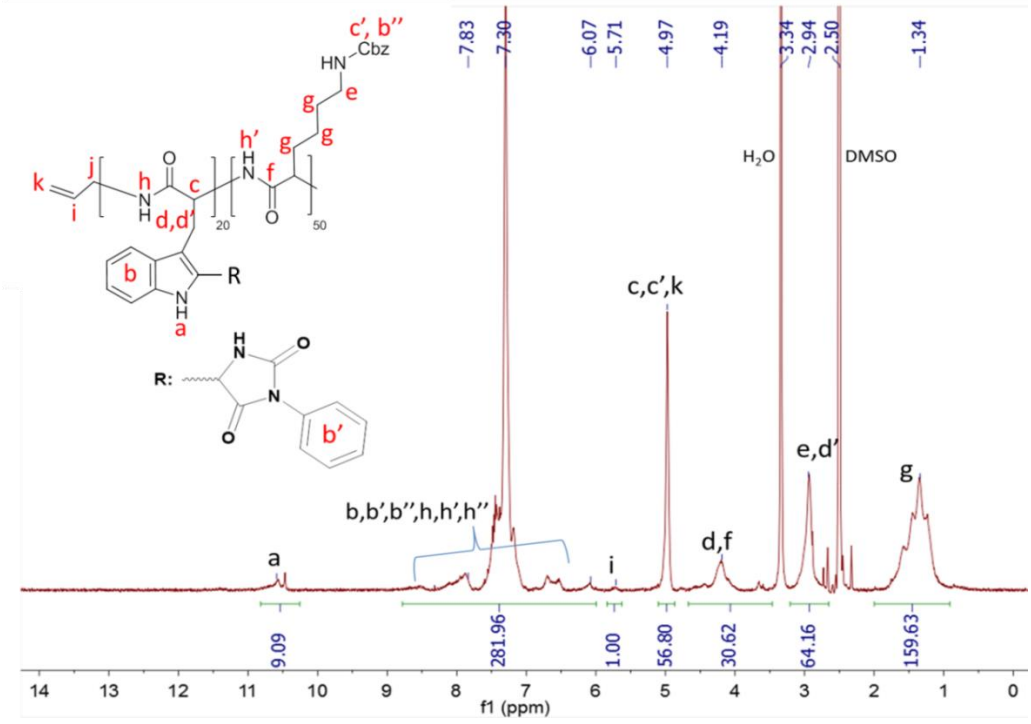

Figure 4.32: ^{1}H-NMR of PTAD functionalized poly(Z-Lys$_{50}$-st-Trp$_{20}$) in dmso-d6.

Thiol-ene reaction was then tested with the allylamine terminated poly(Z-Lysine$_{50}$-st-Trp$_{20}$TAD) (Figure 4.30). PEGylation of the end group was attempted with PEG6K-monothiol under UV irradiation and in the presence of a photoinitiator. The reaction product was washed extensively to remove all unreacted PEG. The NMR spectrum of the polymer clearly shows the presence of PEG suggesting a successful reaction although the reaction yield cannot be quantified by this method (figure 4.33).

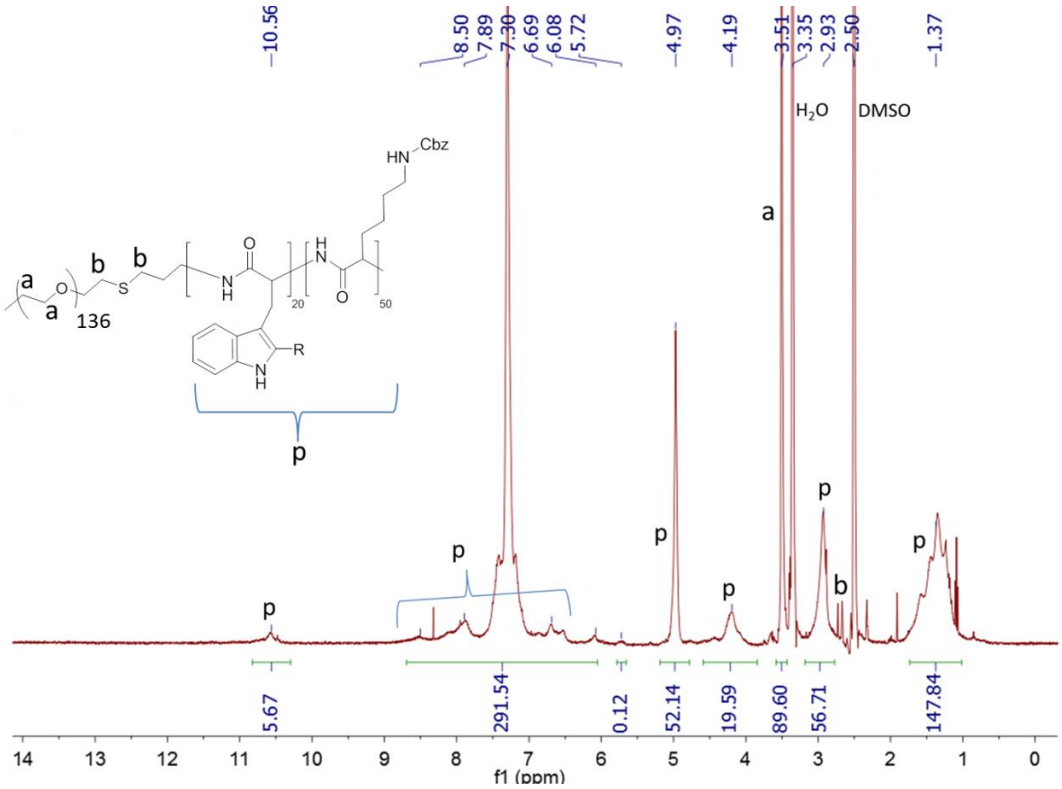

Figure 4.33: ^{1}H-NMR of PEGylated - PTAD functionalized poly(Z-Lys$_{50}$-*st*-Trp$_{20}$) in dmso-d6. New PEG peaks can be seen at 3.51 ppm.

Further evidence for a successful reaction was obtained from SEC analysis. SEC chromatograms confirmed an increase on molecular weight upon PTAD reaction and PEGylation (Figure 4.34). The tailing of the final polymer trace suggests that the end-group reaction with PEG-thiol was not quantitative, a conclusion that is not unreasonable considering the steric aspects of this polymer-polymer reaction. We

believe that the small peaks at ca. 22 min. are due to the polyallylamine formation in allylamine bottle.

While these preliminary results demonstrate the compatibility of the thiol-ene and TAD-Trp reactions, further optimization would be required to gain a better understanding of reaction conditions and selectivity.

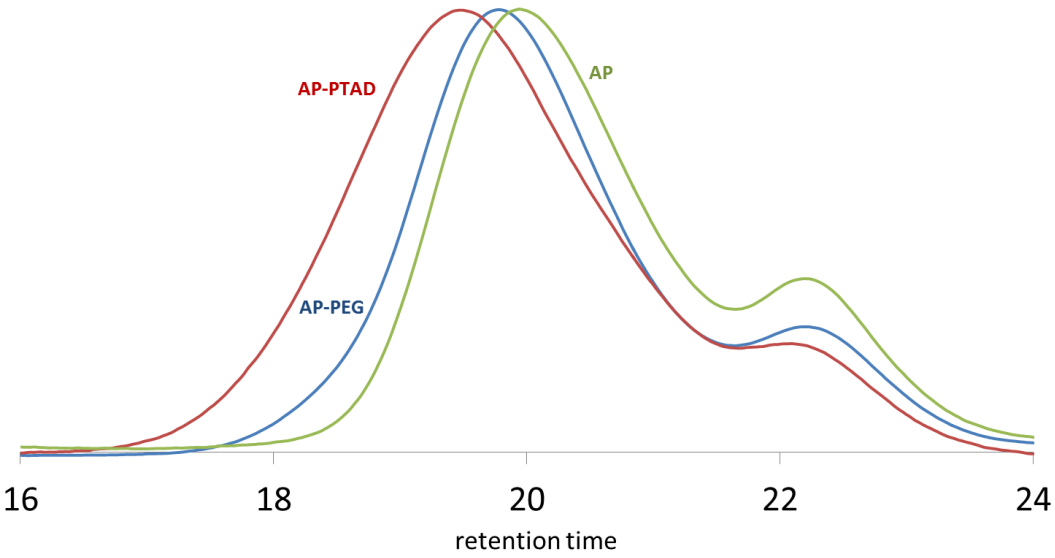

Figure 4.34. GPC chromatogram of allylamine initiated polypeptide (AP, green), its PTAD functionalization (AP-PTAD, red) and PEGylated polypeptide after PTAD attachment (AP-PEG, blue).

4.2.4.2 Azide-Alkyne Functionalization Following PTAD

As a second polymer, propargyl amine initiated copolypeptide was synthesized (Figure 4.35). While according to the polymerization mechanism the copolypeptide must be end-capped with the propargyl group, this is difficult to prove spectroscopically due to the low signal intensity of the propargyl group. The example of the ^{1}H-NMR spectrum is presented in Figure 4.36. The polymer was then reacted with PTAD and the Lys deprotected , which made the copolymer water soluble.

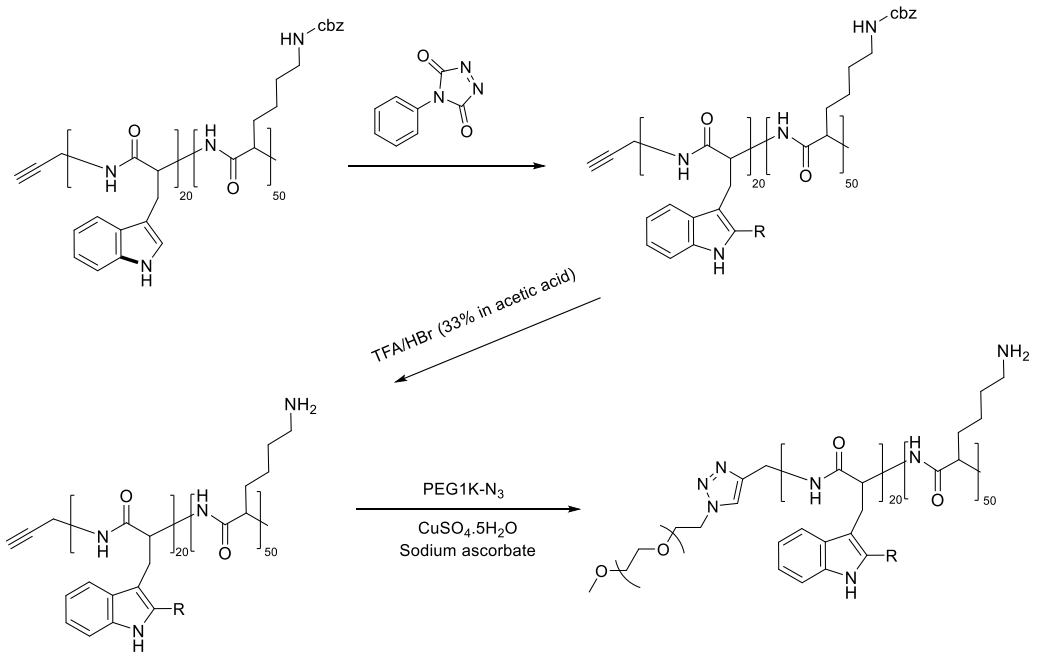

Figure 4.35: Cu-catalyzed cycloaddition followed by PTAD functionalization and deprotection of the Cbz group.

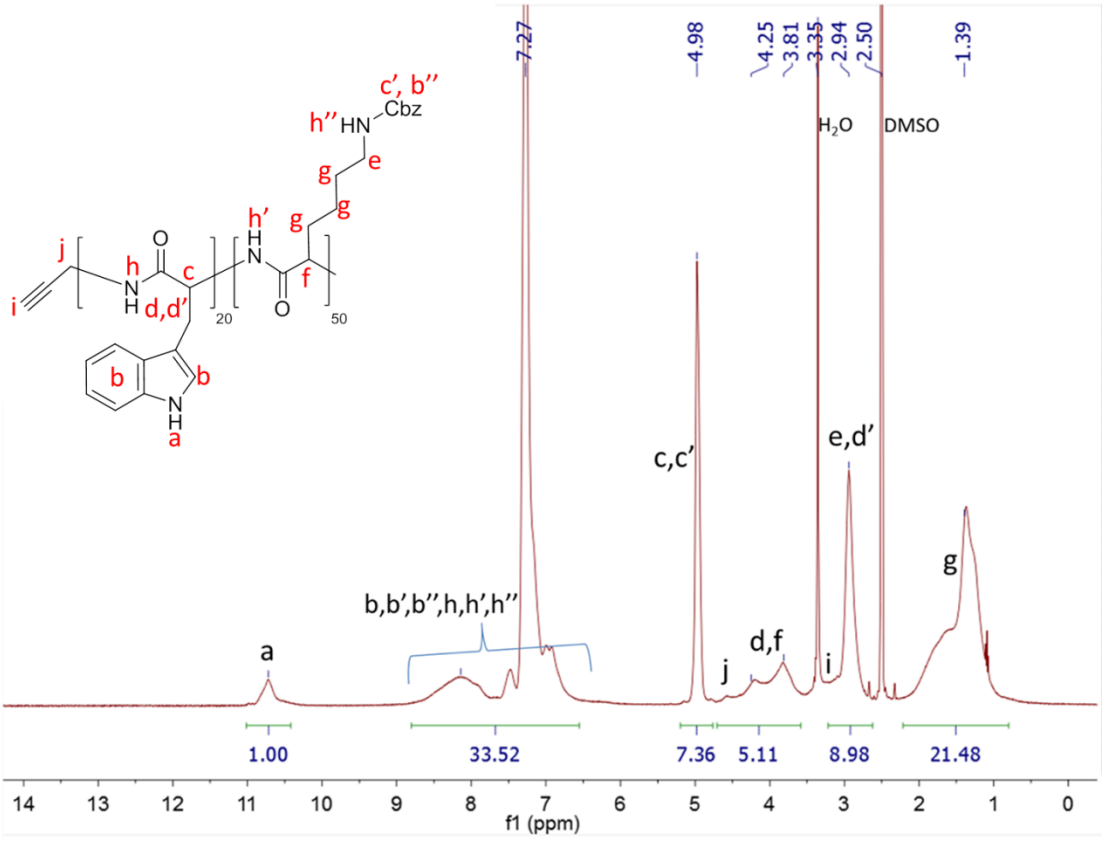

Figure 4.36: ^{1}H-NMR spectrum of propargyl amine initiated poly(Z-Lys$_{50}$-*st*-Trp$_{20}$).

Finally, the propargyl end-group was reacted with an azide functional PEG in a azide/alkyne click reaction. FTIR spectrum of the product showed characteristic PEG-azide (2107 cm^{-1}) signal due to the use of an excess of this reactant. After precipitating in ethanol, the PEG-azide peak has completely disappeared (Figure 4.37) highlighting the efficient removal of the unreacted PEG-azide. NMR data of the purified product display characteristic PEG peaks, which can only be explained from a successful reaction of the PEG-azide with the polymer end-group (Figure 4.38).

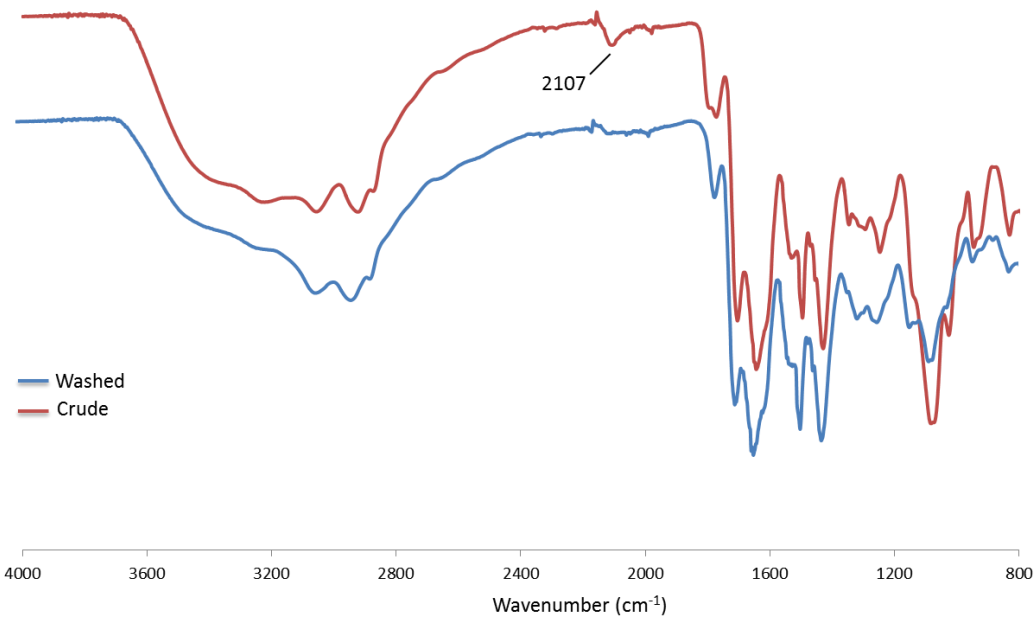

Figure 4.37. IR spectrum of the crude of PEGylated PTAD-polypeptide and purified one.

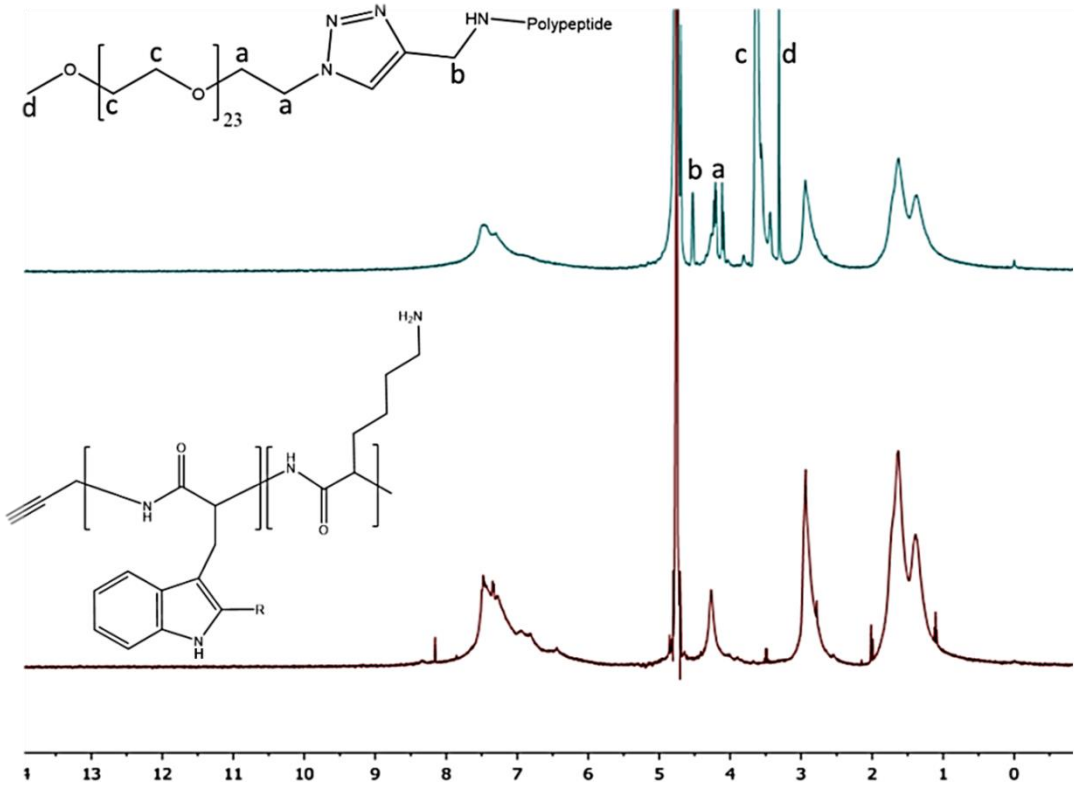

Figure 4.38: ^{1}H-NMR spectra of PTAD functionalized propargylamine initiated (Lys_{50}-*st*-Trp_{20}) i.e. deprotected polypeptide (red) and PEGylated polypeptide (green).

4.3. Conclusion

In conclusion, tryptophan-containing polypeptides with narrow PDIs were prepared by tryptophan NCA and lysine NCA. Successful reaction with TAD derivatives was demonstrated including the reaction with PEG mono and bis-TAD. Preliminary results suggest the compatibility of this reaction with thiol-ene and alkyne-azide click reactions. This TAD-Trp reaction has high potential to be used frequently to modify NCA derived materials due to it is versatile and easy chemistry. Additionally, Trp is a natural amino acid and does not require protection-deprotection chemistry to be compatible with NCA polymerisation, unlike other natural amino acids.

4.4. Experimental

Synthesis of Tryptophan NCA: Tryptophan (10g, 48,97 mmol) was placed into 250 mL three neck round bottom flask and dried in vacuum oven for 2 days at 40^{o}C. Then, 100 mL of anhydrous THF added together with α-pinene (19.8 g, 17mL, 145mmol) under an inert atmosphere. The reflux condenser was placed and temperature set to 50^{o}C. Triphosgene (7g, 23.6 mmol) dissolved in anhydrous THF and added to this mixture dropwise using dropping funnel. The reaction mixture became clear yellow solution after 2-3 hours. Then, half of the solvent was evaporated using rotavap and solution precipitated into cold heptane and kept in -20^{o}C overnight. Semi crystalline-powder precipitate collected by vacuum filtration and recrystallized using 1:1 ethyl acetate/heptane mixture without stopping the stirring while cooling period of crystallization. Yellowish white powder collected by vacuum filtration and dried in the vacuum line. Yield: 7.47 g, 66.2%. ^{1}H-NMR (400 MHz, DMSO, ppm): 3.13-3.19 (dd, 2H), 4.76 (t, 1H), 6.98 (m, 1H), 7.07 (m, 1H), 7.13 (d, 1H), 7.35 (d, 1H), 7.52 (d, 1H), 9.05 (s, 1H), 10.57 (s, 1H). ^{13}C-NMR (400 MHz, DMSO-d6): 26.42, 58.18, 106.98, 111.39, 118.39, 118.57, 121.05, 124.44, 127.15, 135.93, 151.83, 171.23. FTIR(neat, cm^{-1}): 3355, 3002, 1842, 1773, 1618, 1491, 1457, 1432, 1432, 1359, 1337, 1289, 1232, 1177, 1133, 1104, 1081, 1007, 977, 933, 899, 814, 783, 764, 750, 674, 650, 633, 609.

Synthesis of Poly(Lys$_{85}$-Trp$_{15}$): 2600 mg of Lysine NCA (8.5 mmol) and 345 mg of Trp NCA (1.5 mmol) was added into dried schelenck line under inert atmosphere and dissolved in 15 mL DMF. To this solution, 10.7 mg of benzylamine (0.1 mmol) from stock solution was added fast and the solution stirred under vacuum. After, 5-6 hours the solution was precipitated into diethyl ether. The sticky product was dissolved in chloroform and reprecipitated into diethyl ether. Finally, non-sticky powder product was collected by vacuum filtration and dried under vacuum. Yield: 2.23g, 91 %

Synthesis of P6–PTAD: 200mg of poly(lys_{90}-st-trp_{10}) dissolved in 2 mL chloroform/acetonitrile (1:1). Commercially available PTAD (12 mg – theoretically 1 eq. to tryptophan) was dissolved in 0.2 mL acetonitrile and added to the polymer solution. The red color of PTAD was disappeared after 40-60 minutes indicating no more PTAD left in the solution. Then, the solution was precipitated into diethyl ether and collected by vacuum filtration. Isolated yield: 205 mg

Synthesis of P6-TAD Benzoate: 200mg of poly(lys90-st-trp10) dissolved in 2 mL chloroform/acetonitrile (1:1). TAD-Benzoate (17.2 mg, 1eq. to tryptophan, synthesis in chapter 3) was dissolved in 0.2 mL acetonitrile and added to the polymer solution. The red solution became colorless after 10-20 minutes indicating no more TAD left. Then, the solution was precipitated into diethyl ether and collected by vacuum filtration. Isolated yield: 204 mg.

Synthesis of PEG2K- bishydrazine carboxylate: 44 mg Ethyl carbazate dissolved in 2 mL anhydrous THF. To this solution, 65 mg of CDI added in portions over 15 min. Then, 400mg of PEG2K-diamine (dissolved in 2mL) added to the first solution and stirred 24 hours. After, all THF was evaporated by rotavap. The resulting solid dissolved in DI water, filtered and placed into a dialysis bag (0.1-0.5 kDa). The solution was dialyzed for 2 days and product collected as a white powder after freeze-drying. Isolated yield: 381mg

Synthesis of PEG2K-Bisurazole: PEG2K- bis hydrazinecarboxylate (250mg, approx. 0.24 mmol of hydrazine carboxylate end) was dissolved in 5mL of absolute ethanol. To this solution, anhydrous potassium carbonate (66 mg, 0.48 mmol) was added and the mixture was refluxed for 24 hours. Then, all ethanol was evaporated and remaining solid was dissolved in deionized water. The solution was neutralized by HCl carefully

and placed into a dialysis bag. Finally, it was dialyzed against DI water for 2 days and the white product was obtained by freeze drying. Isolated yield: 195mg

Synthesis of PEG2K-TAD: 100mg of PEG2K-Urazole was dissolved in 1 mL of anhydrous chloroform. To this solution, 15 mg of silica nitric acid was added and shake for 15 minutes. Then the solution was filtered and precipitated into diethyl ether. The product was collected as a pink powder. Isolated yield: 79mg, conversion of urazole ends to TADs: 95% from NMR. Giving more time or using higher amount silica would help for full conversion.

PEGylation of P6: 60 mg of P6 was dissolved in chloroform. To this solution, 50 mg of PEG2K-monoTAD was added and stirred for 10 minutes. Then, the solution was precipitated into diethyl ether. The resulting product was characterized by GPC.

Synthesis of Allyl-Poly(Lysine$_{50}$-Trp$_{20}$): 1 g of lysine NCA (3.3 mmol) and 300mg of Tryptophan NCA (1.32 mmol) was placed into an oven dried schelenk tube and dissolved in 10 mL DMF. To this solution, 3.7 mg of allyl amine (0.5 mL from freshly prepared stock) was added and the reaction stirred for 6 hours. Then, the solution was precipitated into diethyl ether. The resulting sticky product was dissolved in chloroform and reprecipitated into diethyl ether to obtain non-sticky powder product.

Synthesis of Allyl-Poly(Z-Lysine$_{50}$-st-Trp$_{20}$)–PTAD: 200 mg of Allyl-Poly(Lysine50-Trp20) was dissolved in 2mL DMF/$CHCl_3$ (1:1). To this solution, 60 mg of PTAD was added and the reaction was stirred for 30 minutes. Then, the solution was precipitated into diethyl ether and the product was collected by vacuum filtration. Isolated yield: 216 mg

Synthesis of Allyl Poly(Z-Lysine$_{50}$-Trp$_{20}$) – PTAD – PEG: 150 mg of Allyl-Poly(Lysine50-Trp20) – PTAD was dissolved in 5 mL of $CHCl_3$. To this solution, 48

mg of PEG-6K Thiol was added together with 2 mg of 2,2-Dimethoxy-2-phenylacetophenone. Then, the reaction solution was irradiated with UV light for 2 hours. Finally, the solution was precipitated into diethyl ether and collected by vacuum filtration. Isolated yield: 162 mg.

Synthesis of Propargyl-Poly(Z-Lysine$_{50}$-Trp$_{20}$): 1 g of lysine NCA (3.3 mmol) and 300mg of Tryptophan NCA (1.32 mmol) was placed into an oven dried schelenk tube and dissolved in 10 mL DMF. To this solution, 3.6 mg of allyl amine (0.5 mL from freshly prepared stock) was added and the reaction stirred for 6 hours. Then, the solution was precipitated into diethyl ether. The resulting sticky product was dissolved in chloroform and reprecipitated into diethyl ether to obtain non-sticky powder product.

Synthesis of Propargyl-Poly(Z-Lysine$_{50}$-st-Trp$_{20}$)-PTAD: 200 mg of Allyl-Poly(Lysine50-Trp20) was dissolved in 2mL DMF/CHCl3 (1:1). To this solution, 60 mg of PTAD was added and the reaction was stirred for 30 minutes. Then, the solution was precipitated into diethyl ether and the product was collected by vacuum filtration. Isolated yield: 221mg

Synthesis of Propargyl-Poly(Lysine$_{50}$-st-Trp$_{20}$)-PTAD: 200 mg of Propargyl-Poly(Z-Lysine50-Trp20) was dissolved in 5 mL of TFA. To this solution, 0.3 mL of HBr (33% in acetic acid) was added and stirred for 5 hours. Then, the solution was precipitated into diethyl ether, washed with excess diethyl ether and dried. The solid was dissolved in deionized water and placed into 3.5 MWCO snake skin dialysis bag. The product was collected by freeze drying after 2-3 days of dialysis. Isolated yield: 134 mg.

Synthesis of Propargyl-Poly(Z-Lysine$_{50}$-Trp$_{20}$)-PTAD-PEG: 60 mg of Propargyl-Poly(Lysine50-Trp20)-PTAD was dissolved in 1 mL of DI water. To this solution, 10 mg of PEG1K-azide was added together with 5 mg $CuSO_4.5H_2O$ and 3.5 mg of sodium ascorbate. The reaction was stirred overnight. Then, the mixture was filtered and the crude product was obtained after evaporation of the water by rotavap. Then, the product was redissolved in a minimum amount of water and precipitated in ethanol. Finally, the product was collected by vacuum filtration and dried on the vacuum line.

4.5 References

(1) Kolb, H. C.; Finn, M. G.; Sharpless, K. B. *Angew. Chemie Int. Ed.* **2001**, *40* (11), 2004–2021.

(2) Barner-Kowollik, C.; Du Prez, F. E.; Espeel, P.; Hawker, C. J.; Junkers, T.; Schlaad, H.; Van Camp, W. *Angew. Chemie - Int. Ed.* **2011**, *50* (1), 60–62.

(3) Chang, P. V; Prescher, J. A.; Sletten, E. M.; Baskin, J. M.; Miller, I. A.; Agard, N. J.; Lo, A.; Bertozzi, C. R. *Proc. Natl. Acad. Sci. U. S. A.* **2010**, *107* (5), 1821–1826.

(4) Hoyle, C. E.; Bowman, C. N. *Angewandte Chemie - International Edition*. 2010, pp 1540–1573.

(5) Carioscia, J. A.; Lu, H.; Stanbury, J. W.; Bowman, C. N. *Dent. Mater.* **2005**, *21* (12), 1137–1143.

(6) Funel, J.-A.; Abele, S. *Angew. Chem. Int. Ed. Engl.* **2013**, *52* (14), 3822–3863.

(7) Cookson, R. C.; Gilani, S. S. H.; Stevens, I. D. R. *Tetrahedron Lett.* **1962**, *3* (14), 615–618.

(8) Cookson, R. C.; Gilani, S. S. H.; Stevens, I. D. R. *J. Chem. Soc. C Org.* **1967**,

1905.

(9) Paquette, L. A.; Doehner Jr, R. F. *J. Org. Chem.* **1980**, *45* (25), 5105–5113.

(10) Stickler, J. C.; Pirkle, W. H. *J. Org. Chem.* **1966**, *31* (10), 3444–3445.

(11) Butler, G. B. *Ind. Eng. Chem. Prod. Res. Dev.* **1980**, *19* (4), 512–528.

(12) Shimizu, M.; Iwasaki, Y.; Yamada, S. *Yakugaku zasshi J. Pharm. Soc. Japan* **1995**, *115* (8), 584–602.

(13) Yasumoto, T.; Takizawa, A. *Biosci. Biotechnol. Biochem.* **1997**, *61* (10), 1775–1777.

(14) Adamo, R.; Allen, M.; Berti, F.a; Danieli, E.; Hu, Q.-Y.;

(15) Baran, P. S.; Guerrero, C. A.; Corey, E. J. *Org. Lett.* **2003**, *5* (11), 1999–2001.

(16) Billiet, S.; De Bruycker, K.; Driessen, F.; Goossens, H.; Van Speybroeck, V.; Winne, J. M.; Du Prez, F. E. *Nat. Chem.* **2014**, *6* (9), 815–821.

(17) Roling, O.; De Bruycker, K.; Vonhören, B.; Stricker, L.; Körsgen, M.; Arlinghaus, H. F.; Ravoo, B. J.; Du Prez, F. E. *Angew. Chemie Int. Ed.* **2015**.

(18) Vonhören, B.; Roling, O.; De Bruycker, K.; Calvo, R.; Du Prez, F. E.; Ravoo, B. J. *ACS Macro Lett.* **2015**, *4* (3), 331–334.

(19) Xiao, L.; Chen, Y.; Zhang, K. *Macromolecules* **2016**, *49* (12), 4452–4461.

(20) Vandewalle, S.; Billiet, S.; Driessen, F.; Du Prez, F. E. *ACS Macro Lett.* **2016**, *5*, 766–771.

(21) Wang, Z.; Yuan, L.; Trenor, N. M.; Vlaminck, L.; Billiet, S.; Sarkar, A.; Du Prez, F. E.; Stefik, M.; Tang, C. *Green Chem.* **2015**, *17* (7), 3806–3818.

(22) Wang, Z.; Zhang, Y.; Yuan, L.; Hayat, J.; Trenor, N. M.; Lamm, M. E.; Vlaminck, L.; Billiet, S.; Du Prez, F. E.; Wang, Z. *ACS Macro Lett.* **2016**, *5* (5), 602–606.

(23) Chen, G.; Gupta, M.; Chan, K.; Gleason, K. K. *Macromol. Rapid Commun.* **2007**, *28* (23), 2205–2209.

(24) Hoogewijs, K.; Buyst, D.; Winne, J. M.; Martins, J. C.; Madder, A. *Chem. Commun.* **2013**, *49* (28), 2927–2929.

(25) Habraken, G. J. M.; Koning, C. E.; Heuts, J. P. A.; Heise, A. *Chem. Commun.* **2009**, No. 24, 3612–3614.

(26) Sun, J.; Schlaad, H. *Macromolecules* **2010**, *43* (10), 4445–4448.

(27) Tang, H.; Zhang, D. *Polym. Chem.* **2011**, *2* (7), 1542.

(28) Krannig, K.-S.; Huang, J.; Heise, A.; Schlaad, H. *Polym. Chem.* **2013**, *4* (14), 3981–3986.

(29) Krannig, K. S.; Schlaad, H. *J. Am. Chem. Soc.* **2012**, *134* (45), 18542–18545.

(30) Huang, Y.; Zeng, Y.; Yang, J.; Zeng, Z.; Zhu, F.; Chen, X. *Chem. Commun. (Camb).* **2011**, *47* (26), 7509–7511.

(31) Fan, J.; Li, R.; He, X.; Seetho, K.; Zhang, F.; Zou, J.; Wooley, K. L. *Polym. Chem.* **2014**, *5* (13), 3977–3981.

(32) Rhodes, A. J.; Deming, T. J. *ACS Macro Lett.* **2013**, *2* (5), 351–354.

(33) Engler, A. C.; Lee, H.; Hammond, P. T. *Angew. Chemie Int. Ed.* **2009**, *48* (49), 9334–9338.

(34) Zhang, R.; Zheng, N.; Song, Z.; Yin, L.; Cheng, J. *Biomaterials* **2014**, *35* (10),

3443–3454.

(35) Shaikh, A. Y.; Das, S.; Pati, D.; Dhaware, V.; Sen Gupta, S.; Hotha, S. *Biomacromolecules* **2014**, *15* (10), 3679–3686.

(36) Xiao, C.; Zhao, C.; He, P.; Tang, Z.; Chen, X.; Jing, X. *Macromol. Rapid Commun.* **2010**, *31* (11), 991–997.

(37) Deming, T. J. *Chem. Rev.* **2015**.

(38) Quadir, M. A.; Martin, M.; Hammond, P. T. *Chemistry of Materials*. 2014, pp 461–476.

(39) Habraken, G. J. M.; Koning, C. E.; Heuts, J. P. A.; Heise, A. *Chem. Commun.* **2009**, No. 24, 3612.

(40) Zhou, J.; Chen, P.; Deng, C.; Meng, F.; Cheng, R.; Zhong, Z. *Macromolecules* **2013**, *46* (17), 6723–6730.

(41) Lu, H.; Wang, J.; Bai, Y.; Lang, J. W.; Liu, S.; Lin, Y.; Cheng, J. *Nat. Commun.* **2011**, *2*, 206–209.

(42) Ciardelli, F.; Fabbri, D.; Pieroni, O.; Fissi, A. *J. Am. Chem. Soc.* **1989**, *111* (9), 3470–3472.

(43) Kotharangannagari, V. K.; Sánchez-Ferrer, A.; Ruokolainen, J.; Mezzenga, R. *Macromolecules* **2011**, *44* (12), 4569–4573.

(44) Bilalis, P.; Varlas, S.; Kiafa, A.; Velentzas, A.; Stravopodis, D.; Iatrou, H. *J. Polym. Sci. Part a-Polymer Chem.* **2016**, *54* (9), 1278–1288.

(45) Kumar, S.; Allard, J.-F.; Morris, D.; Dory, Y. L.; Lepage, M.; Zhao, Y. *J. Mater. Chem.* **2012**, *22* (15), 7252–7257.

(46) Reidy, M. P.; Green, M. M. *Macromolecules* **1990**, *23* (19), 4225–4234.

(47) Shibaev, V.; Palumbo, M.; Peggion, E. *Biopolymers* **1975**, *14* (1), 73–81.

(48) Guillermain, C.; Gallot, B. *Macromol. Chem. Phys.* **2002**, *203* (10–11), 1346–1356.

(49) Schaefer, K. E.; Keller, P.; Deming, T. J. *Macromolecules* **2006**, *39* (1), 19–22.

(50) Fasman, G. D.; Landsberg, M.; Buchwald, M. *Can. J. Chem.* **1965**, *43* (5), 1588–1598.

(51) Xiang, Y.; Si, J.; Zhang, Q.; Liu, Y.; Guo, H. *J. Polym. Sci. Part A Polym. Chem.* **2009**, *47* (3), 925–934.

(52) Cosani, A.; Peggion, E.; Verdini, A. S.; Terbojevich, M. *Biopolymers* **1968**, *6* (7), 963–971.

4.6 Appendix

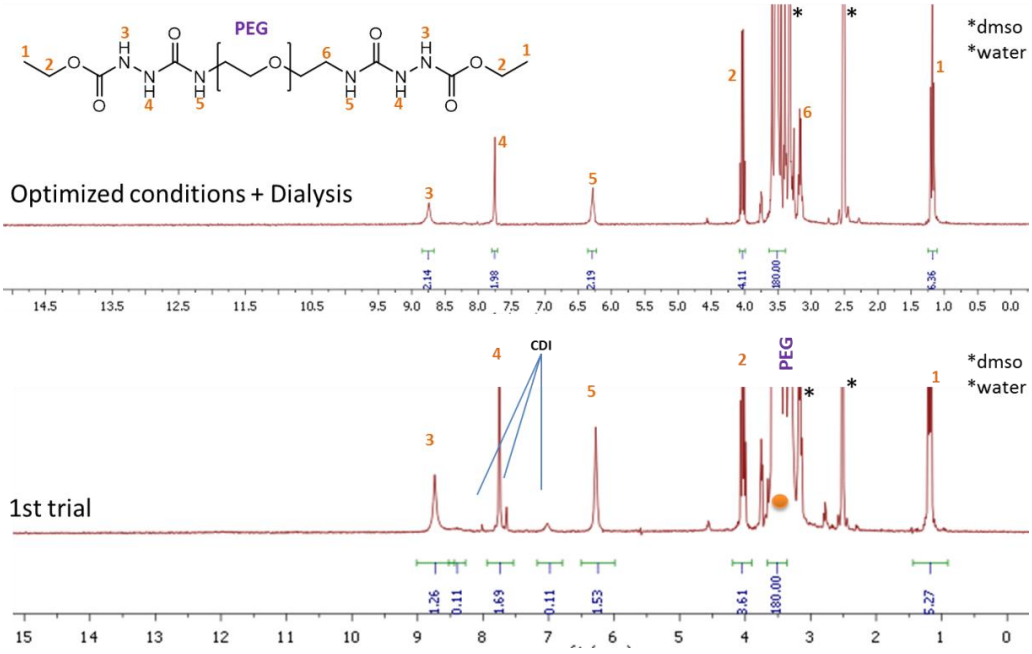

Figure A1: ^{1}H-NMR spectra of PEG2K- bishydrazine carboxylate in dmso-d6.

Dialysis and optimized conditions helped to get rid of CDI impurity.

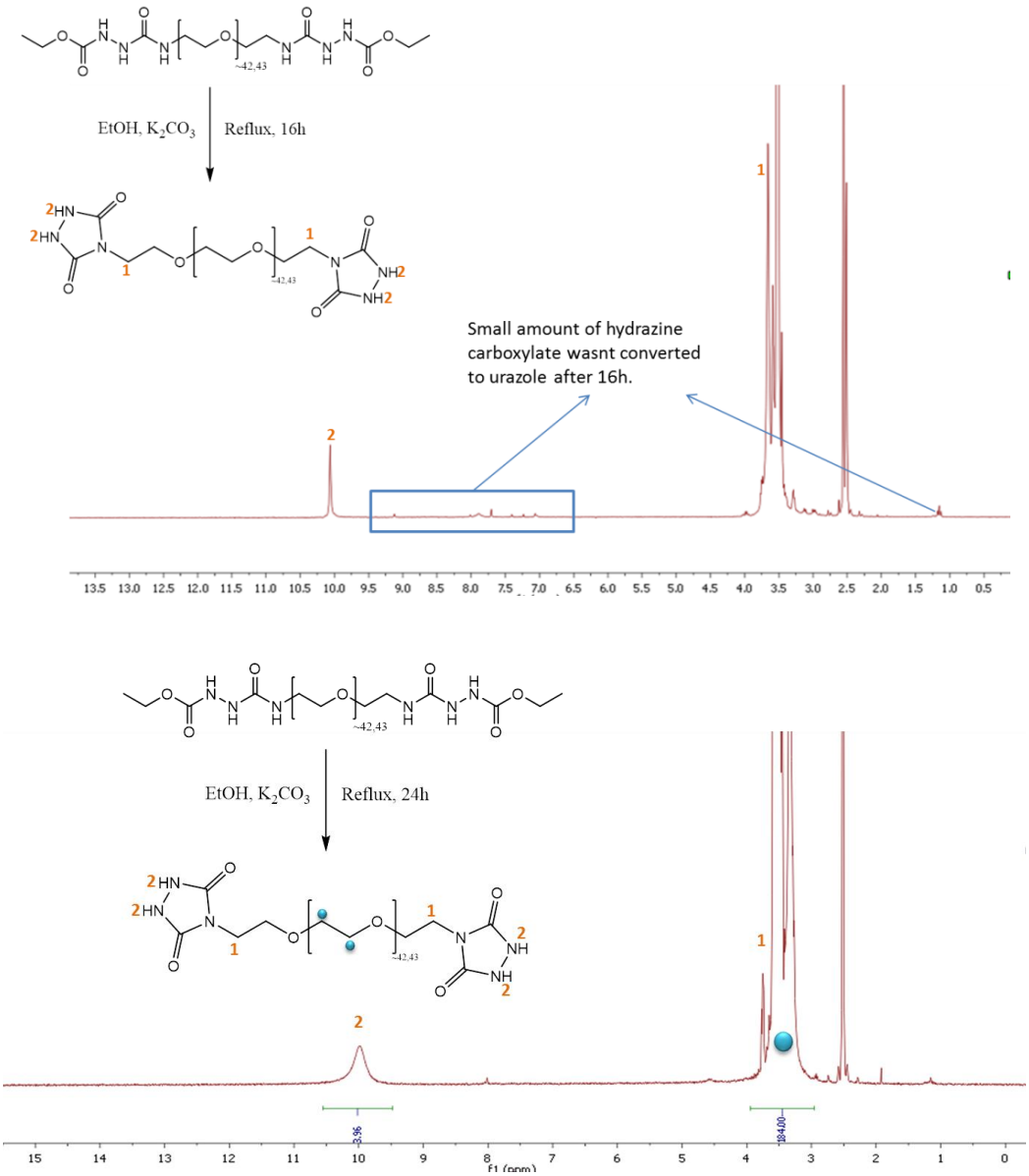

Figure A2: ^{1}H-NMR spectra of PEG2K- bisurazole in dmso-d6. For full conversion at least 24 hours of reflux was needed.

Chapter 5
Tryptophan Based Hydrogels

Abstract

In the previous chapter, it was demonstrated that the TAD-tryptophan reaction is very versatile. This chapter investigates how well-defined polypeptide based hydrogels can be prepared utilizing this reaction. First, a library of co-polypeptides with varying tryptophan content was prepared; then, these copolypeptides were crosslinked using hexamethylene-bisTAD to obtain organogels. Finally, these organogels were converted into hydrogels by removing the hydrophobic protection groups on the amino acids. The gelation kinetics were controlled by either the concentration of crosslinker or tryptophan concentration in the polypeptide. Additionally, it was observed that solvent composition can also be used to control the speed of gelation. Hydrogel microstructures were imaged using SEM and mechanical analyses were completed. Cytotoxicity studies revealed that the hydrogels were not toxic to human mesenchymal cells. TAD-tryptophan crosslinked materials have high potential for use as biomaterials since the composition of amino acids and mechanical properties of these gels can be very easily tuned by this chemistry. In the last part of this chapter, a new type of organohydrogel is reported. This new class of material was obtained by diffusion controlled deprotection of the hydrophobic groups resulting in a macroscopic core-shell type symmetrical hybrid material where the core is hydrophobic and the shell is hydrophilic.

5.1. Introduction

5.1.1 Polypeptide Based Hydrogels

Hydrogels have been used in many applications particularly in biology related fields since their first introduction in 1960 by Wichterle and Lim.[1] In the 1980s, encapsulation of cells by calcium alginate gels[2] and the use of natural polymer hydrogels as burn dressings[3] showed the high potential of hydrogels in real medical applications. Today, numerous types of hydrogels are used or explored in many areas, including pharmaceuticals[4], tissue engineering[5–8], regenerative medicine[9–11], wound dressing[12] and biosensors[13,14]. The high water content of hydrogels allows the movement of small molecules, a critical feature for many bio-applications apart from biodegradability and biocompatibility.[15] Some hydrophilic polymers like PEG (FDA approved) are widely used as crosslinkers to obtain hydrogels[16,17], however, the resulting materials are not biodegradable. Additionally, while PEG itself may be biocompatible, its derivatives such as PEG-acrylate or PEG-isocyanate still contain non-biocompatible functionalities. Moreover, higher molecular weight PEGs are not excreted from the body and accumulate in the liver which may cause health problems.[18]

Natural polymers such as collagen or chitosan may be more suitable for *in vivo* applications than high molecular PEGs because of their biodegradability. Although natural polymers have some advantages such as cell binding sites, they may cause alterations to cell properties.[19] Lack of accessible functional groups, compositional varieties depending on source, non-scalable production, and possible immune responses[20] are among the disadvantages of natural polymers for systematic biomedical applications. Polymers consisting of natural building blocks that grant control over composition and functionalization are interesting alternatives. Aliphatic

polyesters, polypeptides, polyphosphoesters, polyanhydrides and polyurethanes generally meet these criteria, but further modification chemistries should be taken into account.[21]

There are many reports on hydrogels made of NCA derived polypeptide materials.[22,23] Most of these reports are based on stimuli-responsive[23–25] sol-gel behavior or self-assembly of [26–28] diblock amphiphilic copolypeptide. Not only copolypeptides but also copolymer hybrids were reported to form hydrogels. For example, Cho. *et al.* reported a biodegradable hydrogel composed of hexablock hybrids of PEG and PBLG, where α-helical assembly results in supramolecular crosslinking.[29] The role of the PEG is to provide a hydrophilic block, whereas PBLG block is hydrophobic. Due to the amphiphilic diblock character the polymers self-assembled to form supramolecularly crosslinked gel. Another PEG-polypeptide hybrid namely poly(ethylene glycol-*b*-(γ-(2-methoxyethoxy)ester-L-glutamate), was also reported to form hydrogels.[30] In both reports, polypeptide blocks not only provide hydrophobicity but also biodegradability. Biodegradation of the polypeptide blocks breaks the gel network and can thus be used to deliver drugs or biologics. Huang *et al.* reported thermoresponsive gelation of PEG-Tyr block hybrid polymers, where β-sheet formation of the tyrosine block at higher temperatures induces gelation.[31] This is one of few examples showing gelation upon increasing temperature. One drawback of supramolecular hydrogels is their mechanical properties. They are generally too weak to handle and use in real life applications where a strong and stable material is needed. On the other hand, the stimuli-responsive sol-gel behavior of these gels makes them interesting materials for certain applications such as injectable hydrogel systems.[32]

In this chapter, the natural amino acid tryptophan was crosslinked using the TAD click reaction to obtain gels. The details of the reaction were discussed in Chapter 4. To date

there are only two reports on tryptophan bioconjugation.[33–36] The first bioconjugation of tryptophan was reported 2006 by Antos *et al.* (Figure 5.1). A vinyl diazo compound (**1**) was catalyzed with rhodium (II) acetate to obtain rhodium carbenoids (**2**) and tryptophan was conjugated through this intermediate. However, it should be noted that the rhodium carbenoids also reacts with water. Additionally, this reaction only works under very acidic conditions (pH 2).

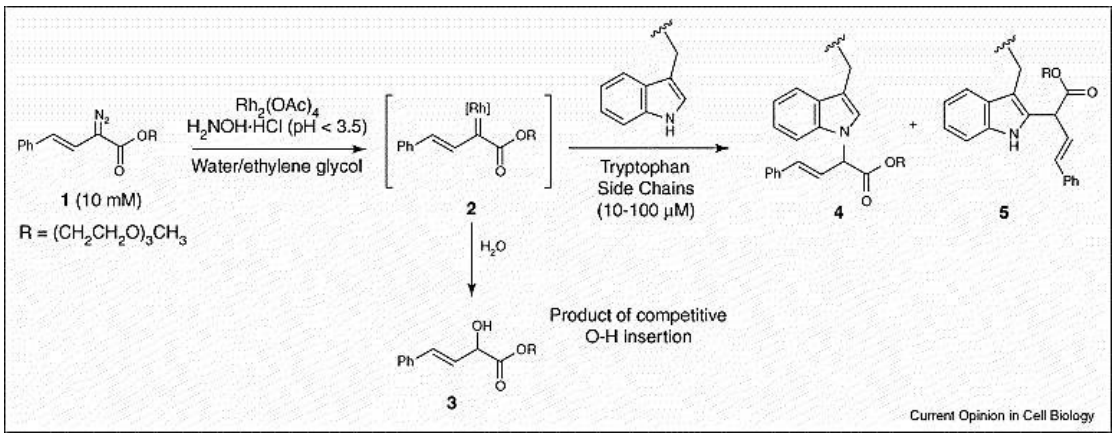

Figure 5.1. Bioconjugation of tryptophan by rhodium carbenoids.[33]

The second method used to conjugate tryptophan was reported in 2016 by Seki *et al.*[36] While investigating serine selective cleavage of a polypeptide by 9-azabicyclo[3,3,1]nonan-3-one-9-oxyl (known as keto-ABNO)[37], they noticed that peptides containing tryptophan formed an adduct. Then, by optimizing the reaction conditions they achieve transition metal free conjugation of tryptophan under mild conditions. (Figure 5.2)

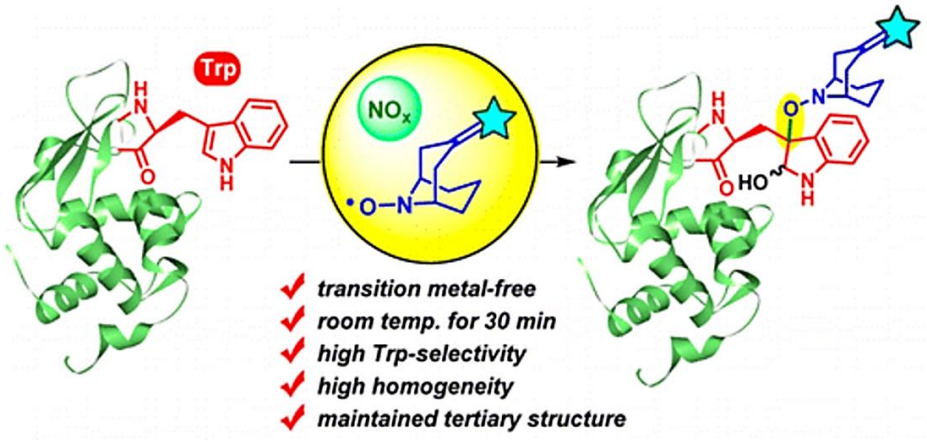

Figure 5.2. Bioconjugation of tryptophan by azabicyclo[3,3,1]nonan-3-one-9-oxyl.[36]

The rare and difficult chemistry on tryptophan suggests that TAD-tryptophan click reaction might be very valuable. However, this reaction is not ideal for tryptophan bioconjugation on natural proteins for two reasons. The gradual decomposition of TAD in an aqueous environment is an impediment for bioconjugation and, as critical, TAD mainly reacts with tyrosine rather than tryptophan (Chapter 3). While the TAD-tryptophan click reaction may not be suitable for protein modification, it is the easiest method to modify NCA derived polypeptides. Firstly, tryptophan NCA does not require protection-deprotection chemistry, which reduces the whole synthesis by two steps. Secondly, it offers freedom for the selection of protection groups of co-amino acid monomers, since no orthogonality is needed. Secondly, TAD is stable in solvents in which protected polypeptides are soluble ($CHCl_3$, DMF, acetonitrile). Therefore, polypeptides can be functionalized at their tryptophan residues immediately after NCA polymerization. Thirdly, tryptophan is a natural amino acid and there is no need for a tedious synthesis to obtain clickable NCA monomers, such as propargyl[38,39] or allyl[40,41] glycine. Another natural amino acid that can be functionalized by different click reaction is thiol containing cysteine. However, cysteine cannot be used as NCA without prior protection of the thiol group.[42,43] Additionally, formation of disulfide bonds might be challenging to work with.

5.1.2 Organohydrogel (Amphiphilic gel)

During hydrogel synthesis, we observed a new type of macroscopic core-shell hydrophobic hydrophilic gel (an amphiphilic gel or organohydrogel). Diffusion controlled deprotection of hydrophobic groups resulted in this new type of organohydrogel. To the best of our knowledge, there have not been any reports on this type of gel or fabrication method (explained further in the Discussion section). However, there are reports on hydrogel-organogel hybrids, where two gels are basically glued to each other[44–46] or two different monomers of high viscosities are polymerized and gelated.[47,48]

In the first approach, adhesion of two type of gels presents difficulties regarding how well the interfaces are connected. Therefore, Biswas *et al.* modeled stacking of two different gels by two different methods. i.e. atom transfer radical polymerization (ATRP) and free radical polymerization (FRP) (Figure 5.3). They found that ATRP gels are weakly connected due to a lack of active radicals.[49] The same group also reported that miktroarm star copolymers enhanced connectivity between the gels.[46]

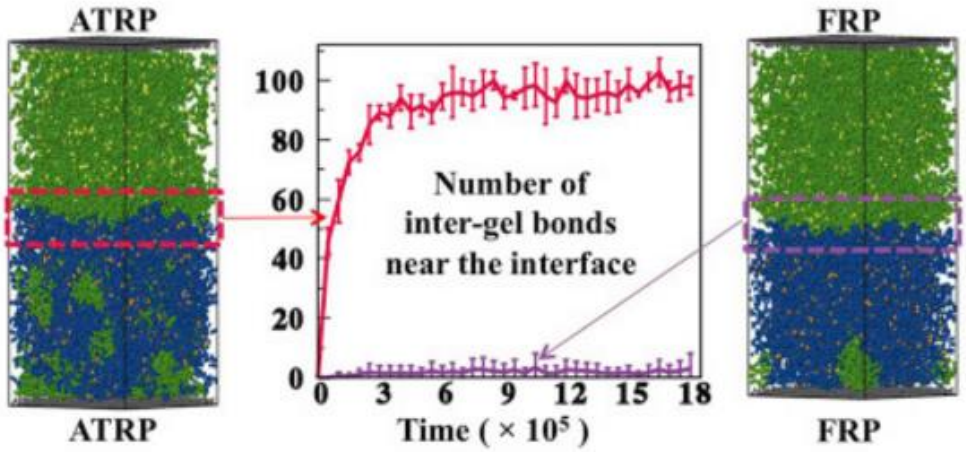

Figure 5.3. Modeling connections between gels shows that free radical polymerization provides better connectivity, compared to ATRP.[49]

Deng *et al.* prepared a hybrid gel by adhering two PEG gels (Figure 5.4).[44] Reversible acylhydrazone reaction was used to bond the PEG hydrogel (synthesized in water) to the PEG organogel (synthesized in anisole).

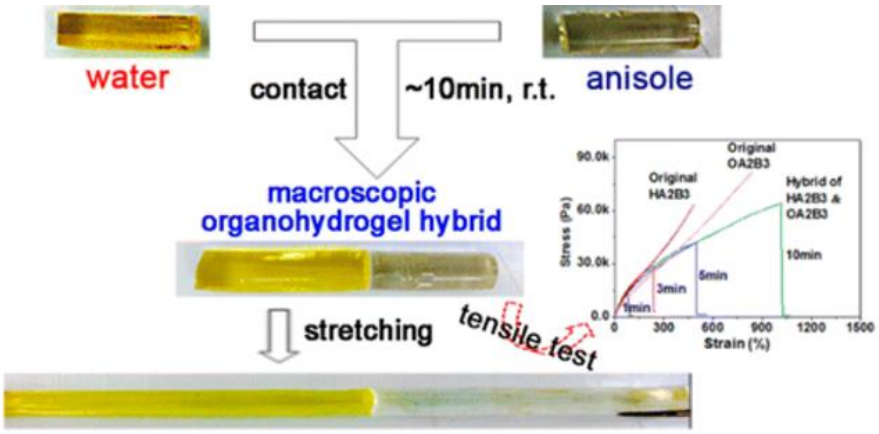

Figure 5.4. Fabrication of macroscopic organohydrogel by rapid adhesion of PEG based organogel and PEG based hydrogel.[44]

Similar to Deng's approach, Yong *et al.* reported a hybrid gel made by initiation of polymerization at the surface of the first gel (Figure 5.5). This work also had similar drawbacks, in particular, questionable interfacial connectivity.

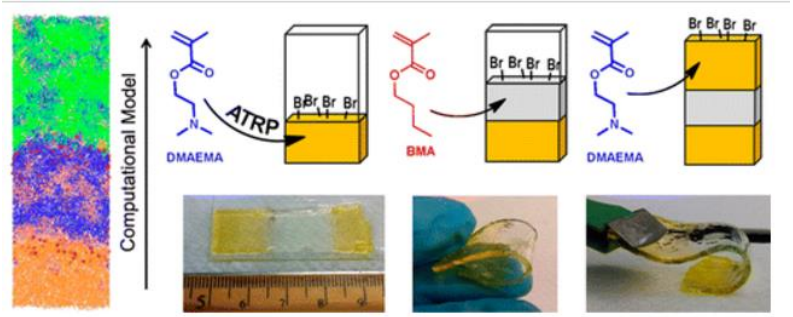

Figure 5.5. Macroscopic organohydrogel by grafting a on a second gel from a first gel.[16]

In the second approach, two monomers or polymers in sufficiently high viscosities are crosslinked, assuming that no diffusion occurs between the different monomer or

polymer regions. However, it is somewhat uncertain whether one distinct region remains “pure” and does not contain monomers or polymers of other region due to diffusion. Crosslinking high viscosity solutions is more suitable for light or heat induced reactions because crosslinking reagents have a longer diffusion time through medium (which is also the rational for the non-mixing for two monomers or polymers). Following this approach, Banik *et al.* reported organohydrogel hybrids that they claim limited diffusion of different monomer or polymer solutions in high viscosities and crosslinked them to obtain chemically and physically distinct regions (Figure 5.6). They also showed that a single monomer N,N-dimethylacrylamide solution can be used with different crosslinkers to obtain organohydrogels with distinct zones.[50]

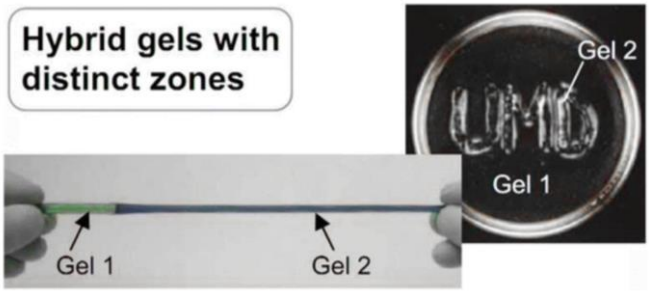

Figure 5.6. Fabrication of macroscopic organohydrogel by preventing diffusion of different monomers and polymers.[50]

In this chapter we report a method of organohydrogel formation that does not rely on adhesion or limiting diffusion of reactants by high viscosities, but rather on the side chain deprotection by natural diffusion control. In our method the connection at the interface is thus not an issue because our gel backbone was initially crosslinked and only the side chains of the polymers are changed. This solves the issue of gel interconnectivity. This finding was further exploited to create hydrogel patterns on a hydrophobic film. We believe that a similar concept can be applied to different polymers with functional side chains, as long as the speed of the reaction taking place

at the side chain is equal to or not much different than the diffusion speed of the modifying agent through the polymer network.

5.2. Results and Discussion

5.2.1 Tryptophan Based Hydrogel

Tryptophan based hydrogels were prepared by crosslinking lysine and glutamic acid containing copolypeptides in their protected forms using hexamethylene-bisTAD (HM-bisTAD) (Figure 5.7). Firstly, TAD-tryptophan crosslinking resulted in a polypeptide organogel. Then, cationic (lysine) and anionic (glutamic acid) hydrogels were obtained by deprotection of the hydrophobic groups of these organogels.

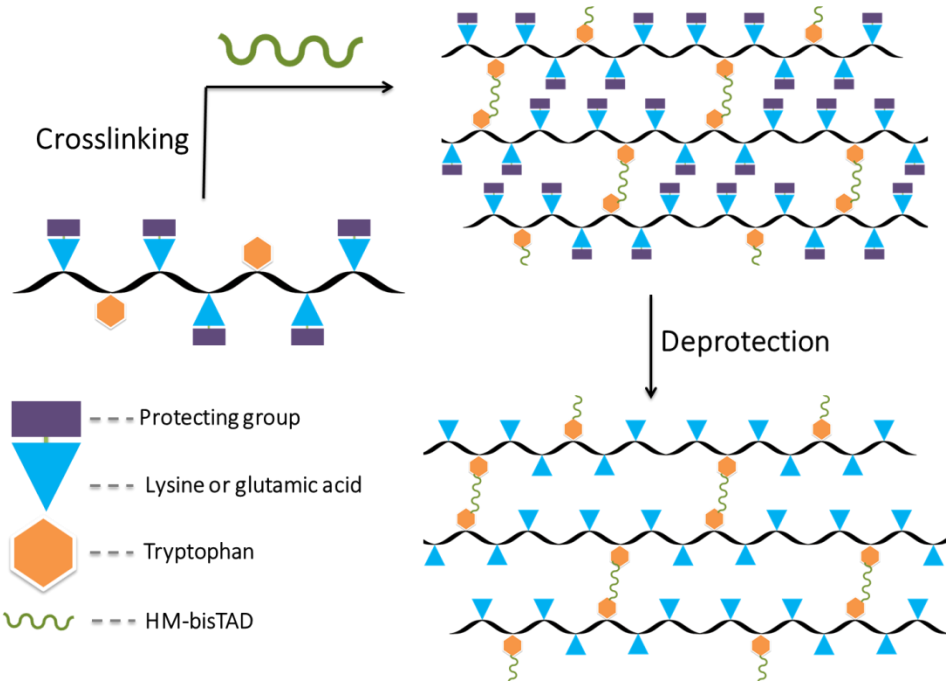

Figure 5.7. Synthesis of hydrogel via TAD-tryptophan crosslinking and deprotection.

5.2.1.1 Copolypeptide Compositions and Gelation Kinetics

A library of tryptophan containing copolypeptides was prepared according to the procedure described in the previous chapter. Table 5.1 shows the properties and

gelation kinetics of the copolypeptides into organogels. The gelation speed was found to be proportional to the amount of tryptophan present. The kinetics of gelation can also be controlled by different solvent compositions. In general, the gelation speed decreases with increasing solvent polarity. Additionally, the concentration of polymer solution can also be used to tune kinetics.

Table 5.1. Summary of the polypeptides used in hydrogel synthesis.

Polymer	Feed Comp.	SEC[a] Mn, Đ	Theo. Mw	% Trp[b]	bisTAD/ Trp	Gelation Time[c]
L1	$Lys_{70}Trp_{30}$	11K, 1.1	23070	24.3	1:2	1-2 min
L1-50	$Lys_{70}Trp_{30}$	11K, 1.1	23070	24.3	1:4	2-3 mins
L2	$Lys_{80}Trp_{20}$	13K, 1.1	23690	15.8	1:2	8 mins
L2-50	$Lys_{80}Trp_{20}$	13K, 1.1	23690	15.8	1:4	1 hour
L3	$Lys_{90}Trp_{10}$	12K, 1.1	24311	7.7	1:2	1.5 hours
B1	$Blg_{70}Trp_{30}$	10K, 1.1	21104	26.6	1:2	1-2 mins
B2	$Blg_{80}Trp_{20}$	12K, 1.1	21424	17.4	1:2	6 mins
B3	$Blg_{90}Trp_{10}$	8K, 1.1	21785	8.6	1:2	40 mins

(a) Measured in DMF against PS. (b) Calculated theoretically. (c) solvent mixture chloroform:acetonitrile (50:50).

SEC results showed that copolymerization of tryptophan with Z-lysine (L-series) and γ-benzyl-glutamate (B-series) resulted in polypeptides with low PDI and symmetrical distributions (Figures 5.8 and 5.9). These polypeptides are soluble in organic solvents, including chloroform and DMF. The choice of solvent is very important to obtain perfect gels. As mentioned before, the TAD-tryptophan reaction is very slow in DMF, which is also a highly hygroscopic solvent. This means that some portion of TAD may be decompose by water (in DMF) unless very high quality anhydrous fresh DMF is used. The TAD-tryptophan reaction is generally very fast in chloroform. This prevents thorough mixing of the reactants before the reaction sets in. We found that a chloroform/acetonitrile mixture is ideal for the crosslinking reactions. The gelation

speed can be controlled by the composition of solvent mixtures, lower concentrations of chloroform resulting in a decreased gelation rate.

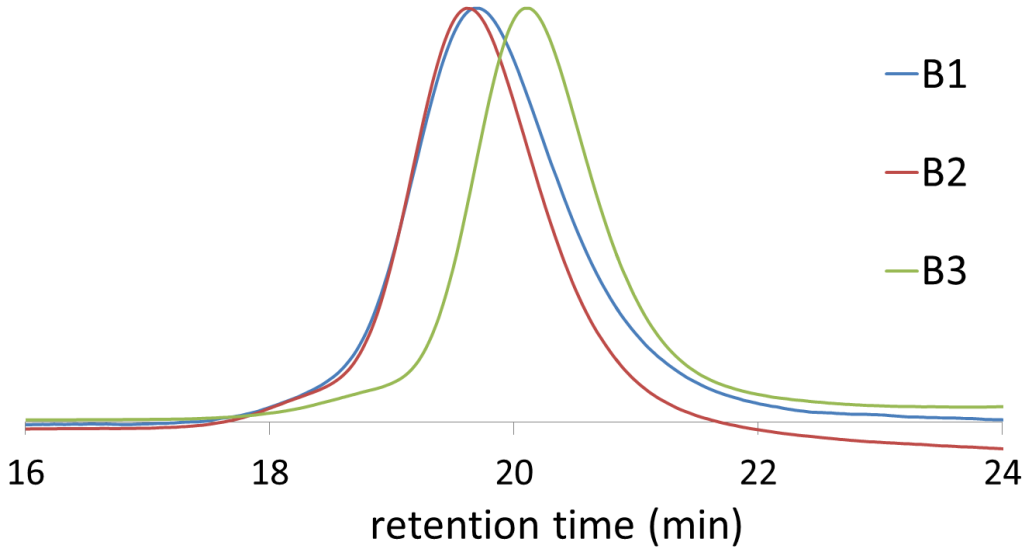

Figure 5.8. GPC chromatograms of the B series. Dispersity is between 1.05 and 1.08.

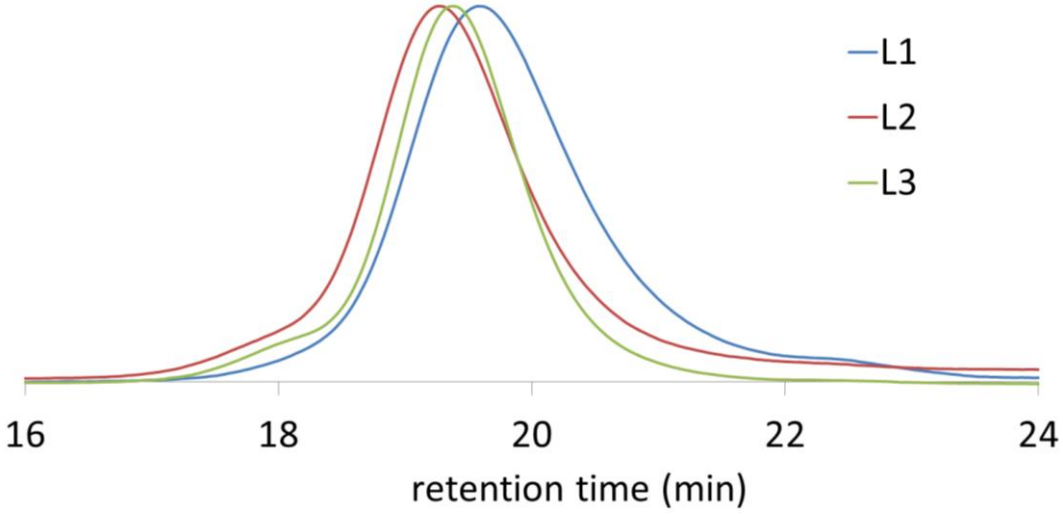

Figure 5.9. GPC chromatograms of the L series. Dispersity is between 1.08 and 1.1.

5.2.1.2 Hydrogel Synthesis

Two different approaches were tested to obtain hydrogels from these polypeptides. The first approach was to make a polypeptide in its deprotected form and crosslink it directly with HM-bisTAD to obtain the hydrogel (Figure 5.10). This approach was

quite limited by the insolubility of the deprotected polypeptide. Indeed, only very short copolypeptides (up to 15-20 repeating units) were soluble in DMF and the crosslinking reaction was quite slow in DMF, approximately 1-3 hours. The second method involved the crosslinking of protected polypeptide first and then deprotecting it to obtain hydrogels (Figure 5.11). This approach allowed us to prepare hydrogels with any length of polypeptide since solubility is not an issue for the protected polypeptides. Additionally, the protected forms do not interfere with the crosslinking reaction whereas a deprotected lysine may react with TAD. Moreover, TAD instability in water also disfavors the first approach.

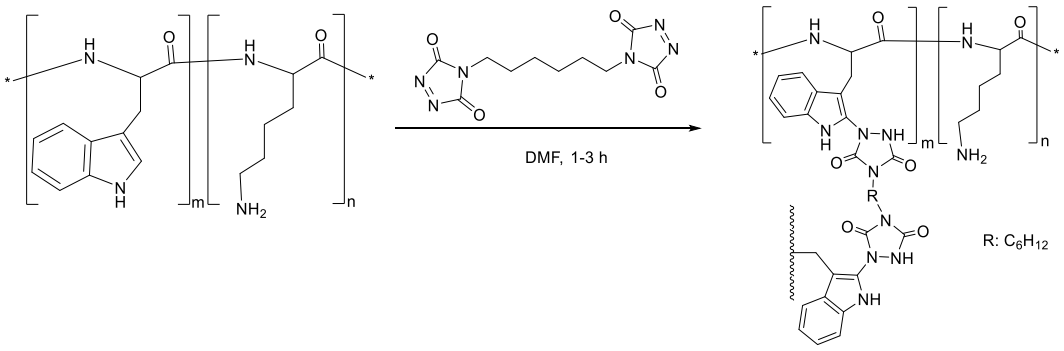

Figure 5.10. TAD crosslinking of Poly(lys-st-trp).

In order to convert organogels into hydrogels, the hydrophobic protecting groups have to be removed. Different protecting groups require individual deprotection methods to convert the organogels into hydrogel. In general, for ionic amino acid residues they have to be ionized after deprotection to obtain a swollen hydrogel. Additionally, washing steps after deprotection should be selected according to the deprotection chemistry. It is important to remove acidic residues or other side products after deprotection, which might otherwise cause hydrolysis of the hydrogel. Here, the hydrogels were washed with DMF to remove all acids. In case of Z-lysine, deprotection with HBr (in acetic acid) followed by washing with deionized water was sufficient to obtain hydrogels. However, in the case of glutamic acid, carboxylic acid

groups require treatment with a K_2CO_3 solution for ionization to achieve hydrophilicity. We observed that if the hydrogels were not washed properly, they break apart due to hydrolysis. On the other hand, properly washed hydrogels were stable for at least 8 months (to date) at room temperature in deionized water.

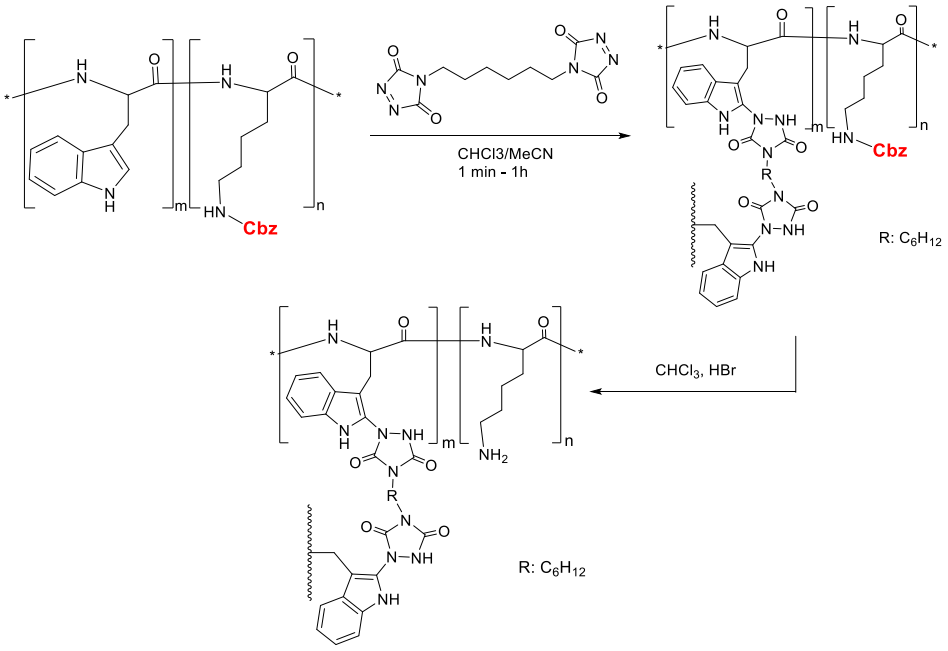

Figure 5.11. TAD crosslinking of poly(Z-lys-*st*-trp) and subsequent deprotection to form hydrogels.

5.2.1.3 Mechanical Analyses of Hydrogels

Organogels of all the copolypeptides described in Table 1 formed elastic and strong materials. Lesser crosslinked organogel have more transparent appearance (Figure 5.12). Sometimes orange colored gels were observed due to small amounts of unreacted TAD left in the gel. Gels obtained from the lysine L-series are denoted as OL# (organogel) and HL# (hydrogel), or accordingly when obtained from the glutamic acid B-series.

Mechanical studies were done on five replicates of each cylindrical shaped gel of approximately 2 cm diameter and 1 cm height Figure 5.13 shows the average results of

these tests. The less crosslinked hydrogels had lower Young moduli (50% crosslinked L1 and L2). Interestingly, there was no significant difference between B1 and B2 unlike between L1 and L2. The results showed that the ranges of the Young moduli of hydrogels are between 2-12 kPa (Figure 5.13). This range is suitable for tissue engineering applications. A recent study showed that optimal elastic modulus is 60 kPa for bone formation and repair.[57] In general, a reasonable modulus for a scaffold is between 0.01kPa-15kPa for hard tissues and 0.0004-0.35 kPa for soft tissues.[58]

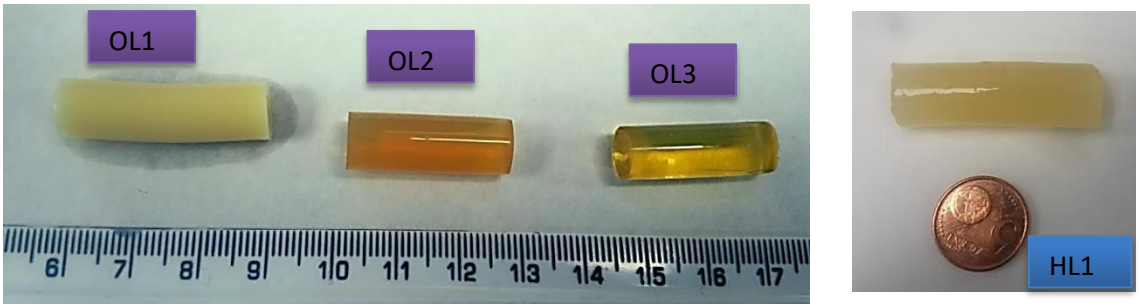

Figure 5.12. Organogels derived from the lysine L-series (OL1, OL2, OL3) and hydrogel of OL1 (HL1). Approximately 50 % crosslinked. The ruler in the photo is metric.

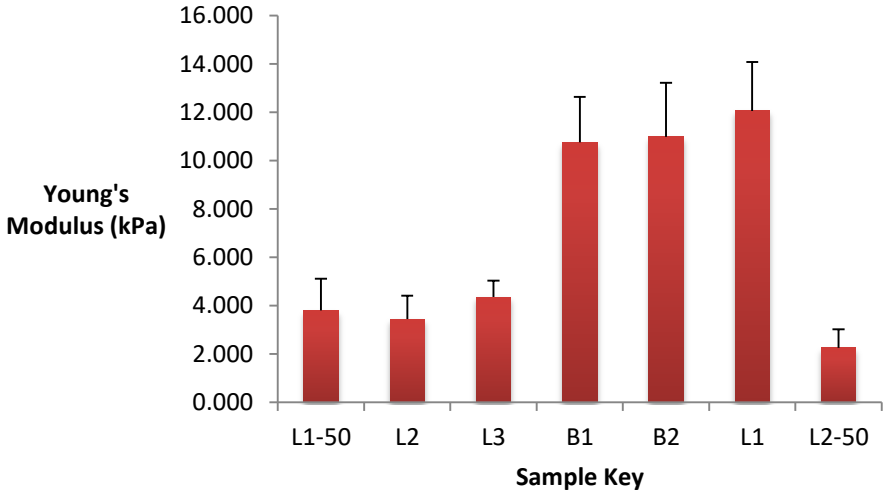

Figure 5.13. Mechanical analyses of hydrogels. These tests were done with hydrogels swollen in PBS buffer. L1 and L2 approximately 50% crosslinked; other samples fully crosslinked.

Unconfined compression testing with impermeable platens was used to determine the effect hydrogel composition on the Young's modulus. Testing was carried out using a Z050 materials testing machine (Zwick/Roell, Germany) equipped with a 5 N S-type load cell. Samples were hydrated in PBS for 1 hour prior to testing and the compression tests were carried out in a bath of PBS. Samples were compressed to 10% strain at a rate of 10%/min. The Young's modulus was then calculated from a fit to the linear region of the stress strain curve. A preload of 5 mN was used to establish contact between the sample and the upper platen in addition to serving as a measure of sample height.

5.2.1.4 Cell Studies

Biocompatibility studies were done on L1 and B1 hydrogels as they contain the highest concentration of crosslinker. Human stem cells were used to investigate cytotoxicity with gel composition. Figure 5.14 shows the result of study and highlights that there is no sign of cell toxicity. In the first 72 hours, cells survived and multiplied as evident from their metabolic activity. At longer exposure time a slight drop of metabolic activity was observed for both gels relative to the cells alone. This effect was more pronounced for the B1 hydrogel at a metabolic activity around 62% after 7 days, while L1 retained a metabolic activity similar to the control group suggesting no cytotoxic effect. Fluorescence microscope image of the cell seeded hydrogels (Figure 5.15) confirm the good cell viability.

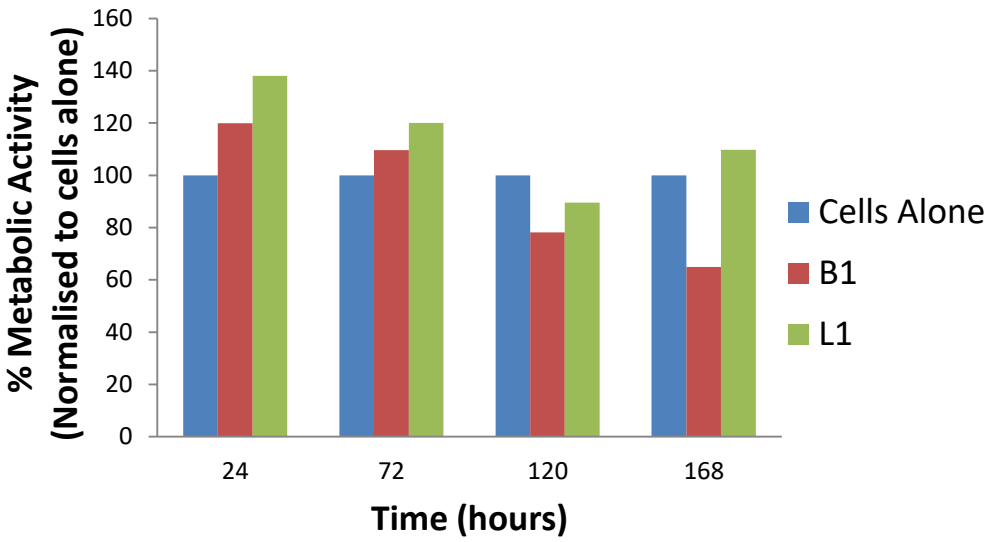

Figure 5.14. Cell viability test of the hydrogels L1 and B1

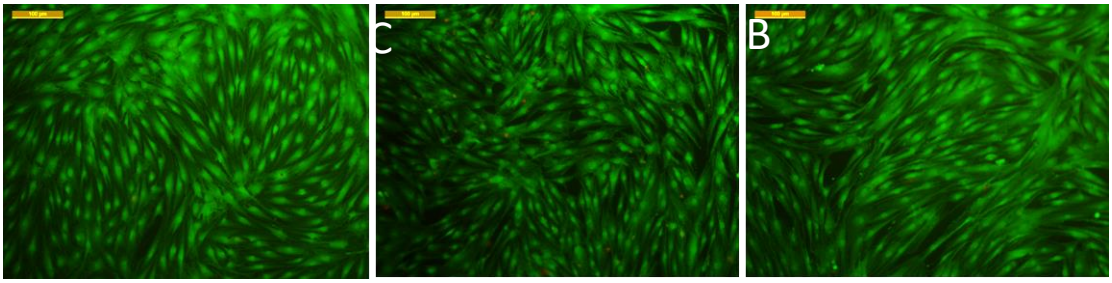

Figure 5.15. Fluorescence microscope images after 72 hours stem cell interactions with hydrogels. C is the control group, B is hydrogel B1 and L is hydrogel L1.

5.2.1.5 SEM Results

SEM images of the hydrogels were taken after freeze drying (Figure 5.16). B1 and B2 did not show a noticeable porous microstructure, whereas the L-gels exhibited this structure. L1-50 and L2 had a homogenous porous structure, and L1 had a heterogeneous pore distribution. The pores of L3 were much bigger and random in sizes. The SEM results show that optimization of gelation parameters has the potential to facilitate porous microstructures.

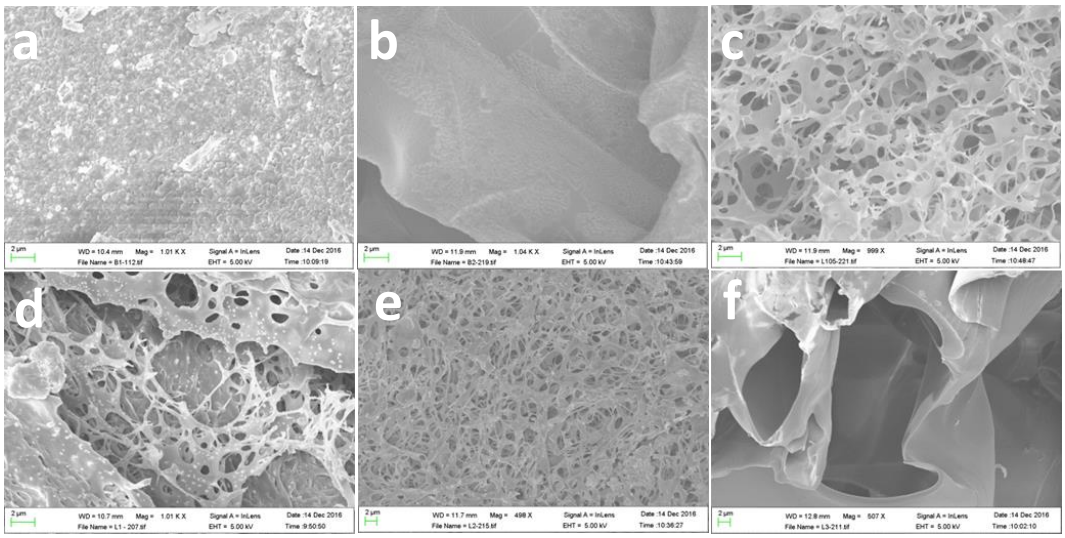

Figure 5.16. SEM images of the freeze-dried gels. **a)** B1 **b)** B2 **c)** L1-50 **d)** L1 **e)** L2 **f)** L3.

5.2.2 A New Class of Organohydrogel

5.2.2.1 The Phenomenon and Synthesis of Organohydrogel

The first trials for converting L series organogels into hydrogels resulted in unusual looking heterogeneous materials where some parts were hydrogel and some parts appeared untouched. After examination of these materials we observed that hydrogel formation occurred at the outside covering an organogel inner material. This observation confirmed that the deprotection of the hydrogel begins from the outer surface and follows the diffusion of the deprotecting agent. We believe that this is due to the slow diffusion of acid in a solid hydrophobic gel network (deprotection speed $\geq$ diffusion speed). It was hypothesized that the slow diffusion was caused by the shrinking of the deprotected networks (deprotection medium is a poor solvent for hydrogel) (Figure 5.17). Having these findings in hand, we tested this hypothesis by preparing smooth cylindrical gels and deprotected them under gentle conditions (non-stirring). The very first test was done with a short polypeptide with a composition of poly(Z-Lys_{10}-*st*-Trp_5) which is soluble in DMF in its protected and deprotected form.

After crosslinking with HM-bisTAD (Figure 18a), the organogel was placed into a TFA/$CHCl_3$ solvent mixture and treated with HBr (in acetic acid) (Figure 5.18b). After 1-2 hours, the material was taken from the solution and washed with diethyl ether. At this stage the material had shrunk and became opaque. Finally, it was placed into DMF and left until fully swollen (Figure 5.18c). Two distinct regions (as symmetrical core-shells) were observed (Figure 5.18c) where unreacted hydrophobic HM-bisTAD residues accumulated in the hydrophobic core.

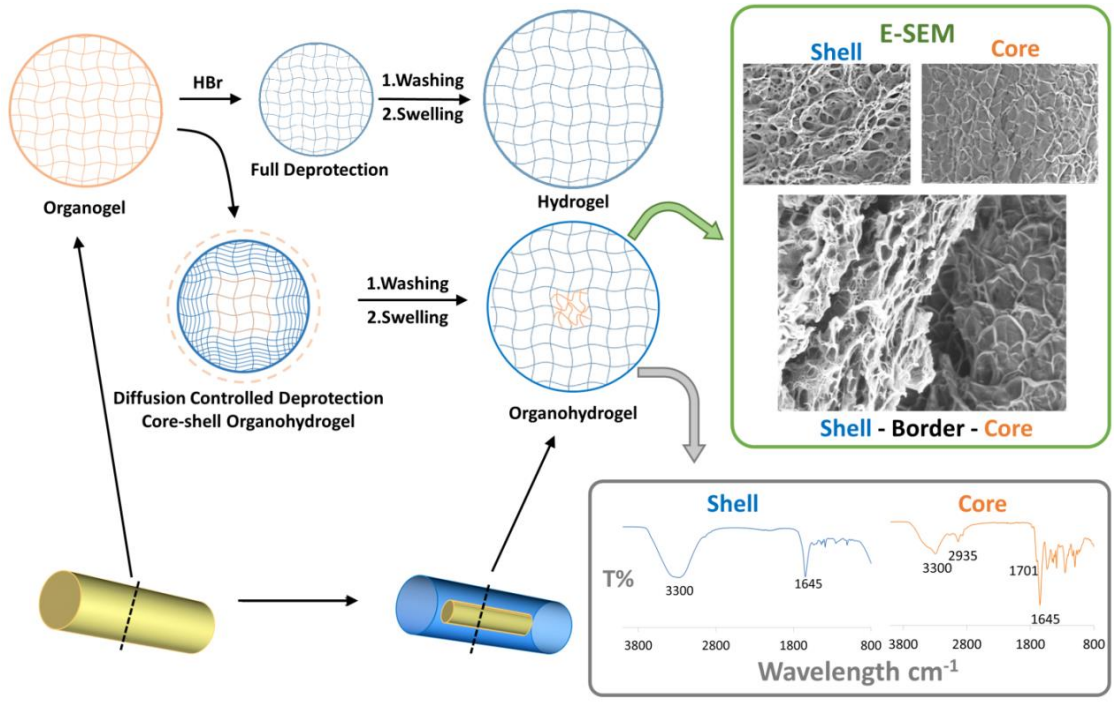

Figure 5.17. Schematic illustration of organohydrogel synthesis.

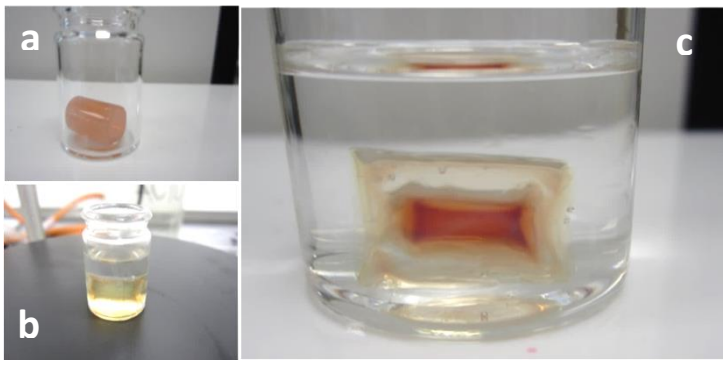

Figure 5.18. Partial deprotection of organogel. a) Organogel having unreacted TAD b) The gel in (**a**) was placed into deprotection medium c) Partially deprotected gel washed and swollen in DMF

We further tested organohydrogel formation with longer chain polypeptides such as poly(Lys_{70}-*st*-Trp_{30}), Mw:11K, and observed the same core shell structure after optimization of deprotection time and acid amount. The timing of the deprotection procedure is critical as for overnight deprotection and 1:4 (CBz:HBr) equivalent acids, the material completely turned into a hydrogel. On the other hand, decreasing the time to 1h under the same condition resulted in an organohydrogel. The main difference of these longer polypeptide chains was the opacity in DMF, so the core-shell structure was not seen as clearly as in Figure 5.18c. However, in water the transparent hydrogel shell and opaque core was easily distinguishable (Figure 5.19).

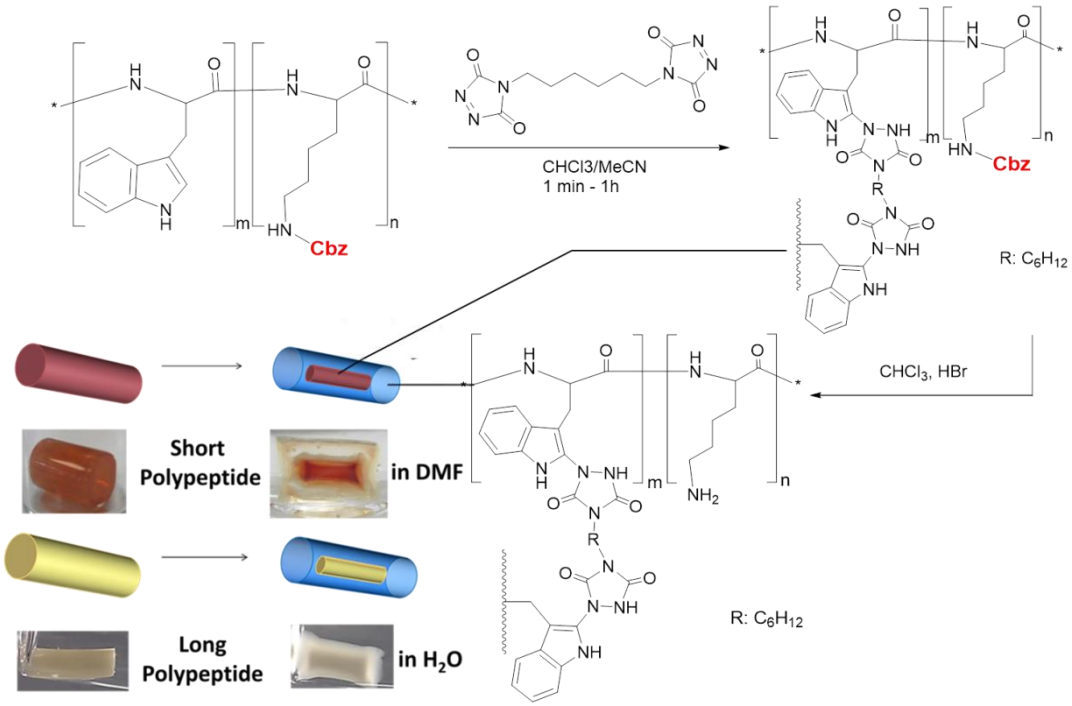

Figure 5.19. Organohydrogel synthesis by partial deprotection of CBZ groups on lysine.

5.2.2.2 SEM and ESEM Results

SEM (Figure 5.20) and ESEM (Figure 5.21) images demonstrate that the shell network expanded while the core network was collapsed. Interestingly, they belong to the same network since the material backbone and crosslinking was not affected during CBZ group removal.

When all organic solvent was removed from the core by washing, the material became extremely hard and brittle at the core level and very soft at the shell level. At this stage, the organohydrogel's composition is similar to a peach (very soft hydrophilic shell and with a hard seed at the core). This made cutting of the gel challenging because of core breakage. Therefore, there is a slight height difference between the regions in both the SEM and ESEM images. However, the difference between core and shell is easily distinguishable with both analyses.

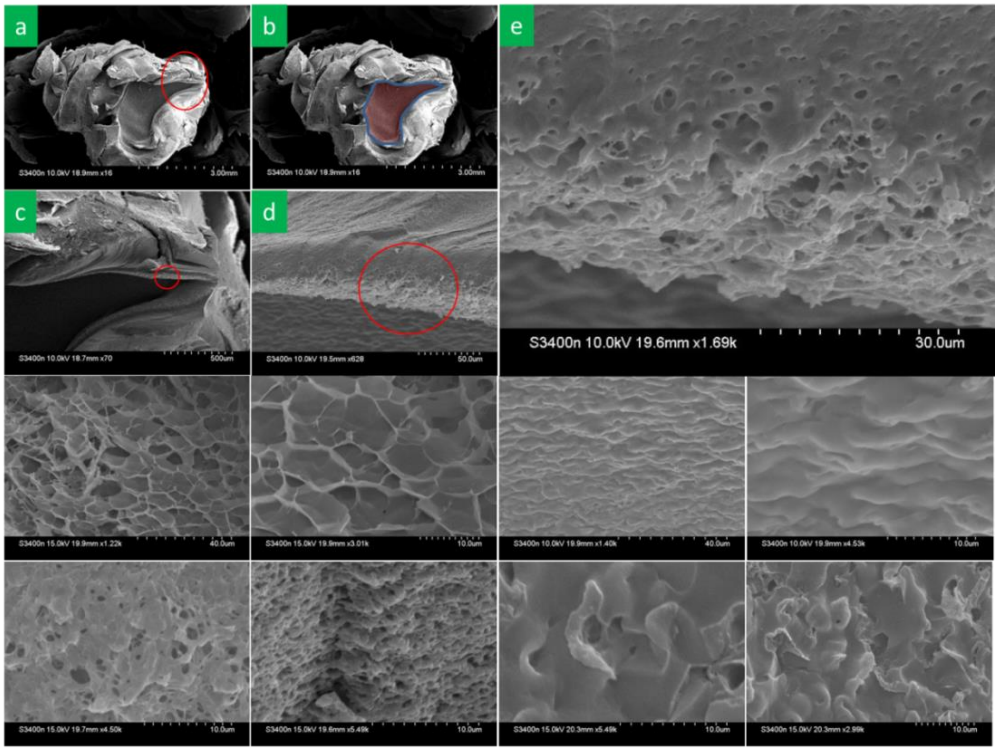

Figure 5.20. SEM images of a hybrid gel after freeze drying. **a** represents freeze dried gel. **b**, **c** and **d** zoomed circles. Border (e) image scale is 30µm.

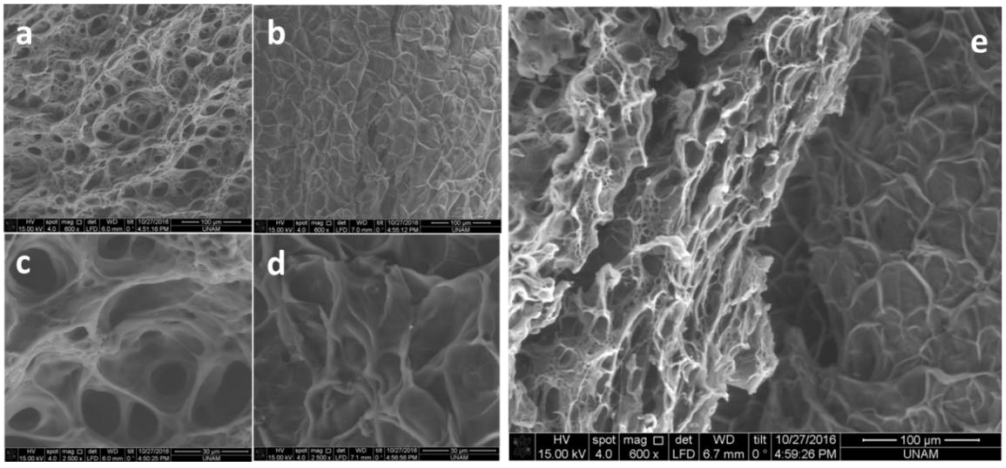

Figure 5.21. ESEM images of a wet hybrid gel. a) Shell-100 µm b) Core-100 µm c) Shell-30 µm d) Core-30 µm and e) Border-100 µm

5.2.2.3 Dyeing of the Material

Hydrophobic hexamethylene-bisTAD has a distinguishable red color which was used to monitor hydrophobic or non-deprotected areas of the gel. Figure 5.22 shows representative examples of synthesized organohydrogels. Initially, we started the washing steps with diethylether after treatment with acid. Then we realized that it creates internal pressure inside the gel, due to the high vapor pressure of ether and the heat produced by mixing the washing solvents. As a result, gels cracked (Figure 5.22 a) and therefore, this method was abandoned and gels only washed with excess DMF.

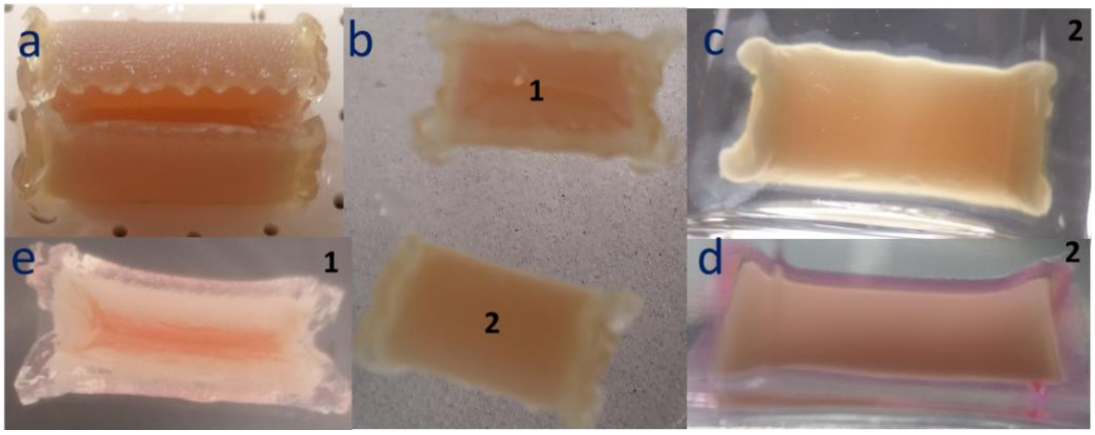

Figure 5.22. a) A cracked gel due to internal pressure of trace ether which increased with the heat of DMF-H_2O mixing. **b)** The gel broken into two almost identical pieces **c)** The piece (2) was washed with excess DMF to remove unreacted TAD – this photo was taken in H_2O. **d)** TAD free gel was placed into Rhodamine B solution overnight and washed. **e)** Piece (1) was washed partial with DMF to show TAD free and TAD containing areas and then dyed with Rhodamine B to show hydrophilic areas.

Similiarly, a core-shell organohydrogel was dyed with Rhodamine B when it is one piece (Figure 5.23a). Then it was cut into half and observed that core was not dyed (Figure 5.23b). Another gel was kept in THF and dyed with Reichardt's dye. After swollen in water the core was seen dyed (Figure 5.23c).

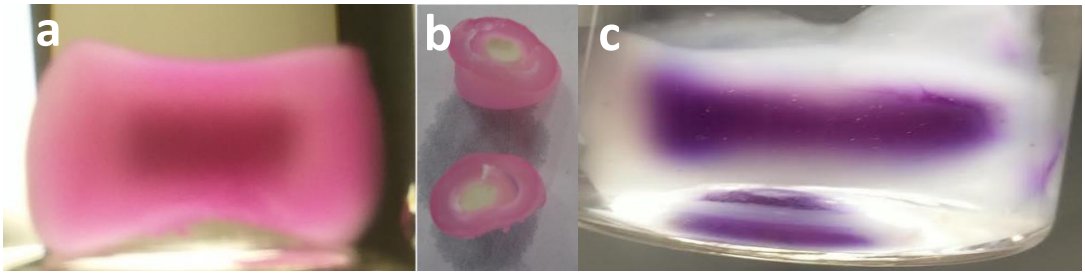

Figure 5.23. a) Excess-TAD free gel was dyed with Rhodamine B. **b)** The gel was cut into pieces showing that the core was not dyed with Rhodamine B, **c)** Another organohydrogel was dyed with Reichardt's dye in THF followed by resweeling in water, showing hydrophic dye in the core.

5.2.2.4 Patterning of Organogel Film

TAD-tryptophan crosslinked gels can be made in any shape such as cylinder, film or the shape of a mold. Thin films of polypeptide gel were prepared in glass petri dishes (Figure 24). Then, deprotection of different regions was achieved by placing drops of deprotecting acid as patterns on the organogel. IR spectrum showed exactly the same results for deprotected (patterned) and protected (untouched) parts. This is because the patterned layer was thin and sits on a protected film. Then the gels were covered with an aqueous solution of hydrophilic Rhodamine B. After washing only the patterned parts were dyed pink indicating the presence of Rhodamine B in these hydrophilic regions. We believe that by optimizing conditions and with better equipment or setup, this method will provide complex patterns for different type of applications. For example, 3D-printers can be utilized through a double-syringe mixer where one syringe contains polypeptide and a crosslinker is in the other syringe. Partial deprotection of different shapes forms completely unique hybrid materials.

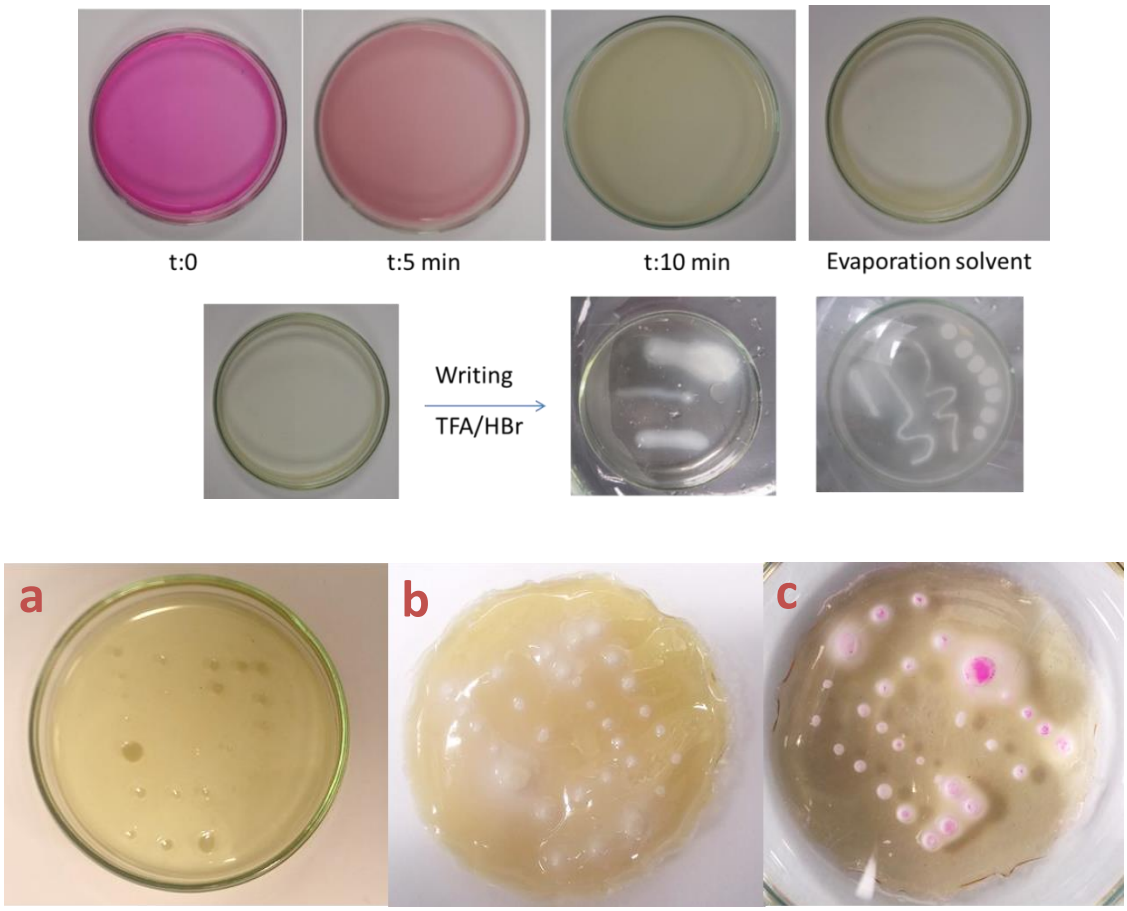

Figure 5.24. Top: mixing a P6 with HM-bisTAD at different times. a) HBr solution was dropped by TLC capillary tube to create a pattern b) Patterned film washed with DMF and water c) Washed film was dyed with Rhodamine B.

5.3. Conclusions

In conclusion, tryptophan-TAD chemistry was used to crosslink tryptophan containing statistical copolypeptides. Hydrogels were obtained by removal of hydrophobic protection group of lysine and glutamic acid. Cytotoxicity essay, mechanical analyses and SEM results showed that these hydrogels has a high potential to be used as biomaterials.

Observation of diffusion controlled deprotection of hydrophobic groups was exploited to create new class of core-shell type organohydrogels. Similarly, this concept was used to create thin hydrophilic patterns on a hydrophobic film.

5.4. Experimental

Synthesis of the organogels: In general, 150 mg of polypeptide was dissolved in 1.5 mL chloroform-acetonitrile (1:1) mixture. To this solution, HM-TAD from a stock solution (33 mg/mL in chloroform-acetonitrile 1:2) was quickly added and the solution was shaken vigorously for 20-30 seconds. Then, the solution was kept standing for gelation. The gelation time was determined by the vial tilting method.

Synthesis of the hydrogels: The organogel obtained was placed into an oven dried vial and approximately 10 mL of chloroform was added. To this mixture, 1 mL of HBr in acetic acid (33%) was added and stirred for 8 hours. Then, solvent was removed by decanting. After, the gel was washed with chloroform twice and placed into a vial containing 15 mL of anhydrous DMF. The gel was kept for 30 minutes in this solution and solution refreshed with DMF again. This step was repeated for 4 times. Then, the gel was taken and placed into a beaker containing ice cold-deionized water. The shrunken gel, specifically lysine containing gels, started to swell in water. At this step the gel was dialyzed against deionized water for 2 days to remove the DMF.

Glutamic acid containing gels (B1 and B2) were swelled in basic aqueous solution at pH 10.5-11. After, 1 or 2 days the completely swelled gel was then dialyzed with deionized water to neutralize the solution.

Importantly, if the gels start breaking apart in the dialysis step, it indicates that there is still acid left in the gel. To prevent this, less HBr and given longer times for deprotection or increase the number of DMF steps can be used. A well washed gel should be in one piece and strong enough to hold and squeeze slightly.

Synthesis of the core-shell hybrid gel: An L series organogel was obtained in accordance with the procedure above. Then, it was placed into an oven dried vial and

10 mL of chloroform was added with 0.5 mL HBr (33% in acetic acid). The mixture was shaken and let stand for 1 hour. Then, the solvent was removed by decanting. Afterwards, the gel was washed with chloroform twice and placed into vial containing 15 mL of anhydrous DMF. The gel was kept for 30 minutes in this solution and then the solution was refreshed with DMF again. This step was repeated for 4 times. Then, the gel was taken and placed into beaker containing ice cold-deionized water. The shrunken gel was started to swell in water for lysine containing gels. At this step the gel was dialyzed against deionized water for 2 days to remove the DMF. Different procedures such as 0.1 mL HBr and overnight reaction also resulted in similar core-shell organohydrogels.

During washing steps, the immiscible layer of previous solvent (like chloroform) also follows a diffusion pattern while leaving the gel. Therefore, in cases of complete deprotection, it could be assumed that the completely deprotected hydrogel is a core-shell organohydrogel. To distinguish between two, the gel should be washed very well. A succesfull core-shell organohydrogel should keep its hard, opaque, symmetric core after washing, deswelling in different medium or reswelling after freeze drying. If this structure is not present, it indicates that gel was already a hydrogel and the pattern observed was only solvent differences trapped in the gel. In this case the procedure can be optimized by reducing acid amount or reaction time to obtain a proper core-shell organohydrogel.

Patterning trials on organogel film: 500 mg of an L series polypeptide was dissolved in 7.5 mL chloroform-acetonitrile (1:1). Next, 50 mg HM-bisTAD in 1.5 mL chloroform-acetonitrile (1:1) was added to the solution and shaken. Then, the solution was slowly added into a clean glass petri dish with a Pasteur pipette. After 10-20 min the pink color of the TAD disappeared, indicating there is no free TAD left in the film.

The film was left for 2-3 hours in open air to remove most of the solvent absorbed by the gel. Then, using a commercially available TLC capillary tube a 1/10 diluted solution of HBr (33% in acetic acid) in chloroform was put on the gel as droplets. After, 15 minutes the droplets and the film were washed with DMF and then with deionized water.

Dying the core-shell hybrid gel: Gels were placed into a beaker containing Rhodamine B (20mg/L) and kept overnight. Then, dyed gels were dialyzed against deionized water for 2 days and the water was refreshed at least 3 times a day. The same procedure was also applied to the patterned film. To test dying of the core, a gel was placed in 200 mL THF and immediately started to shrink. Then, Reichardt's dye (~5-10 mg) was dissolved and the gel was kept in this solution overnight. Finally, the gel was dialyzed with deionized water for 2 days by and the water was refreshed at least 3 times a day.

5.5 References

(1) Wichterle, O.; Lim, D. *Nature* **1960**, *185* (4706), 117–118.

(2) Lim, F.; Sun, A. M. *Science,* **1980**, *210* (4472), 908 LP-910.

(3) Yannas, I. V; Lee, E.; Orgill, D. P.; Skrabut, E. M.; Murphy, G. F. *Proc. Natl. Acad. Sci. U. S. A.* **1989**, *86* (3), 933–937.

(4) Kashyap, N.; Kumar, N.; Kumar, M. N. V. R. *Crit. Rev. Ther. Drug Carrier Syst.* **2005**, *22* (2), 107–150.

(5) Drury, J. L.; Mooney, D. J. *Biomaterials* **2003**, *24* (24), 4337–4351.

(6) Lee, K. Y.; Mooney, D. J. *Chem. Rev.* **2001**, *101* (7), 1869–1880.

(7) Langer, R., *Nat. Biotechnol.*, **1994**, 12, 689-693.

(8) Gunatillake, P. A.; Adhikari, R. *Eur Cell Mater* **2003**, *5* (1), 1–16.

(9) Saul, J. M.; Williams, D. F. In *Handbook of Polymer Applications in Medicine and Medical Devices*; **2013**; pp 279–302.

(10) Slaughter, B. B. V; Slaughter, B. B. V; Khurshid, S. S.; Khurshid, S. S.; Fisher, O. Z.; Fisher, O. Z.; Khademhosseini, A.; Khademhosseini, A.; Peppas, N. A.; Peppas, N. A. *Adv. Mater.* **2009**, *21* (32–33), 3307–3329.

(11) Lin, C. C.; Anseth, K. S. *Pharmaceutical Research*. **2009**, pp 631–643.

(12) Wokalek, H. Patent, US5076265 A, **1991.**

(13) Peppas, N. A.; Van Blarcom, D. S. *J. Control. Release* **2016**, *240*, 142–150.

(14) Han, I. S.; Magda, J. J.; Lew, S. L.; San Jean, Y., Patent, WO2001081890 A2 **2003.**

(15) Hoffman, A. S. *Adv. Drug Deliv. Rev.* **2012**, *64*, 18–23.

(16) Papavasiliou, G.; Sokic, S.; Turturro, M. *Intechopen* **2012**, 111–134.

(17) Männistö, M.; Vanderkerken, S.; Toncheva, V.; Elomaa, M.; Ruponen, M.; Schacht, E.; Urtti, A. *J. Control. Release* **2002**, *83* (1), 169–182.

(18) Veronese, F. M.; Pasut, G. *Drug Discov. Today* **2005**, *10* (21), 1451–1458.

(19) Vaissiere, G.; Chevallay, B.; Herbage, D.; Damour, O. *Med. Biol. Eng. Comput.* **2000**, *38* (2), 205–210.

(20) Hersel, U.; Dahmen, C.; Kessler, H. *Biomaterials*. **2003**, pp 4385–4415.

(21) Benoit, D. S. W.; Anseth, K. S. *Biomaterials* **2005**, *26* (25), 5209–5220.

(22) Satriano, C.; Messina, G. M. L.; Marino, C.; Aiello, I.; Conte, E.; Mendola, D. La; Distefano, D. A.; D'Alessandro, F.; Pappalardo, G.; Impellizzeri, G. *J. Colloid Interface Sci.* **2010**, *341* (2), 232–239.

(23) Tian, H.; Tang, Z.; Zhuang, X.; Chen, X.; Jing, X. *Prog. Polym. Sci.* **2012**, *37* (2), 237–280.

(24) Huang, J.; Heise, A. *Chem. Soc. Rev.* **2013**, *42* (17), 7373–7390.

(25) He, X.; Fan, J.; Wooley, K. L. *Chemistry - An Asian Journal*. **2016**, pp 437–447.

(26) Huang, J.; Heise, A. *Chem. Soc. Rev.* **2013**, *42* (17), 7373–7390.

(27) Zhang, S.; Li, Z. *J. Polym. Sci. Part B Polym. Phys.* **2013**, *51* (7), 546–555.

(28) Nowak, A. P.; Breedveld, V.; Pakstis, L.; Ozbas, B.; Pine, D. J.; Pochan, D.; Deming, T. J. *Nature* **2002**, *417* (6887), 424–428.

(29) Pakstis, L. M.; Ozbas, B.; Hales, K. D.; Nowak, A. P.; Deming, T. J.; Pochan, D. *Biomacromolecules* **2004**, *5* (2), 312–318.

(30) Pochan, D. J.; Pakstis, L.; Ozbas, B.; Nowak, A. P.; Deming, T. J. *Macromolecules* **2002**, *35* (14), 5358–5360.

(31) Cho, C.-S.; Jeong, Y.-I.; Kim, S.-H.; Nah, J.-W.; Kubota, M.; Komoto, T. *Polymer*, **2000**, *41* (14), 5185–5193.

(32) Zhang, S.; Fu, W.; Li, Z. *Polym. Chem.* **2014**, *5* (10), 3346–3351.

(33) Huang, J.; Hastings, C. L.; Duffy, G. P.; Kelly, H. M.; Raeburn, J.; Adams, D. J.; Heise, A. *Biomacromolecules* **2012**, *14* (1), 200–206.

(34) Nguyen, M. K.; Lee, D. S. *Macromol. Biosci.* **2010**, *10* (6), 563–579.

(35) Antos, J. M.; Francis, M. B. *J. Am. Chem. Soc.* **2004**, *126* (33), 10256–10257.

(36) Sletten, E. M.; Bertozzi, C. R. *Angew. Chemie Int. Ed.* **2009**, *48* (38), 6974–6998.

(37) Antos, J. M.; Francis, M. B. *Curr. Opin. Chem. Biol.* **2006**, *10* (3), 253–262.

(38) Seki, Y.; Ishiyama, T.; Sasaki, D.; Abe, J.; Sohma, Y.; Oisaki, K.; Kanai, M. *J. Am. Chem. Soc.* **2016**, *138* (34), 10798–10801.

(39) Seki, Y.; Tanabe, K.; Sasaki, D.; Sohma, Y.; Oisaki, K.; Kanai, M. *Angew. Chemie Int. Ed.* **2014**, *53* (25), 6501–6505.

(40) Engler, A. C.; Lee, H.; Hammond, P. T. *Angew. Chemie Int. Ed.* **2009**, *48* (49), 9334–9338.

(41) Quadir, M. A.; Martin, M.; Hammond, P. T. *Chemistry of Materials*. **2014**, pp 461–476.

(42) Robinson, J. W.; Schlaad, H. *Chem. Commun.* **2012**, *48* (63), 7835–7837.

(43) Krannig, K.-S.; Huang, J.; Heise, A.; Schlaad, H. *Polym. Chem.* **2013**, *4* (14), 3981–3986.

(44) Wong, M. S.; Cha, J. N.; Choi, K.-S.; Deming, T. J.; Stucky, G. D. *Nano Lett.* **2002**, *2* (6), 583–587.

(45) Habraken, G. J. M.; Koning, C. E.; Heuts, J. P. A.; Heise, A. *Chem. Commun.* **2009**, No. 24, 3612–3614.

(46) Deng, G.; Ma, Q.; Yu, H.; Zhang, Y.; Yan, Z.; Liu, F.; Liu, C.; Jiang, H.; Chen, Y. *ACS Macro Lett.* **2015**, *4* (4), 467–471.

(47) Yong, X.; Simakova, A.; Averick, S.; Gutierrez, J.; Kuksenok, O.; Balazs, A. C.; Matyjaszewski, K. *Macromolecules* **2015**, *48* (4), 1169–1178.

(48) Beziau, A.; Singh, A.; de Menezes, R. N. L.; Ding, H.; Simakova, A.; Kuksenok, O.; Balazs, A. C.; Kowalewski, T.; Matyjaszewski, K. *Polymer* **2016**, *101*, 406–414.

(49) Hu, Z.; Zhang, X.; Li, Y. *Science.* **1995**, *269* (5223), 525 LP-527.

(50) Hu, Z.; Chen, Y.; Wang, C.; Zheng, Y.; Li, Y. *Nature* **1998**, *393* (6681), 149–152.

(51) Biswas, S.; Singh, A.; Beziau, A.; Kowalewski, T.; Matyjaszewski, K.; Balazs, A. C. *Polymer*. **2017**, *111*, 214–221.

(52) Banik, S. J.; Fernandes, N. J.; Thomas, P. C.; Raghavan, S. R. *Macromolecules* **2012**, *45* (14), 5712–5717.

(53) Li, P.; Poon, Y. F.; Li, W.; Zhu, H.-Y.; Yeap, S. H.; Cao, Y.; Qi, X.; Zhou, C.; Lamrani, M.; Beuerman, R. W.; Kang, E.-T.; Mu, Y.; Li, C. M.; Chang, M. W.; Jan Leong, S. S.; Chan-Park, M. B. *Nat. Mater.* **2011**, *10* (2), 149–156.

(54) Veiga, A. S.; Schneider, J. P. *Biopolymers*. 2013, pp 637–644.

(55) Ng, V. W. L.; Chan, J. M. W.; Sardon, H.; Ono, R. J.; García, J. M.; Yang, Y. Y.; Hedrick, J. L. *Advanced Drug Delivery Reviews*. 2014, pp 46–62.

(56) Kim, B.; La Flamme, K.; Peppas, N. A. *J. Appl. Polym. Sci.* **2003**, *89* (6), 1606–1613.

(57) Huebsch, Nathaniel, et al., *Nat. mater.*, **2015** 14.12 (2015): 1269

(58) Hollister, Scott J., *Nat. Mater.*, **2005** 4.7: 518.

Chapter 6
Conclusion and outlook

The aim of this Ph.D. project was to synthesize cross-linked polypeptide based hydrogels derived from N-carboxyanhydride polymerization. The focus was on the development of a method that allows the fabrication of mechanically strong gels which may find application in tissue engineering or drug delivery.

In Chapter 2 we have attempted to crosslink tyrosine containing polypeptides by Horseradish Peroxidase enzyme. Varieties of polypeptides have been tested for crosslinking but none of them formed a hydrogel. Having tyrosine polypeptides in our hand we searched for alternative tyrosine selective reactions in literature. This led to the investigation of triazolinedione (TAD) compounds as crosslinking agents for copolypeptides in Chapter 3. TAD compounds were synthesized and tyrosine-TAD reactions was optimized for our polypeptides. In this chapter we have successfully functionalized tyrosine containing polypeptides by PTAD, TAD-carboxylic acid and crosslinked those polypeptide by HM-bisTAD. The main challenge and limitation for tyrosine-TAD reaction was the instability of TAD compounds in aqueous conditions. In Chapter 4, switching from tyrosine to tryptophan has opened a new way to functionalize copolypeptides. Unlike most of the functional amino acids, tryptophan did not require protection-deprotection chemistry for polymerization. Additionally, tryptophan-TAD reaction has been carried out in organic solvents in which TADs are stable. Demonstration of successful co-click reaction showed that this method has high potential to prepare well defined polypeptides with an ease. In the last chapter, the TAD-tryptophan reaction was utilized to obtain mechanically strong hydrogels. The versatility of the reaction has provided the consistency and the reproducibility for fabrication of polypeptide based hydrogels. Control over gelation kinetics was

achieved by varying the amount of tryptophan in the copolypeptide. At the end of this chapter a new type of organohydrogel was reported. It was formed by deprotection of Cbz groups of lysine via diffusion control.

While the Trytophan-TAD reaction can be used to conjugate polypeptides, applying this reaction for crosslinking has higher future potential for bioapplications. Synthesis of functional TADs is challenging which probably limits its applicability in the conjugation/functionalization of polymers. Difunctional, hydrophobic TADs can, however, readily been synthesized and stored. Their reaction with tryptophan is fast and selective, which makes it ideally suited for cross-linking reactions. In continuation of this work, the design of biomedically relevant hydrogels by this technique should be focused on. For example, 3D-printers can be utilized to create very complex hydrogels by using double-syringe mixer where one syringe contains polypeptide and a TAD crosslinker in the other syringe. It could be done by choosing proper composition of solvents, polymer/TAD. The gelation time can be tuned to 1 second or much lower to achieve a fast 3D printing. On the other hand 3D printed molds can be used to fabricate complex shape hydrogels.

In future, new approaches to pattern cross-linked polypeptides should also be investigated.